Fabrication and Use of Conducting Polymer Linear Actuators

by

Timothy Andrew Fofonoff

B.Sc., Engineering Physics (2000)
B.Sc., Computer Science (2000)
University of Saskatchewan
S.M., Mechanical Engineering (2003)
Massachusetts Institute of Technology

Submitted to the Department of Mechanical Engineering
in partial fulfillment of the requirements for the degree of

Doctor of Philosophy

at the

MASSACHUSETTS INSTITUTE OF TECHNOLOGY

June 2008

Author .....
Department of Mechanical Engineering
May 23, 2008

Certified by .....
Ian W. Hunter
Hatsopoulos Professor of Mechanical Engineering
Thesis Supervisor

Accepted by .....
Lallit Anand
Chairman, Department Committee on Graduate Students

Fabrication and Use of Conducting Polymer Linear Actuators

by

Timothy Andrew Fofonoff

Submitted to the Department of Mechanical Engineering
on May 23, 2008, in partial fulfillment of the
requirements for the degree of
Doctor of Philosophy

Abstract

The development of biomimetic devices will benefit from the incorporation of actuators with combinations of properties common to biological systems, for example low density, controllable mechanical flexibility, and compact size. Conducting polymers, such as polypyrrole, exhibit muscle-like properties and the potential to provide the above capabilities while delivering significant forces over useful displacements. Current conducting polymer linear actuators, however, are generally limited to displacements of less than 0.5 mm, forces of less than 1 N, and cycle frequencies of less than 0.1 Hz. These materials are rarely tested on a length scale of more than a few millimeters, and their incorporation into real applications has to date been limited.

This work focuses on improving and scaling conducting polymer linear actuators for application in macroscale systems. A new fabrication method is described that delivers polypyrrole ribbons with uniform thicknesses of 10 to 30 μm, widths of 20 μm to 20 mm, and lengths exceeding 5 m. A second method is described where a conductive gold layer is incorporated into the ribbons and is shown to enhance performance and mitigate limiting effects common to longer conducting polymer actuators. Additionally, parallel actuation is explored as a method to achieve greater forces without compromising actuation speed. The integration of these actuators into stand alone systems that include joints and flexures has yielded novel techniques in amplifying motion while minimizing friction, improving electrical connection, and increasing actuator lifetime. The challenges of incorporating these actuators into an example biomimetic system are discussed and an approach is introduced. These methods and systems are shown to have increased conducting polymer linear actuator displacement output, force output, and actuation speed each by a full order of magnitude, thus bringing this technology closer to practical incorporation and use in biomimetic systems.

Thesis Supervisor: Ian W. Hunter
Title: Hatsopoulos Professor of Mechanical Engineering

Acknowledgments

I will always cherish my time at MIT. I still remember my sense of wonder the first summer I spent at the MIT BioInstrumentation Lab. I can confidently say that it inspired me to work harder, to work smarter, and to fearlessly tackle extremely complex and sometimes seemingly impossible projects without looking back. I can't help but feel that I have been part of something very special. There really are so many people who have made and continue to make MIT the unique place it is today, and I'd like to begin with a shoot out to the whole community: Thanks! Three groups that have been especially good to me during my time as a graduate student and deserve my special thanks are the Mechanical Engineering Department, the Institute for Soldier Nanotechnologies, and the Venture Mentoring Service.

I would like to thank my thesis advisor, Professor Ian Hunter, who has supported me for so long on numerous projects, and who has guided me while still allowing me the freedom to explore what I felt like exploring, to try what I felt like trying, and to build what I felt like building. His renaissance-like passion for knowledge over an enormous breadth of disciplines has been an inspiration to me.

I would like to acknowledge several members of the BioInstrumentation Lab's polymer group, Rachel Pytel, Nate Vandersteeg, Priam Pillai, Bryan Ruddy, Angela Chen, Nate Wiedenman, and Patrick Anquetil, with whom I have had many lengthy and fruitful discussions. I would also like to acknowledge the work of John Madden, Peter Madden, Mike Del Zio, and Bryan Schmid for pioneering methods, constructing equipment, and conducting studies upon which my work builds.

Thinking back on the years I have spent earning this degree, there are many colleagues I'd like to thank for lending a hand when needed, and for making the lab such an enjoyable place to work. They include Brian Hemond, Cathy Hogan, Andrew Taberner, James Tangorra, Scott McEuen, Bryan Crane, Robert David, Ariel Hermannson, and Mike Garcia-Webb. Kate Melvin has also been especially helpful and thoughtful.

Two labmates in particular deserve a special mention: Craig Forest and Nathan

Ball. I have many fond memories of discussions and activities of all kinds with these guys, and they have been great sounding boards for many of my plans and ideas. I know that working together, whether solving a problem, discussing an issue, or just having fun, has helped us all to grow, and I have a high regard for what I am sure will be long lasting friendships.

Finally, I would like to thank my parents, Ann and Dan Fofonoff, for their unwavering support of all of my studies, and for being so trusting in my making the choices that are best for me. Seeing their pride at the end of this long road has really been a treat. And, most of all, because she has been right there with me through this entire process, I would like to thank my love, Leslie Deutsch, for being so patient with me and for being there with me while I walked this long and sometimes not so straight road.

Contents

List of Figures

List of Tables

Chapter 1

Introduction

1.1 Motivation

Actuators are all around us. They are inside my fingers as I type this thesis, inside my cat twitching as she sleeps next to me, and inside the steering mechanisms of the airplane I see flying in the sky outside the window. Actuators allow us to control our environment, move ourselves, and in a general and real way: do work. Perhaps the actuators we are familiar with most are those within our own bodies. Our muscles allow us to move about as well as to displace other objects, and in today's world, to control a wide range of devices made to accept a human input. These devices also often contain actuators, and while they sometimes have similarities to our own muscle actuators in their output, they most often are very different in makeup, capabilities, control, and operation.

It has long been an aspiration of humankind to mimic the processes, behaviors, and movements found in nature. A good deal of effort is today put toward the creation of biologically inspired systems, or *bioinspired* systems, that attempt to mimic natural phenomena, including motion. Animal motion appears fluid, responsive, and is generally efficient, and there is significant interest in the creation of *biomimetic* systems that would exhibit similar qualities. While a motorized propeller can propel a boat, submarine, or robot through the ocean, dolphins and fish can accomplish this task much more quietly, efficiently, and elegantly. There is certainly a desire for

robots to be made more lifelike. And, although there are certainly aesthetic reasons for this, animal movement is often much more efficient and responsive than that of human made machines. For example, my cat has a sense of balance and control that would be very difficult for an artificial machine to match. Its speed, power, and energy output are all very impressive when compared to a state of the art human made machine of similar size. Much of this has to do with the animal's complex control system, or nervous system, but its actuators, or muscles, are a significant component as well.

Our muscles can often appear much simpler than they really are. Upon closer inspection, we see they are immensely complex and are coupled with equally complex control, energy delivery, and repair systems. The notion of creating *artificial* muscles has been an attractive prospect for some time. Skeletal muscle's ability to perform desirable tasks quickly and with an acceptable level of control, such as moving an object or repositioning the body, while adhering to compact and flexible geometries make it very attractive when compared to conventional systems that could accomplish similar tasks. Some applications in particular, such as exoskeletons, wearable rehabilitation devices, and platforms for the study of animal movement are envisioned to be obvious candidates for the application of artificial muscles.

1.2 Artificial muscles

Several technologies have been developed that are often now classified as artificial muscles. A key component separating an *artificial muscle* from a conventional actuator is its ability to directly generate sizable strains at reasonable stresses. This leads to a capability of directly driving a load without a gearbox or other mechanisms that would add size, increase complexity, and reduce efficiency. Thorough reviews of these technologies have been produced [10, 9]. Table 1.1 presents a list of several artificial muscle technologies along with their advantages and disadvantages [9].

A large variety of actuators have been created to date. They utilize an extensive variety of materials in a large array of configurations to accomplish a fundamentally

Actuator	Advantages	Disadvantages	Comments
Mammalian Skeletal Muscle	Large strains (20 %). Moderate Stress (350 kPa blocking). Variable stiffness. High energy fuel (20-40 MJ/kg). Efficient (~ 40 %). Good work density (< 40 kJ/kg). High cycle life (by regeneration).	Not yet an engineering material. Narrow temperature range of operation. No catch state (expends energy to maintain a force w/o moving, unlike mollusk muscle).	Incredibly elegant mechanism that is a challenge to emulate. Muscle is a 3D nanofabricated system with integrated sensors, energy delivery, waste/heat removal, local energy supply and repair mechanisms.
Dielectric Elastomers	Large strain (20% - 380 %). Moderate stress (several MPa peak). Large work density (10k to 3.4 MJ/m^3). Moderate to high bandwidth (10 Hz to > 1 kHz). Low cost. Low current. Good electromechanical coupling & efficiency (> 15 % typical, 90 % max).	High voltages (> 1 kV) and fields (~150 MV/m). Typically requires DC-DC converters. Compliant ($E \sim 1$ MPa). Pre-stretching mechanisms currently add substantial mass and volume, reducing actual work density and stress.	Potential to lower fields using high dielectric materials. Small devices are favored for high frequency operation eg. MEMS. (due to the more efficient heat transfer which prevents thermal degradation, and the higher resonant frequencies). Starting materials are readily available.
Relaxor Ferroelectric Polymers	Moderate strain (< 7 %). High stress (45 MPa blocking). Very high work density (up to 1 MJ/m^3 internal strain). Stiff (400 MPa). Strong coupling (0.4) & efficiency. Low current.	High voltages (typically > 1kV) and fields (~150 MV/m). Typically need DC-DC converters. Synthesis of typical materials involves environmentally regulated substances. Cycle life is unclear & may be limited by electrode fatigue and dissipation. Limited temperature range.	Lower voltages and fields are being achieved using new high dielectric composites. Small devices are favored for high frequency operation eg. MEMS. Unique combination of high stiffness, moderate strain & reasonable efficiency.
Liquid Crystal Elastomers	Large strains in thermally induced materials (45%). Moderate strains in field induced materials (2-4 %). High coupling (75%) in electrical materials.	Subject to creep. Thermal versions are slow unless very thin or photoactivated. High fields (1-25 MV/m). Low efficiency in thermal materials.	New material with much promise and much characterization to be done. Photo-activation has been achieved.
Conducting Polymers	High stress (34 MPa max, 5 MPa typical). Moderate strain (~ 2 %). Low voltage (~ 2 V). High work density (100 kJ/m^3). Stiff polymers (~ 1 GPa).	Low electromechanical coupling. Currently slow (several hertz maximum to obtain full strain). Typically needs encapsulation.	Promising for low voltage applications. Speed and power will improve dramatically at small scales.
Molecular Actuators	Large strain (20 %). Moderate to high stress (> 1 MPa). Low voltage (2 V). High work density (> 100 kJ/m^3)	Currently slow. Need encapsulation.	Great promise of overcoming many of the shortcomings of conducting polymer actuators, but still very early in development.
Carbon Nanotubes	High stress (> 10 MPa). Low voltage (2 V). Very large operating temperature range.	Small strain (0.2 % typical). Currently has low coupling. Materials are presently expensive.	Great potential as bulk materials approach properties of individual nanotubes.
Ionic Polymer Metal Composites (IPMC)	Low Voltage (< 10 V). Large displacement (mechanical amplification built into the structure).	Low coupling and efficiency. Usually no catch state (consumes energy in holding a position). Requires encapsulation.	IPMC driven toys and demonstration kits are available.
Thermally Activated Shape Memory Alloys	Very high stress (200 MPa). Unmatched specific power (> 100 kW/kg). Moderate to large strain (1-8 %). Low voltage (actual voltage depends on wiring). Great work density (> 1 MJ/m^3)	Difficult to control (usually run between fully contracted and fully extended but not between). Large currents and low efficiencies (<5%). Cycle life is very short at large strain amplitudes.	Readily available. Generally thought of as slow, but can achieve millisecond response times using short high current pulses and water cooling.
Ferromagnetic Shape Memory Alloys	High stress (< 9 MPa). High frequency (> 100 Hz). Moderate strain (up to 10%). High coupling (75%).	Bulky magnets are required which greatly reduce the work density. Costly single crystal materials.	Operates in compression and thus needs a restoring force. Displacement is typically all or nothing, as intermediate states are difficult to reach reproducibly. Commercially available.

Table 1.1: Summary comparing several actuator technologies (from [9]).

similar result: The application of a force or torque to a load. Of particular interest is the linear actuator. Whereas a rotary motor produces a rotational output in the form of torque at a given angular velocity, a linear actuator produces a force at a given velocity. An interesting subtlety is that mechanisms can be applied to linear

and rotational actuators in order to effectively switch between the two output modes. For example, a linear actuator can be pinned at a hinge or joint in order to cause motion along an angular path, and the output from a rotational actuator can be applied through a pinion on a rack to produce linear motion. Even with this in mind, however, it is anticipated that many applications would benefit from a direct drive configuration. The absence of a gearbox or similarly performing mechanism would positively effect the system's size, complexity, and efficiency.

1.3 Conducting polymer actuators

Conducting polymer actuators, such as those based on polypyrrole, offer muscle-like properties that could be useful in the creation of biomimetic devices [11, 12, 1]. These properties include a high power-to-mass ratio, inherent compliance, and direct-drive capability. In carefully measured experiments, performed at a small scale, their output capabilities have indeed appeared promising. They can generate stresses of 5 MPa [13] and strains of up to 12% [14], while operating in a desirable voltage range (less than 5 V).

Conducting polymers, as a group, consist of polymers which have unique conjugated backbone structures that facilitate the delocalization of electrons along those chains. With the addition of a dopant to complete the electron delocalization, these materials can be substantially conductive. For example, polypyrrole, the polymer model that forms the basis for this work, has a conductivity of about 5×10^4 S/m.

A conducting polymer, such as polypyrrole, undergoes volumetric changes as its oxidation state is altered electrochemically. This actuation is the result of the diffusion of ions in and out of the polymer bulk in order to balance the applied charge [12, 15]. Figure 1-1 shows the actuation mechanism of conducting polymer actuators. A voltage potential is applied between the conducting polymer film and a non-reactive counter electrode, causing positive charge to develop throughout the polymer film, which then drives negative ions in to balance the charge. In practice, a reference electrode and potentiostat are used in order to more accurately control the potential

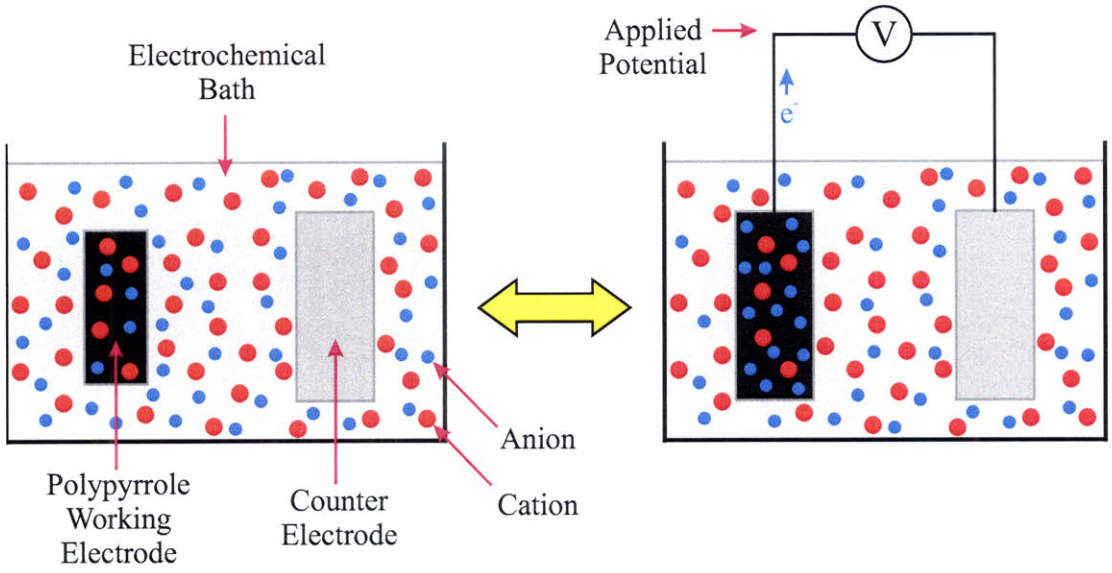

Figure 1-1: Schematic showing the electrochemical actuation of polypyrrole. A voltage potential is applied between the working and counter electrodes of the electrochemical cell, here causing the polypyrrole film to swell with ingressing anions.

or charge imposed on the conducting polymer working electrode. The electrochemical bath is chosen to have anions and cations with different sizes, so that either the anion or cation will diffuse more quickly than the other. In Figure 1-1, the anion is shown as the more mobile ion.

Two common categories of conducting polymer based actuators are layered actuators and linear actuators.

1.3.1 Layered actuators

Although not the focus of this thesis, layered conducting polymer actuators deserve mention due to their prominence in the literature [3, 16, 17, 18, 19, 20, 21, 1]. Layered polymer actuators, often referred to as bilayers or trilayers, can be fabricated in a variety of ways, but have a common actuation mode. One or two active layers are made to contract and expand with respect to a passive layer or an opposing active layer. The net effect is an amplification of a moderate strain (1-2%) in order to produce a deflection that is readily observed [3]. These actuators can be used in an electrolyte bath, or in air, by utilizing a central ionically conducting gel layer [20].

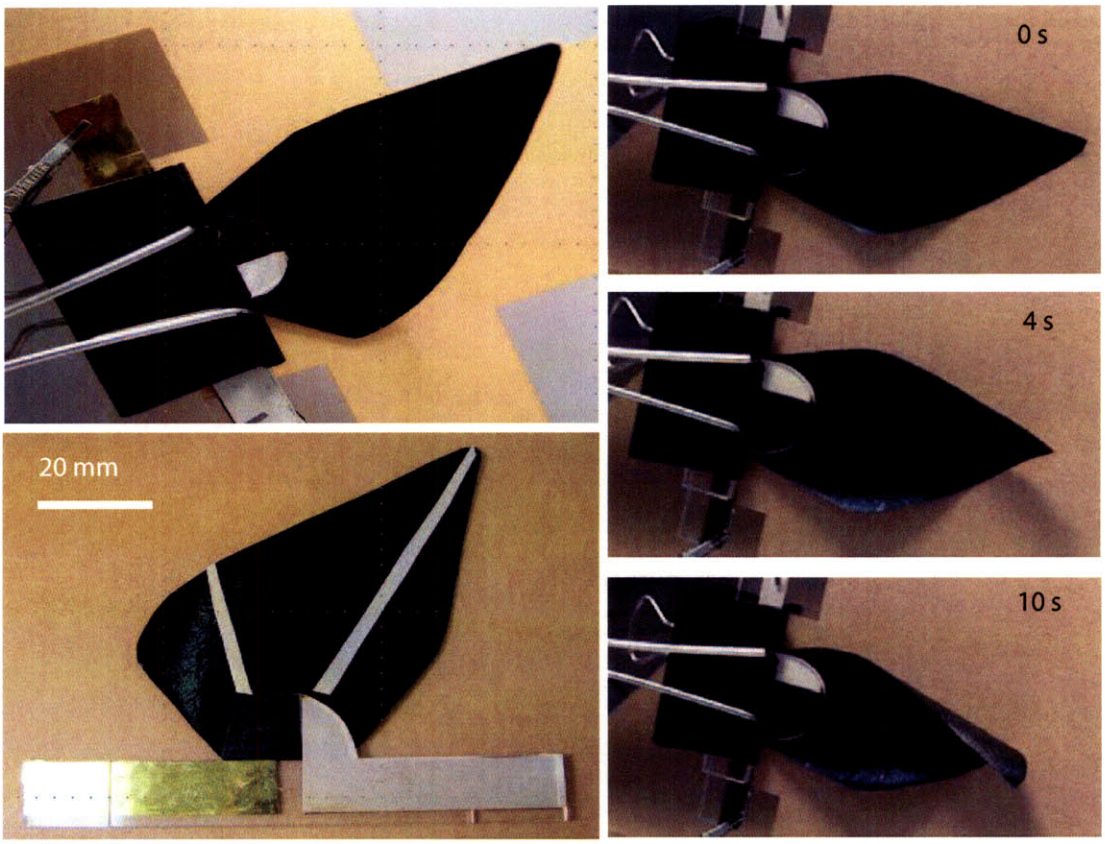

Figure 1-2: A polypyrrole a based trilayer fin that was fabricated in order to make cupping motions (from [1]).

Although the curving geometry produced by layered actuators can provide for interesting demonstrations, it is not able to produce substantial forces. Still, applications have been proposed for these types of actuators where large forces are not required [18, 21]. Figure 1-2 shows a conducting polymer based trilayer fin that was fabricated in order to make cupping motions. Full contraction of the fin takes 10 s.

It has been shown that adding additional layers to these layered conducting polymer actuators increases force generation to a point [3, 22], but not sufficiently to compete with uniaxially loaded conducting polymer linear actuators.

1.3.2 Linear actuators

A conducting polymer linear actuator, in its simplest form, consists of a ribbon of polymer film connected at its two ends. Normally, one or both of these connections

also serve as the electrical connection used to charge and discharge the film with respect to a counter electrode, thus causing an expansion or contraction. In a linear actuator, the film is preloaded to an initial stress of 0.5 MPa to 5 MPa. The preload force may be provided by means of a hanging mass, a stretched elastomer, or an actively driven force feedback system as is often the case during actuator characterization. During the actuation cycle, this force may be altered or held constant. These techniques will be discussed in Chapter 4.

Linear polymer actuators have advantages over layered actuators. They are generally able to produce greater forces and are more easily preloaded and attached. Layered actuators are limited in their configurability in that they generally produce one single bending motion, and it is difficult to configure and attach a layered actuator so that its curving motion is able to deliver a sizable and consistent force. Linear polymer actuators are always used preloaded, which is generally easier to work with when designing complementary hardware. Linear actuators can also be scaled more easily than layered actuators. A linear actuator's fundamental behavior does not appreciably change when its dimensions are altered. Generated stresses and strains, as well as required preloading stresses can be predictably calculated. This is not to say that there are no difficulties to overcome in scaling linear polymer actuators for greater power delivery, but the challenge is more palatable. It is because of conducting polymer linear actuators' promise in scaling that they have become the focus of this thesis.

Most applications at the macroscale will require larger movements and larger forces than those typically produced to date [23]. These limitations are largely due to the physical dimensions of the manufactured materials. In increasing the size of the actuators, however, several significant issues become more pronounced and must be considered. For example, if an electrical connection is made at a single end of a polymer strip, the sizeable resistance of the polymer causes an ohmic potential drop along the length of the polymer which impacts its performance as an actuator [12, 23, 3]. This effect is of increased importance for longer films. Additionally, as an actuator is made wider, nonlinear effects such as rippling across a ribbon in tension

are increased. Also, because strain rate is related to the diffusion of the ions into and out of the polymer, it is impacted by the thickness of the polymer [12, 24, 3]. Thicker films tend to move more slowly. The ability to tension and manually adjust the polymer in response to swelling and creep also plays a larger role at the macroscale. In order for polypyrrole and similar actuating polymers to be readily used as macroscale engineering components, these issues need to be addressed.

Chapter 2

Review of conducting polymer actuators

In this chapter, the development of conducting polymer actuators is reviewed. Particular attention is paid to polypyrrole, the longstanding conducting polymer of choice at the MIT BioInstrumentation Laboratory and the base material for the actuators presented in this thesis.

2.1 Introduction

Conducting polymers, as a group, consist of polymers which have unique conjugated backbone structures that facilitate the delocalization of electrons along those chains [25]. For this reason, they are also referred to as conjugated polymers or π-electron conjugated conducting polymers [26, 11]. The first publication regarding a conducting polymer, polyacetylene, was published in 1977 [27], and three of the authors, Heeger, Shirakawa, and MacDiarmid, were awarded the Nobel prize in chemistry for this work in 2000 [28]. Figure 2-1 shows schematics of the most common conducting polymers where the conjugation is represented by alternating single and double bonds.

The molecules shown in Figure 2-1 lack mobile charge, and a dopant must be present in order to properly complete the electron delocalization [25]. The addition of this dopant dramatically increases the resulting material's conductivity, effectively

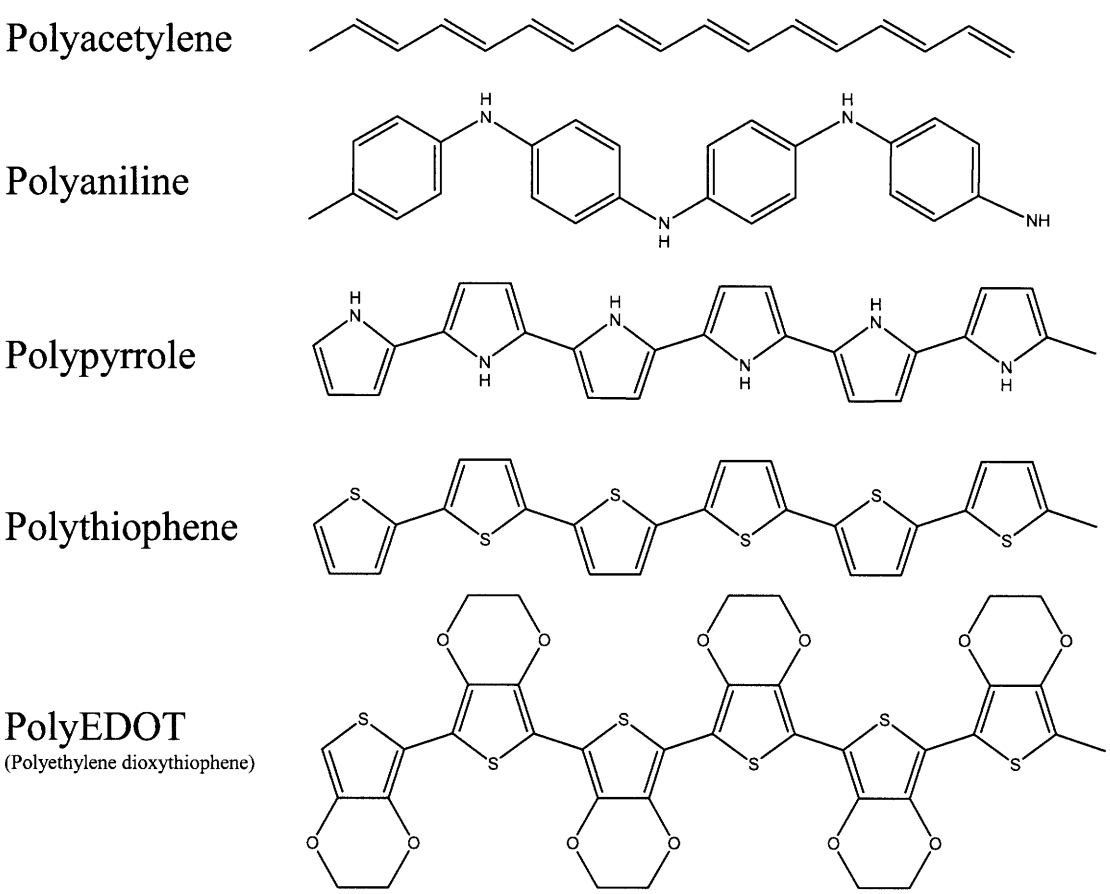

Figure 2-1: Schematic showing the bond structures of common conducting polymers (from [2]).

bringing the polymer from a semiconducting state to a conducting state. A schematic depicting this process is shown for polypyrrole in Figure 2-2.

Of the conducting polymers shown in Figure 2-1, polyaniline and polypyrrole have been found to demonstrate the largest active stresses and strains, and have therefore largely become the focus of conducting polymer actuator development. Polyaniline, although shown to be more processable than polypyrrole [29, 30, 31], has the disadvantage of requiring an acidic bath for operation [32, 33]. Polypyrrole, however, has been shown to actuate in a variety of environments [34, 9], including in aqueous solutions [35, 36].

Conducting polymers can be synthesized both chemically [37, 38] and electrochemically [39, 40, 15], although electrodeposited films generally yield more consistent and

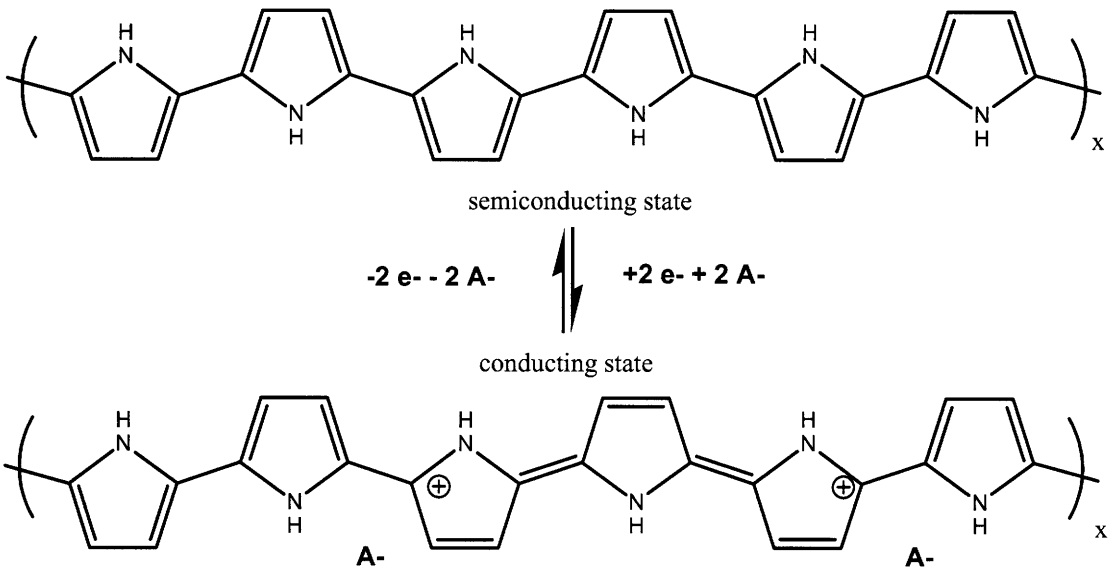

Figure 2-2: Schematic showing the doping and dedoping of polypyrrole. A- represents anions and e- represents electrons (from [2]).

desirable morphologies [6]. Electrodeposition is performed in an electrochemical cell consisting of a working electrode and a counter electrode, both with large nonreactive surfaces, positioned in an electrolyte bath that contains anions and cations in a solvent. A constant current is applied to the cell and a polymer film is electrodeposited at the working electrode. During deposition, as polymer chains *grow* at the working electrode, their conjugation increases and their oxidation potential decreases, resulting in oxidized polymer chains [41]. Anions from the solution move into the matrix of growing polymer chains in order to balance the charge, ultimately leading to a *doped* conducting polymer film. The specifics of conducting polymer electropolymerization are still debated. Sadki *et al.* have published a comprehensive review covering several possible chain growth mechanisms [41]. More on fabrication processes, including a standard recipe for electrodepositing polypyrrole, can be found in Chapter 3.

An important characteristic of conducting polymers is that their oxidative state can be altered electrochemically. That is, one can oxidize and reduce a conducting polymer film by removing or adding electrons from it. This is accomplished by applying a voltage potential to the polymer film in an electrochemical cell. Figure 2-3 shows a schematic of a basic electrochemical cell used to change the oxidative state

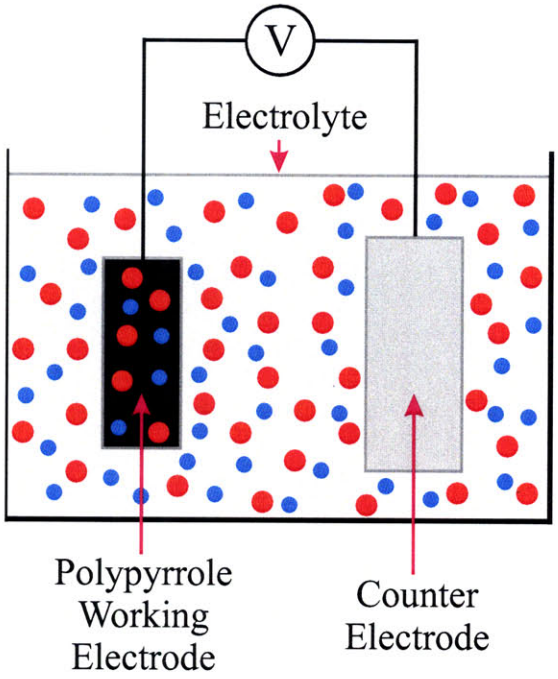

Figure 2-3: Schematic of a basic electrochemical cell used to change the oxidative state of a conducting polymer.

of a conducting polymer. The cell consists of a working electrode, made up of conducting polymer film, and a counter electrode, made up of a nonreactive conducting material, such as stainless steel, carbon fiber paper, or a second conducting polymer film. The electrodes are suspended in an electrolyte bath.

2.2 Actuation mechanism

Early development of conducting polymers was focused on their electrical properties and their use in battery applications, and it was during this work that a volume change was observed during oxidation and reduction in an electrochemical cell [28, 42, 43], leading to conducting polymers being proposed as actuators [44, 42]. It has since been determined that the observed volume change observed during the redox cycle is a result of counter ions moving into and out of the conducting polymer in order to balance the charge [34, 45].

Figure 1-1 showed a schematic depicting a conducting polymer expanding due to

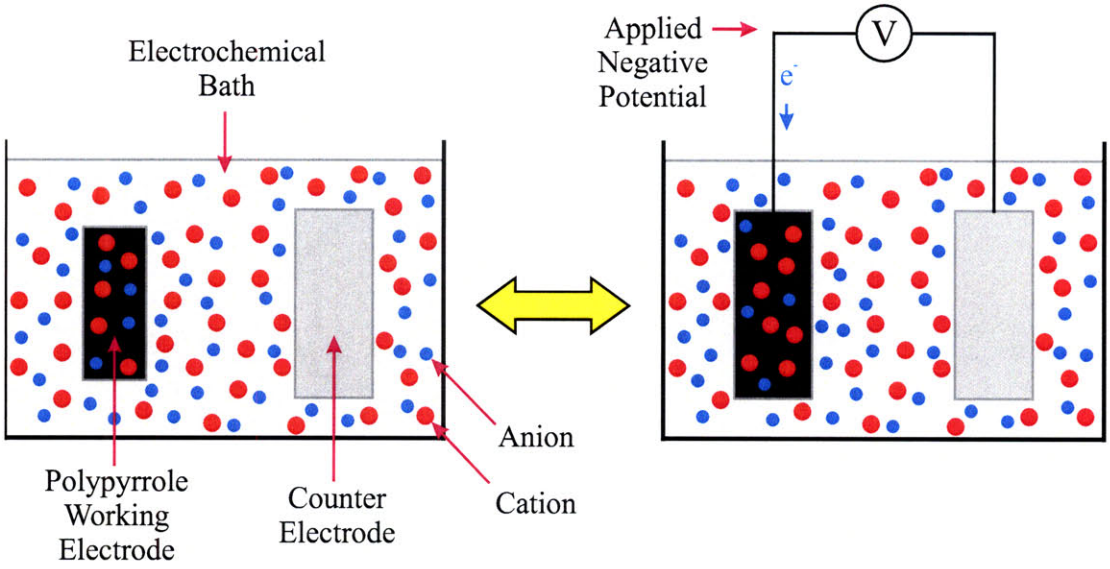

Figure 2-4: Schematic of a basic electrochemical cell used to change the oxidative state of a conducting polymer. The conducting polymer undergoes increases and decreases in volume as it takes up or lets out ions while actuated in an electrochemical cell.

the ingress of anions that results from the removal of electrons during its oxidation. When a positive voltage is imposed on the film, electrons are removed (and holes are added), and ions diffuse in or out of the film to balance the charge. A system that works in this way is an electrochemical bath of 0.05 to 0.1 M tetraethylammonium hexafluorophosphate ($TEAPF_6$) in propylene carbonate, where the tetraethylammonium (TEA^+) cations move much more slowly than the smaller hexafluorophosphate (PF_6^-) anions. Other electrolyte choices such 1-butyl-3-methylimidazolium hexafluorophosphate ($BMIMPF_6$), commonly referred to as a *liquid salt*, can lead to an opposite response, where the $BMIM^+$ cation will dominate the actuation. This response is demonstrated in Figure 2-4.

A circuit model for the electrochemical system of Figure 2-4 is shown in Figure 2-5 [24, 3, 7]. In the figure, R_S represents the solution resistance, C_{DL} represents the double layer capacitance at the polymer/electrolyte interface, and Z_d represents the impedance of ions diffusing into and out of the conducting polymer. It should be noted that the solution resistance term can be made to include the wiring and contact resistance at the film [3], as well as the electrical resistance of the polymer

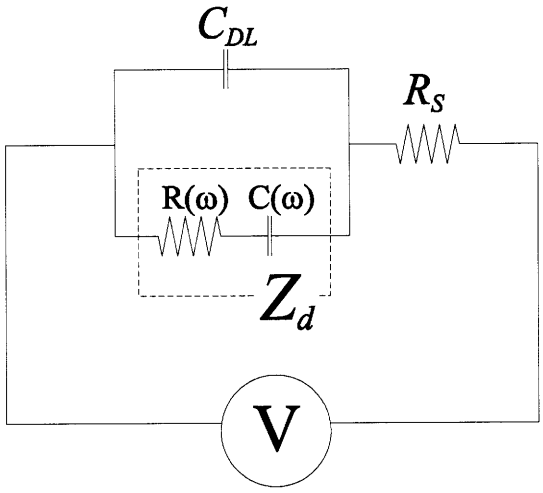

Figure 2-5: A circuit model for a conducting polymer in an electrochemical cell (from [3]).

[5], both of which can be appreciable.

J. Madden, in his PhD thesis [24], developed the diffusive elastic model (DEM) which predicts the electrical and mechanical behavior of a thin film conducting polymer actuated in an electrochemical cell. The model relates actuation to by the diffusion of ions into and out of the film through an elastic, metallic polymer matrix [7]. The model is in the form of an admittance, $Y(s)$, for the polymer strip, and is given by

$$Y(s) = \frac{s}{R} \frac{\frac{1}{\sqrt{\tau_{DDL}}} tanh(\sqrt{s\,\tau_D}) + \sqrt{s}}{\frac{\sqrt{s}}{\tau_{RC}} + s^{3/2} + \frac{s}{\sqrt{\tau_{DDL}}} tanh(\sqrt{s\,\tau_D})}, \tag{2.1}$$

where s is the Laplace variable and R is the series resistance. The diffusion based time constant, τ_D, relates to the concentration of ions in the polymer film, and is given by

$$\tau_D = \frac{a^2}{4D}, \tag{2.2}$$

where a is the film thickness, and D is the diffusion constant. τ_{RC} is the time constant related to charging the double layer, and is given by

$$\tau_{RC} = R\,C_{dl}, \tag{2.3}$$

where C_{dl} is the double layer capacitance. And finally, τ_{DDL} is the time constant related to the diffusion of ions through the double layer thickness, and is given by

$$\tau_{DDL} = \frac{\delta^2}{D}, \tag{2.4}$$

where δ is the thickness of the double layer. The admittance relates the current through the polymer $I(s)$, to the voltage $V(s)$ by

$$I(s) = Y(s)V(s). \tag{2.5}$$

Finally, the stain, $\epsilon(s)$, is given by

$$\epsilon(s) = \alpha \frac{Y(s)\,V(s)}{s\,LWa} + \frac{\sigma(s)}{E(s)}, \tag{2.6}$$

where σ is the stress applied to the film, E is the elastic modulus of the polymer, and L,W, and a are the length, width, and thickness of the polymer film. α is the strain to charge density ratio of the conducting polymer (about 10^{-10} m^3/C for PF_6^- doped polypyrrole) [12].

The DEM has been demonstrated to match experiments over a wide range of frequencies [24, 46, 3, 12]. It is a difficult equation to work with, however, because its solution in the time domain cannot be expressed in closed form [3]. The model is a very useful tool in investigating the dependencies of actuation, though, especially relating to the time constants.

Simpler models have been shown to work well for certain cases. For example, experimental data has been shown to fit well with a model consisting of two time constants [47, 7]. N. Vandesteeg, in a study of the effect of temperature on actuation, relates these time constants to electrical and diffusion related phenomena [7]. While these effects are interconnected, and some of the physical meaning of the DEM may be lost, this simpler model is attractive when actuator performance improvements are to be compared. The time constants relating to actuation will be revisited in Chapter 5.

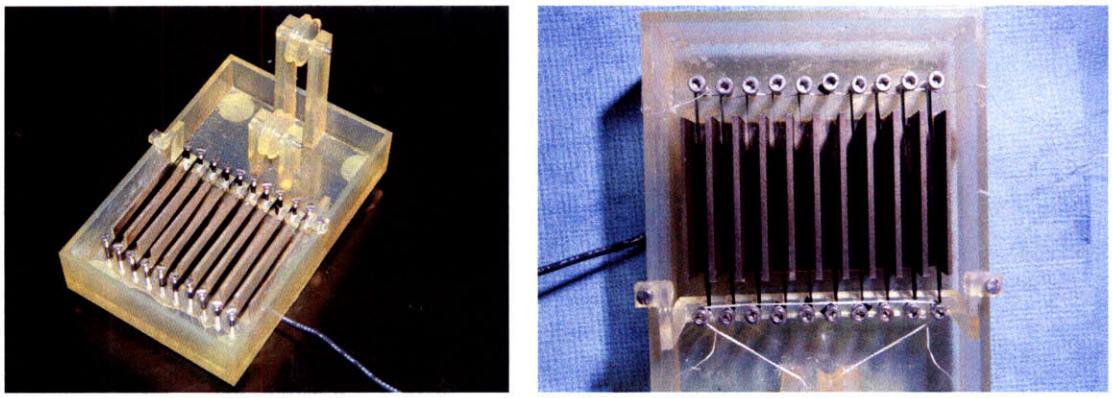

Figure 2-6: An early effort in parallel actuation (from [4, 1]).

2.3 Macroscale actuation

One question that must be asked is: *Does this performance scale as the characteristic dimensions of the actuator are scaled up*? The simplest answer is: *No.* There are two primary reasons for this: 1) Difficulties in manufacturing large uniform films, and 2) Time constants unfavorably increase as the physical dimensions of these films are increased. Imperfections or flaws in fabricated films become more noticeable when one moves to a larger format. Additionally, manufacturing methods to date have focused on the fabrication of small films, normally on the range of a few millimeters. Efforts have been undertaken to mitigate the effects of scaling the films, and some progress has been made [1, 4, 23]. Two approaches for delivering large forces are highlighted below.

One approach that has been investigated for increasing force output is parallel actuation, where several linear actuators are made to work together against a larger force [23, 13, 48]. This eliminates the need to drastically increase the thickness of the individual actuators, thus maintaining their response time. Parallel actuation will be discussed in detail in Chapter 5. A previous effort in parallel actuation, created by M. Del Zio of the BioInstrumentation Laboratory [4, 1], is shown in Figure 2-6. At the time of its creation, this device was the state of the art in terms of high force generating devices utilizing conducting polymer linear actuators.

The device utilizes a series of stainless steel screws to individually tension a series

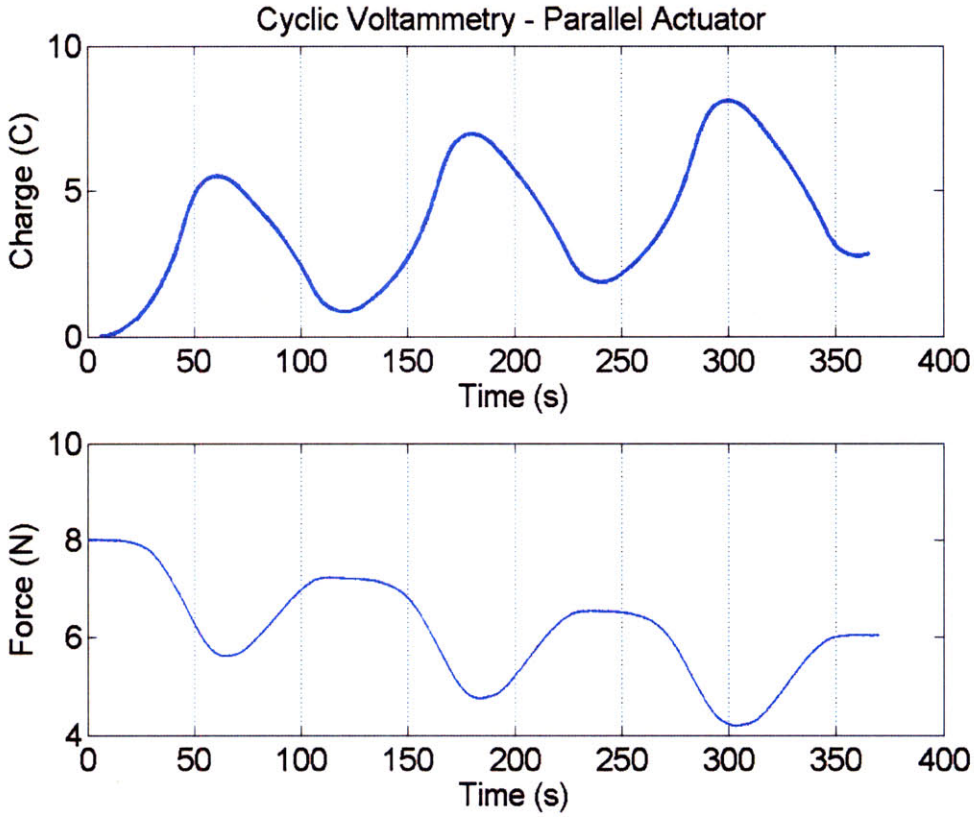

Figure 2-7: Data showing resulting actuation achieved using the parallel actuator shown in Figure 2-6 (from [4, 1]).

of ten 5 mm $\times$ 20μm $\times$ 60 mm polypyrrole ribbons equally. The capstan effect, in combination with machined slits in the screws, is utilized to hold the polymers in place. A metal counter electrode, with fins rising between the tensioned ribbons can be seen in Figure 2-6. The bath itself, and the other supporting hardware, were manufactured using stereolithography, a 3D printing process. Pulleys are used to guide a tensioned member that is then preloaded. Figure 2-7 shows some data that were recorded using the parallel actuating device shown in Figure 2-6.

Although 2 N of force is observed with this system, the experiment shown in Figure 2-7 was run in isometric mode. That is, no movement or mechanical work was achieved. The force output was 60% less than anticipated and was attributed to uneven tensioning of the polypyrrole actuators [4]. Also evident in the data is that the device suffered from creep. Although the approach showed promise, the system also

suffered from friction, which restricted its movement and its ability to do mechanical work. This data was significant in that 2 N was the upper end of force ever generated by conducing polymer based actuators, but it also highlights some of the challenges that needed yet to be overcome.

The device shown above demonstrated an approach for reducing the time constant relating to diffusion, but it still relied on the ribbons themselves to distribute the inputted charge along their lengths. An appreciable ohmic drop is expected of conducting polymer ribbons of this size. From bilayer work, it is known that the addition of a conducting layer can help distribute charge and increase actuation speed. Some groups have investigated incorporating metal conductors into linear actuators as well [49, 23, 14, 5, 50, 22].

One approach to adding a conducting element to a conducting polymer linear actuator undertaken by J. Ding, G. Spinks *et al.* [5, 23] is shown in Figure 2-8. A polypyrrole helix tube is achieved by winding 25 to 50 μm platinum wires around a larger 125 to 350 μm platinum wire and then electrodepositing polypyrrole onto the combination. Actuators 60 mm in length were typically achieved [5]. The larger wire is then removed and the smaller wire remains to help distribute charge. A variety of combinations can be achieved by adding more wires during deposition and bundling deposited helixes together [23].

With linear actuators fabricated in this way, the authors report using a nine-fiber bundled sample to achieve a 0.5% strain with a 2 N preload [23], a figure they tout as the highest force to date achieved using polypyrrole based actuators where an appreciable stain is observed. They do not report the speed of this actuation, however. Using parallel assemblies of helix fibers, they report achieving 0.4% strain at a 0.6 N preload. Interestingly, like in the parallel actuation system above, these authors also report encountered difficulties in equally tensioning the fibers in their assembly. The authors have utilized actuators of this type in a new type of Braille cell [5, 51].

It is clear that in addition to the above mentioned restrictions on scaling up conducting polymer linear actuator size, several other challenges related to the use of

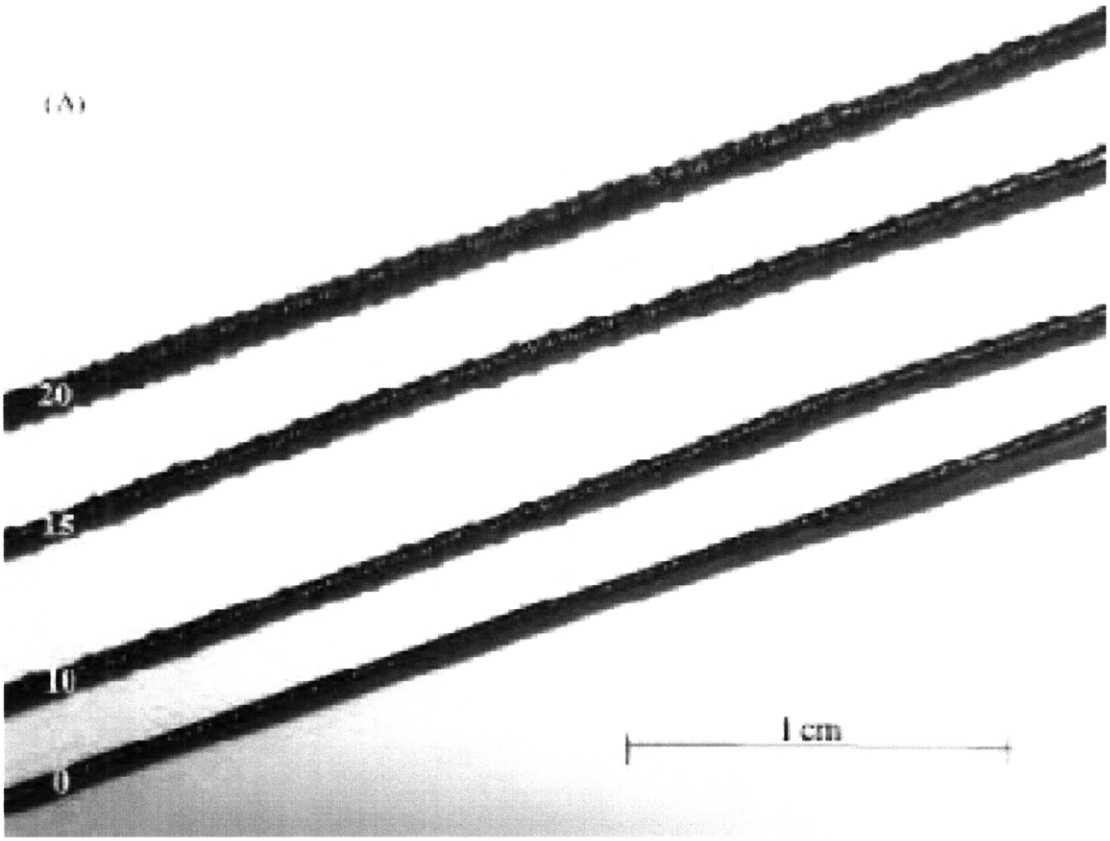

Figure 2-8: Photographs of hollow polymer tubes with helical interconnecting platinum wires. From top down, the pitches of the helices are 2000 turns/m, 1500 turns/m, and 1000 turns/m. A hollow tube with no helix is also displayed at the bottom of the photograph (from [5]).

conducting polymer actuators need to be addressed or controlled in order transform them into a useable engineering material. These challenges include: electrical and mechanical attachment, system friction and inefficiencies, creep, encapsulation, lifetime, and control.

Other notable efforts that have reported generating strains against sizable isotonic preload forces include 0.25 N by Sonoda *et al.* [52], 0.45 N by Della Santa *et al.* [26], and 0.8 N by Spinks *et al.* [49]. It should also be noted that commercial efforts have been made to develop electroactive polymer actuators. One such effort is Eamex of Japan. Although quantitative data and detailed descriptions are difficult to obtain, interesting videos and other information are available [53].

The fabrication, characterization, and application of conducting polymers at larger

scales are the focus of this thesis and are explored in depth in the chapters that follow.

Chapter 3

Actuator fabrication

Polypyrrole is one of the most studied of the conducting polymers largely because it is the most resilient to handling. Several procedures have been worked out over time that produce desirable films. It has been the conducting polymer workhorse for some time in the MIT BioInstrumentation Laboratory, and it was an obvious choice as the material model for work on scaling conducting polymer linear actuators.

In this chapter, a new method for creating large scale conducting polymer linear actuators is introduced. This method has produced ribbon actuators two orders of magnitude longer than any previously reported. First, a preferred deposition process is highlighted. This is followed by a method for creating long ribbons from these deposited materials for use as linear actuators. A method developed for incorporating conductors onto the films in order to increase their performance as linear actuators is then explained. Next is a discussion on further increasing manufacturing scale and automation. And finally, other approaches and material choices relating to the encapsulation of linear actuators are discussed.

3.1 Introduction

Like many conducting polymers, polypyrrole cannot be reversibly dissolved or melted. The material's resilience to chemical solvents and heat comes at a cost, however, as this significantly limits processing options. For example, polypyrrole cannot be

readily cast or molded. And, although polypyrrole can be deposited chemically, higher quality films are obtained using electrodeposition-based processes in electrochemical cells under controlled conditions. Because these higher quality films are of primary interest for use as linear actuators (indeed most other techniques cannot yield a free standing film that can be adequately preloaded for actuation), it was decided that they would form the basis of the scaling work on conducting polymer linear actuators. It should be noted, however, that the procedures described below could be applied to all electrodeposited materials as well as possibly some materials created using other means, such as chemical or vapor deposition techniques.

The material that serves as the basis for the actuator development below, as well as the characterization that follows, is hexafluororphosphate (PF_6^-) doped polypyrrole, using what has become legitimately the *standard deposition* of polypyrrole at the MIT BioInstrumentation Laboratory. As described below, the deposition is run using purified chemicals under controlled conditions, and yielded material has been found to produce films of uniform conductivity and morphology [6] that can be handled with relative ease, and that exhibit good, and especially reliable or repeatable actuator performance [24, 15, 6].

It was decided that the *standard deposition* onto a glassy carbon crucible would be a good starting point for the creation of long conducting polymer ribbons for use as linear actuators. Computer numerically controlled (CNC) equipment at the BioInstrumentation Laboratory was utilized in order to do proof of concept creation of long polymer ribbons with accurate and uniform physical dimensions. Attention was then diverted to mitigating a reported limitation of longer conducting polymer actuators caused by a potential drop that develops along these materials due to their finite conductivity [23, 3]. Because charge must travel along longer paths and at higher densities in linear actuators with larger aspect ratios, this resistive effect becomes responsible for the dominating time constant limiting actuation speed as these actuators are lengthened. This limitation of longer conducting polymer linear actuators was tackled by adding a nonreactive conductive layer to the polymer films. The limiting effect caused by the material's finite conductivity as well as improvements

in performance resulting from the incorporation of the conductor into the actuators are studied in detail in Section 5.3 and Section 5.4 of Chapter 5. The procedures used to achieve these advancements can be found in the chapter sections below.

3.2 Polymer synthesis

3.2.1 Standard deposition

The polymer synthesis procedure that follows is derived from a procedure developed by Yamaura and colleagues [39, 40] and enhanced by Madden and colleagues over time [15, 24, 3, 54, 6], mostly by more accurately controlling the steps and parameters of the process. It has become the *standard recipe* for producing (PF_6^-) doped polypyrrole at the MIT BioInstrumentation Laboratory.

Polypyrrole films are electrodeposited gavanostatically in a two electrode electrochemical cell onto the outer surface of a 75 mm diameter glassy carbon cylindrical crucible oriented vertically and submerged approximately 75 mm in a solution containing 0.05 M of distilled pyrrole (Sigma-Aldrich, [55]) and 0.05 M tetraethylammonium hexafluorophosphate ($TEAPF_6$) (Sigma-Aldrich) in propylene carbonate (Sigma-Aldrich) with 1% (by volume) distilled water. For the counter electrode, a concentric sheet of copper or stainless steel is used. Figure 3-1 shows a schematic of the setup used for electrodepositing polypyrrole on a glassy carbon crucible.

Prior to deposition, the solution is saturated with nitrogen by bubbling nitrogen gas through it while slowly mixing the constituents. The solution is then chilled to -40°C prior to applying current to the electrochemical cell. The deposition is generally run at a current density of 0.9 to 1.2 A/m^2 for 10 to 12 hours, and delivers a typical film thickness of 20 to 25 μm. The current is controlled by a Princeton Applied VW2 16 channel multichannel potentiostat [56], and the temperature is held steady using a Cincinnati Sub-Zero temperature chamber [57]. Figure 3-2 shows setups for two depositions ready to run simultaneously, but independently, in the environmental chamber. In the left deposition, 316L stainless steel is used as the counter electrode

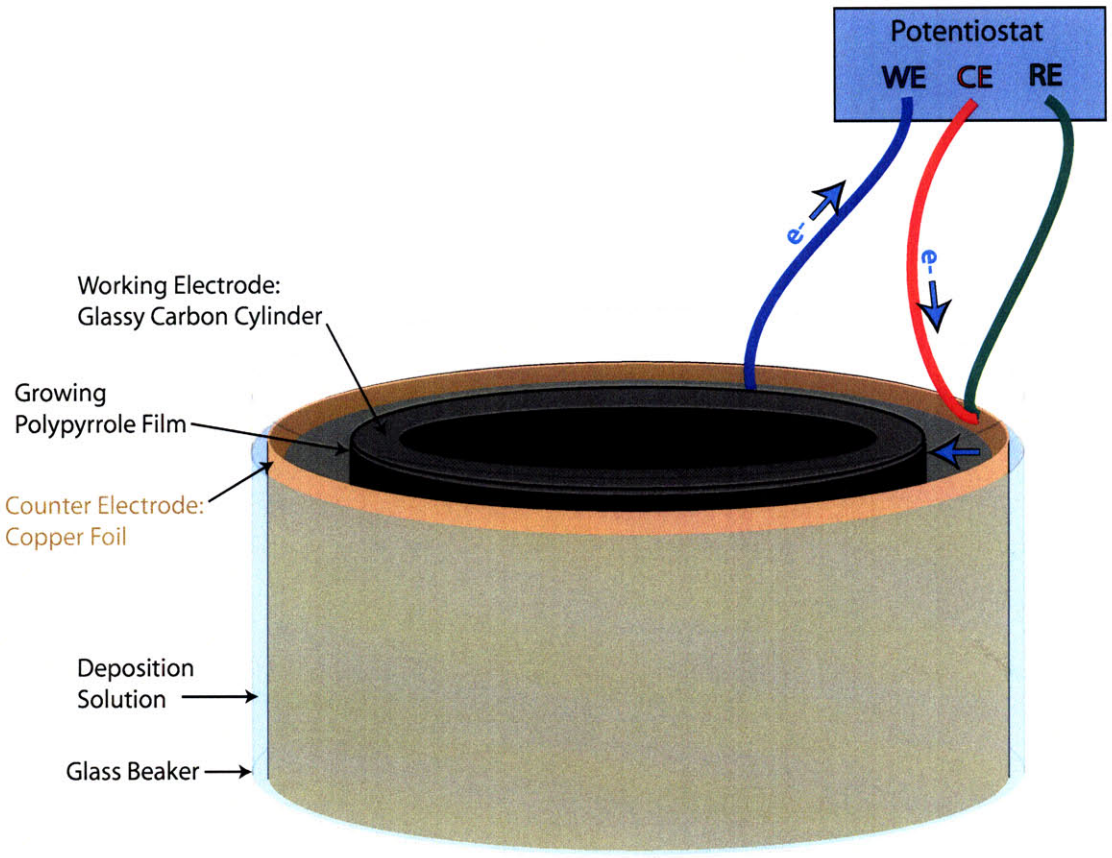

Figure 3-1: A schematic showing the setup used for electrodepositing polypyrrole films (from [6]). The electrochemical cell consists of a glassy carbon cylindrical crucible working electrode and a concentric copper foil counter electrode in a deposition bath containing pyrrole monomer, $TEAPF_6$, and water in propylene carbonate. In this two electrode configuration, the reference electrode is also connected to the metal counter electrode and a potential is applied between the two electrodes by the potentiostat in order to produce a constant current as shown. Pyrrole oxidation occurs at the working electrode, slowly building up a polypyrrole film.

material, and in the right deposition, copper is similarly used. Acetal spacers, specially designed and fabricated using laser machining, are used to accurately position the crucibles in the center of their baths, as well as keep the distance to the counter electrodes uniform. Polyimide based tape is often used to mask the upper and lower edges of the crucible in order to decrease film removal difficulties that can occur at the crucible ends.

The above parameters yield PF_6^- doped polypyrrole films with typical conductivities of 3 to 5 $\times 10^4$ S/m, an elastic modulus of about 0.2 GPa, and an ultimate tensile

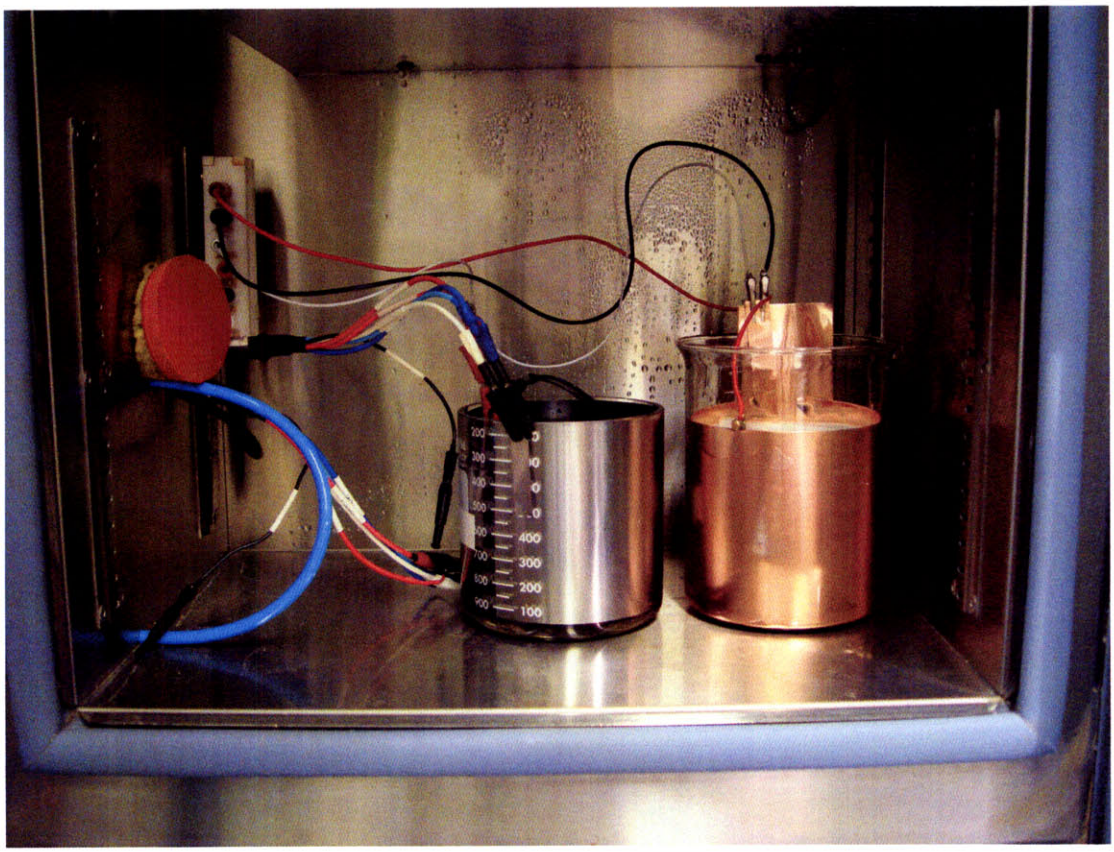

Figure 3-2: Two deposition setups are shown in the environmental chamber prior to final chilling and running the electrodepositions. The red wires are connected to the working electrode crucibles, and the reference electrodes and counter electrodes are connected to the concentric metal electrodes in a two electrode configuration, as depicted in Figure 3-1.

strength of about 30 MPa [6]. Following synthesis, the polypyrrole coated crucible is removed from the solution, rinsed with a solution of 0.05 M $TEAPF_6$ in propylene carbonate to remove any unpolymerized pyrrole monomer, and allowed to warm to room temperature. Following electrodeposition, the polypyrrole film is well adhered to the glassy carbon crucible. The film is allowed to dry in air for 24 hours or more, which causes the film to shrink or tighten up on the crucible and allows it to be more easily removed. Figure 3-3 shows the result of the deposition process.

The glassy carbon crucibles used were produced by HTW Hochtemperatur-Werkstoffe GmbH [58] using their SIGRADUR G grade material. These crucibles have a thickness of 3 mm and a resistivity of 4.5×10^{-5} Ωm [58] or a conductivity of 2.2×10^{4} S/m.

Figure 3-3: A polypyrrole film that has been electrodeposited onto a glassy carbon crucible. The top end surface of this crucible is masked with a black tape. The upper and lower edges of the crucible were masked with a polyimide tape during deposition and removed before this photo was taken, thus revealing the difference between the shiny crucible finish and the matte polypyrrole film.

The above procedure reliably produces good films. Variation in quality can occur, however. Care must be taken to properly center the crucibles in order to ensure uniform deposition. Use of the above mentioned spacers aid in this. Complete chilling of the solution to -40°C prior to applying current to the electrochemical cell will minimize cross-linking and branching of the growing polymer chains during the process, ultimately creating a more conductive and uniform film [6]. Also, the use of distilled pyrrole, kept chilled and away from light and oxygen, will give the best result. A yellowish color to the pyrrole monomer, as well as a yielded discolored polypyrrole film, as opposed to a typical solid black film, are both signs that the pyrrole may have deteriorated prior to deposition.

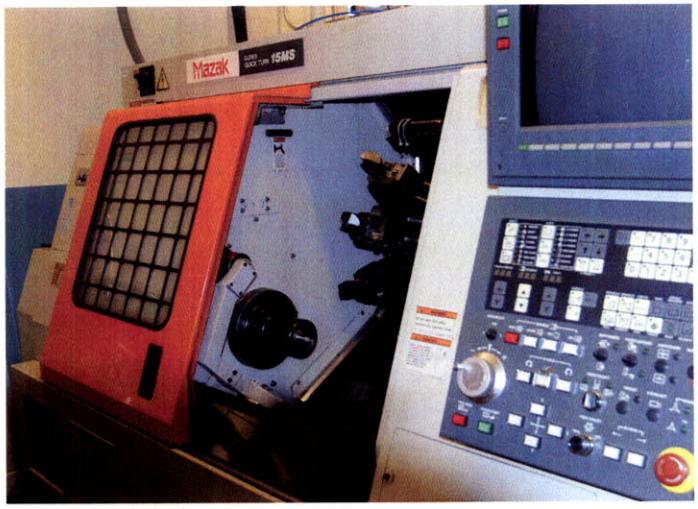

Figure 3-4: The BioInstrumentation Lab's Mazak Super Quick Turn 15MS turning center (Photo credit: Serge Lafontaine).

3.2.2 Other deposition variations

Variations to the above procedure are certainly possible, and some will produce very similar films. For example, one can change the counter electrode material. Copper and stainless steel have both been found to perform well. Glassy carbon has also been used as a counter electrode. Tetrabutylammonium hexafluorophosphate ($TBAPF_6$) can be substituted for the $TEAPF_6$ and will equally produce good films. Replacing the glassy carbon substrate at the working electrode with alternate materials like stainless steel or gold, however, normally yields films with less desirable surface morphologies [6]. It is possible that in addition to glassy carbon being inert, its limited conductivity, relatively matched to that of polypyrrole, may help homogeneously distribute charge during electrodeposition, especially at the smallest scales, and aid in producing a smooth, uniform film. When experimentation with depositions on a smaller scale is desired, smaller, flat 25 mm $\times$ 25 mm $\times$ 3 mm substrates of glassy carbon, also manufactued by HWT, have been found to work well.

3.3 Polymer slicing

Ribbons are sliced from polypyrrole that has been electrodeposited onto a glassy carbon crucible as described in Section 3.2. This is accomplished using a custom built tool mounted into a Mazak Super Quick Turn 15MS turning center (Figure 3-4) by slicing a spiral along the film in a manner similar to cutting a thread. For this task, a custom designed tool was fabricated that incorporates a straight razor blade and can be mounted onto the Mazak tool turret. The tool allows for precision angular adjustment of the razor blade in order to set it at a pitch angle that corresponds to the desired ribbon width, normally very close to 90°. The tool also incorporates springs that serve to preload the blade against the crucible during cutting, and will accommodate for any difference in the radius along the crucible or its position. This custom tool is shown in Figure 3-5.

The glassy carbon cylindrical crucible, coated with the electrodeposited polypyrrole film during polymer synthesis, is mounted horizontally onto the main axis of a Mazak turning center as depicted in (Figure 3-6) using a machined plastic receptacle that fits to one of the machine's 16C collets. The outer surface of this receptacle fits snug with the inner surface of the crucible. Tape is used to prevent the crucible from turning during the slicing operation.

A threading operation is performed on the Mazak, normally run using G-Code generated in FeatureCAM [59] in order to accurately slice the polymer into one continuous ribbon. A example of this G-Code and information on its use can be found in Appendix A. Figure 3-6 shows polypyrrole being sliced from a glassy carbon crucible in the Mazak turning center.

After running the tool over the polymer film in the prescribed spiral pattern, the resulting ribbon is still adhered to the crucible. It is removed by manually applying a small off-tangent force to the polymer in order to peel it from the crucible. The resulting ribbon is then run onto spool mounted parallel to the crucible. This spool is rotated to supply the tension required to peel the polymer from the crucible, while the crucible is appropriately rotated using the Mazak manual C-Axis controls. This

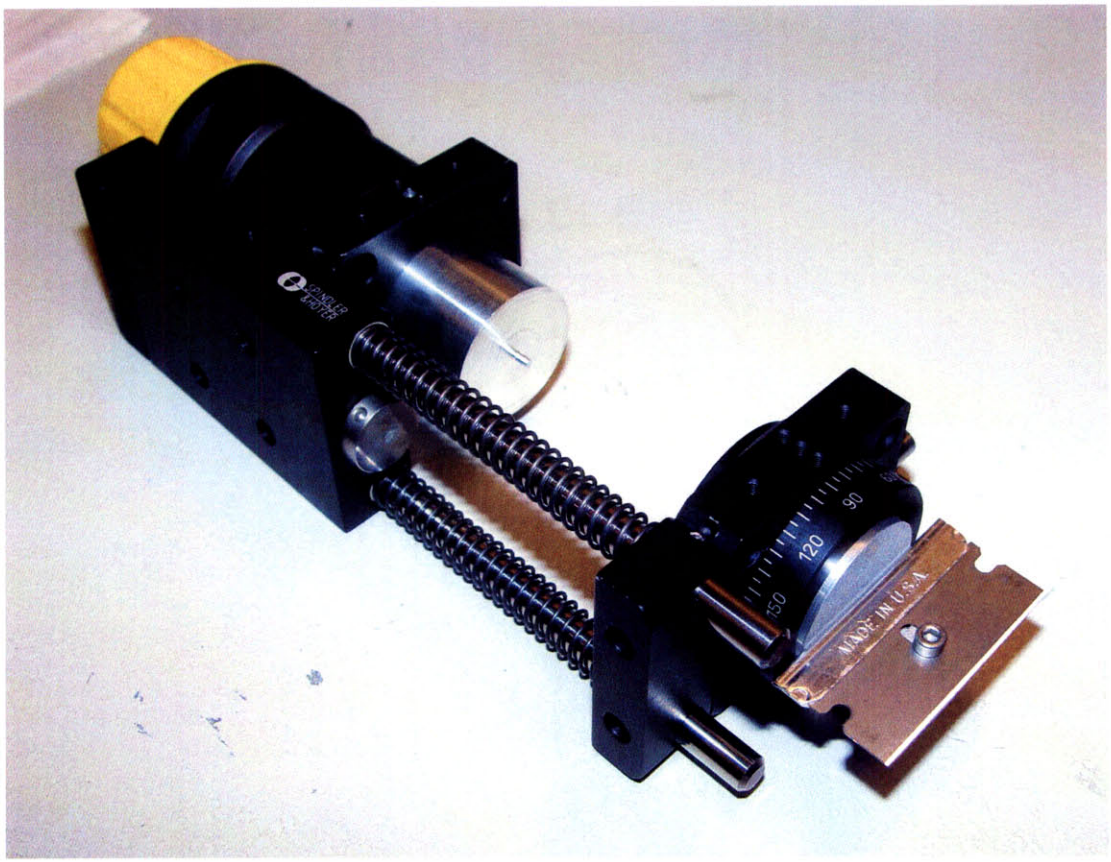

Figure 3-5: A custom built polymer slicing tool, designed to mount into the Mazak turning center.

procedure is depicted in Figure 3-7 and the yielded product is shown in Figure 3-8.

The custom tool developed for polymer ribbon production was found to be adequately stiff and to deliver the necessary preload for slicing the polymer to a range of widths. Polymer ribbons with lengths exceeding 5 m have been manufactured using this technique. The ultimate length of the yielded polymer, l, is related to the surface area of the crucible by

$$l = \frac{A}{w}, \tag{3.1}$$

where w is the desired width of the ribbon and A is the total area of the deposition, given by

$$A = \pi\, d\, h. \tag{3.2}$$

Here, d is the diameter of the crucible used and h is the usable height of the deposition

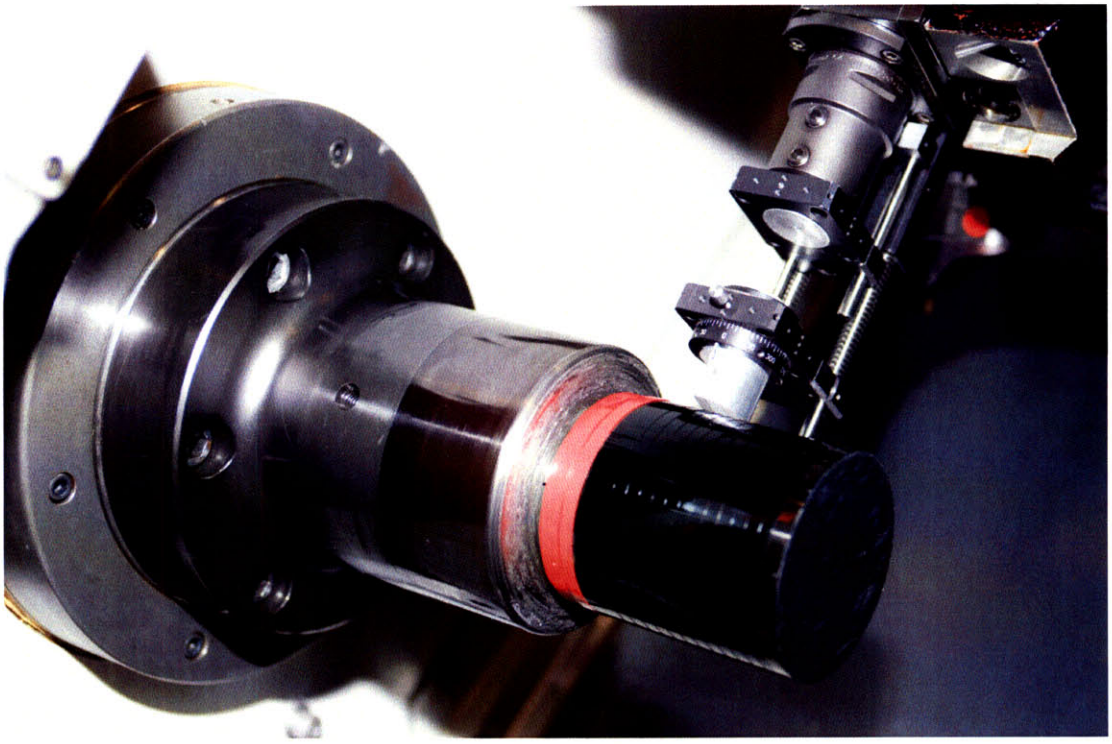

Figure 3-6: Polypyrrole is shown sliced on a glassy carbon crucible in the Mazak turning center.

along the crucible axis.

At times, it was found useful to slice single rings of polymer by setting the desired width by indexing the tool along the crucible axis, moving in the tool to apply the cutting force, and then rotating the crucible by one turn. This abbreviated procedure allows for the fabrication of ribbons of a variety of selected widths without wasting any of the deposited polypyrrole. The resulting ribbons are of course in this case limited in length to the circumference of the crucible.

Ribbons with widths as fine as 20 μm have been fabricated using the above procedure, as demonstrated in Figure 3-9 and Figure 3-10. The ribbons in this image contain a gold layer, the application of which will be discussed in Section 3.4. After slicing finer than about 0.5 mm, the ribbons become much more likely to peel during slicing and become tangled. This generally reduces the reliability of generating single or continuous long ribbons. To achieve finer continuous threads, more study of the forces at the blade-polymer and polymer-crucible is required. Further automation

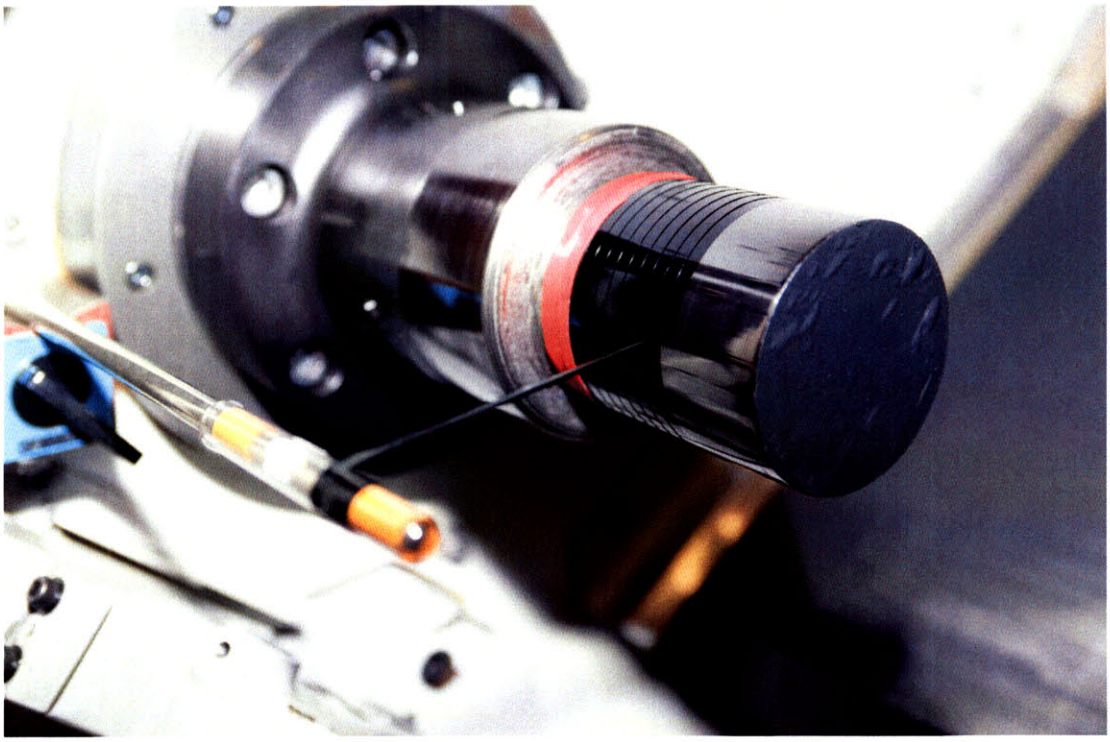

Figure 3-7: Polypyrrole is shown being removed from a glassy carbon crucible after being sliced in the Mazak turning center.

and additional hardware, perhaps to simultaneously peel the polymer while cutting, could also help extend this process to finer widths.

3.4 Conductor incorporation

As the length of a conduction polymer ribbon is increased, so is its resistance. When a voltage is applied at one end of a conducting polymer ribbon, where its length is significantly longer than this width, a voltage drop appears along the ribbon. This ohmic voltage drop has the effect of slowing actuation, and is discussed in detail in Section 5.3. A process has been developed in order to reduce this effect. The process includes the incorporation of a nonreactive conductive layer into the film. Electroplating was explored as a deposition method to achieve this layer, and was found to work well. Gold was chosen for this layer due to its nonreactive nature, high conductivity, and its ability to be electroplated evenly at small thicknesses.

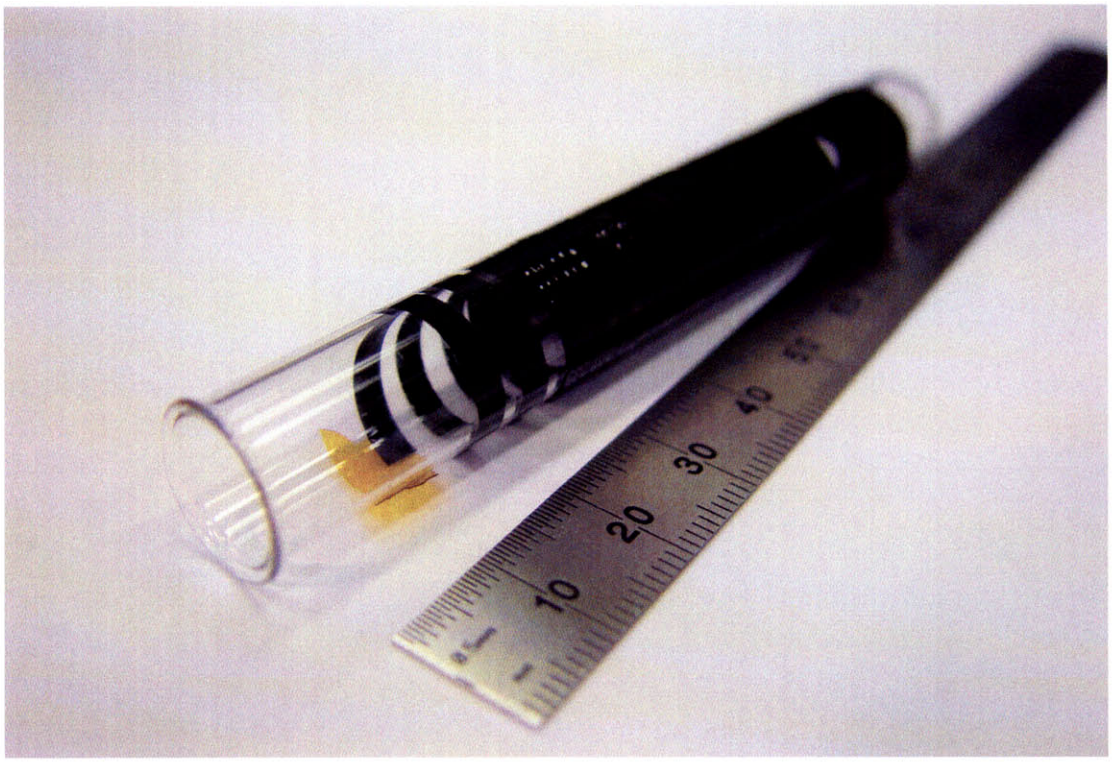

Figure 3-8: A 3 mm wide polypyrrole ribbon is shown wound around a test tube.

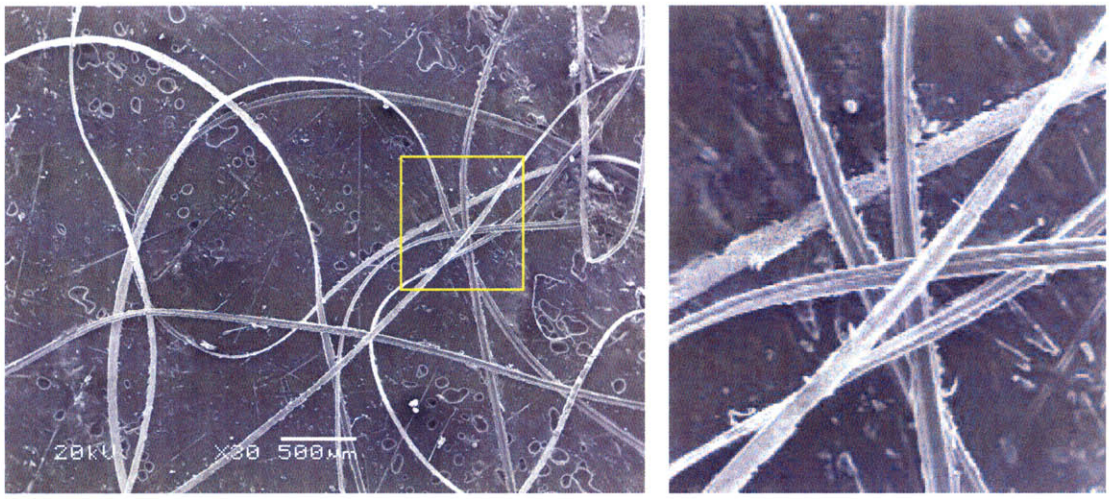

Figure 3-9: SEM images showing gold backed polypyrrole ribbons sliced to about 50 μm. The right image is a zoom in of the area in the highlighted rectangle (Images by Nate Wiedenman).

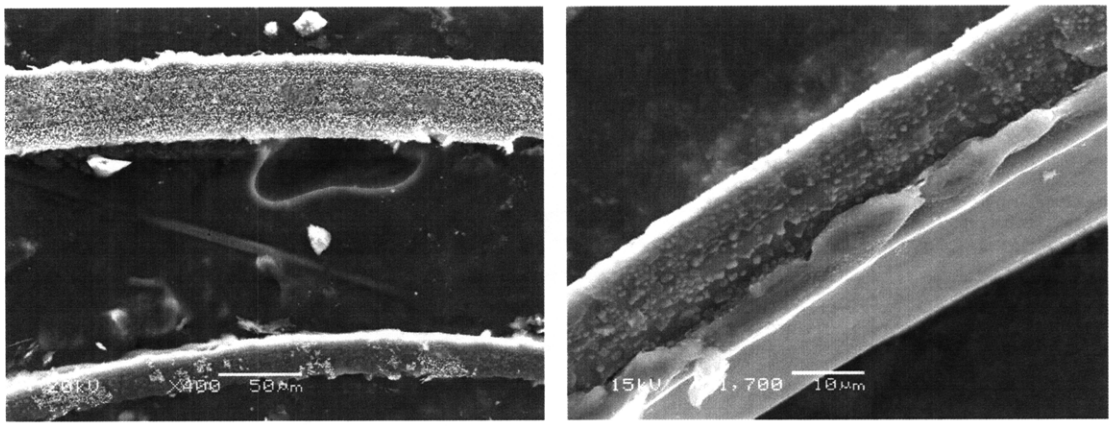

Figure 3-10: SEM images showing gold backed polypyrrole ribbons sliced to about 50 μm. The gold layer can be seen in the left image, and the cut edge can be seen in the right image (Images by Nate Wiedenman).

The conductor deposition process is run prior to polymer electrodeposition. A cleaned and spotless glassy carbon crucible is placed in an electrochemical cell with a geometry identical to that used for polymer electrodeposition. Again the glassy carbon crucible serves as the working electrode, and a concentric 316L stainless steel foil is used as the counter electrode. A ready made neutral non-cyanide gold plating solution, Techni Gold 25 ES RTU, was chosen. The plating solution is manufactured by Technic, Inc. [60], and is designed to yield soft pure gold deposits suitable for electrical applications. The deposition is run galvanostatically with the crucible as the working electrode, but this time negative with respect to the stainless steel counter electrode. Usually when electroplating, an activator or strike deposition is used to increase adhesion of the thicker outer deposited layer. It this case, however, it is desirable that the deposition is not strongly adhered, and is therefore run alone. The inert and smooth glassy carbon substrate also aids in reducing the adhesion of the gold layer. Figure 3-11 shows a glassy carbon crucible that has been electroplated with gold.

Custom made acetal spacers were used during the electroplating process to ensure the concentricity of the crucible and the counter electrode during deposition. The deposition is normally run at a constant current of 10.75 A/m^2 (1 ASF), which corresponds to 190 mA for a 75 mm diameter crucible with 75 mm submerged. This

Figure 3-11: Glassy carbon crucible that has been electroplated with gold prior to being electrodeposited with polypyrrole.

current density leads to a calculated deposition rate of 3.79×10^{-10} m/s. The first depositions were run for 3 to 12 minutes, giving thicknesses of 68 to 270 nm. Following the deposition, the crucible is dipped in a beaker of distilled water as a rinse, allowed to air dry, and then used in the polymer electrodeposition process as discussed in Section 3.2. Care is made not to contact the gold layer, as it will easily rub off the crucible.

The gold layer was found to adhere very strongly to the electrodeposited polypyrrole. The gold layer appears integrally bonded to the pyrrole and peeling of gold from the polypyrrole has never been observed. It is interesting that the polymer electrodeposits, or *grows*, so well on the gold layer, even though growing on solid metal films yields less desirable films [6]. The electrodeposition essentially occurs as if the gold layer was not present. Figure 3-12 shows gold backed polypyrrole ribbon actuators partially removed from a glassy carbon crucible.

It has been observed that the gold backed polymer ribbons are much less adhered to the glassy carbon crucible following the polymer electrodeposition. This allows the

Figure 3-12: Gold backed polypyrrole ribbon actuators partially removed from a glassy carbon crucible.

ribbons to be removed more easily, with less force (possibly no force) being required to peel them from the substrate, thus often delivering a better quality product and larger yield. Because the gold layer effectively acts as a releasing agent, this method opens the door for reliably manufacturing much thinner free standing films than was previously possible, since removal of those films after deposition was a prohibitive logistical challenge to their use. Figure 3-13 shows gold backed polymer ribbons after they were removed from the glassy carbon crucible.

3.5 Next steps

3.5.1 Larger scale

Figure 3-14 shows larger crucibles that enable the creation of larger polymer films using the method described above. For the generation of more film in general, batch processing can be applied. The longest step in the overall fabrication process of these ribbons is by far the electrodeposition of the conducting polymer. By batch processing

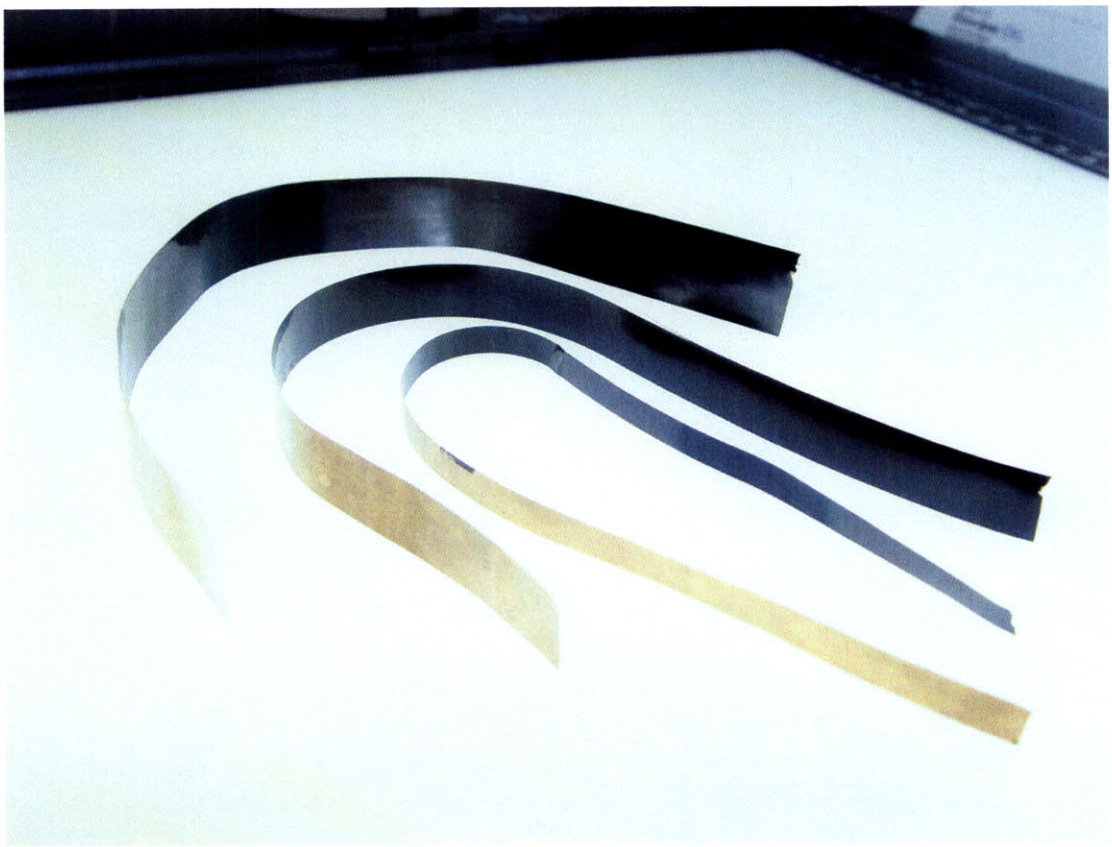

Figure 3-13: Polypyrrole ribbons with a well adhered gold layer.

Figure 3-14: Larger crucibles that enable the creation of longer conducting polymer ribbons.

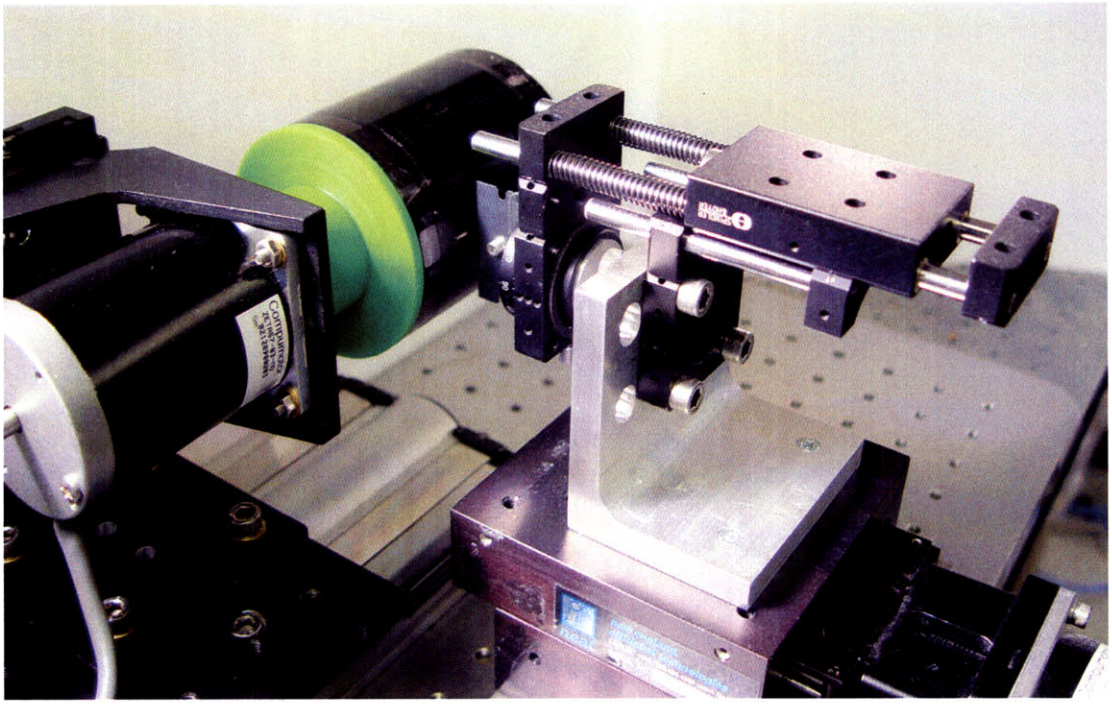

Figure 3-15: A stand alone polymer slicing machine. Conducting polymers are sliced from the glassy carbon crucible shown mounted horizontally.

several crucibles simultaneously, much more polymer could be created simultaneously.

3.5.2 Further automation

The Mazak turning center has been shown to be a useful tool for creating polymer ribbons. It's ability to accurately and stiffly produce the desired spiral pattern enabled the ribbons to be created accurately. It may be desirable, however, to create a stand alone machine dedicated and optimized for creating these ribbons. Figure 3-15 shows such a stand alone machine. The machine, which includes stepper motor driven precision stages, provides an experimental platform that can be more easily accessed when trying new techniques or optimizing the slicing tool. It is hoped that a polymer removal device can be added to this setup in order to more reliably create ribbons of small width (micrometers) and long length (meters). This setup can also be used in manual mode to produce ribbons of constant width.

3.5.3 Additional approaches

For many applications, it is desirable to achieve a final ribbon that has polypyrrole on both sides of the conducting layer. This could be achieved by modifying the processes above in a number of ways. First, two gold backed ribbons could be used back to back, either bonded together somehow, or perhaps not. A second option is to follow the final removal of the gold backed polymer with a second polymer electrodeposition process. The deposition could be allowed to proceed on both sides of the film (the gold and polypyrrole sides), or the polypyrrole side could be masked, perhaps with temporary tape, or perhaps with an encapsulant such as silicon. Or, the electrodeposition could be conducted in an electrochemical cell where the geometry strongly favors a deposition on the gold side of the ribbon. A third option is to lay down the conducting layer on top of a previously deposited polymer layer. This could be done by electroplating or sputtering, for example. Some attempts were made at electroplating onto pyrrole, but the chemistry of the plating solutions used proved problematic.

Laminated, stacked, or fused parallel linear actuators are of interest, especially when large forces are desired. Parallel actuation will be discussed in more detail in Chapter 5. To achieve bonded multilayer actuators, ionic reservoir layers are required. The use of gel layers, similar to those used in the layered actuators discussed in Chapter 2, may be advantageous. Another option is the use of layers of mesh, ether elastic enough to not strongly effect actuation, or machined with a geometry that allows for the required movement. Nylon meshes were successfully used in some of the devices in Chapter 5 to separate the working and counter electrodes.

3.5.4 Additional materials

Electroactive polymers, such as polypyrrole, require an ionic reservoir to supply the ions required for actuation. For this reason, these actuators are characterized in an electrolyte bath. When these actuators are applied to a system, the bath must be incorporated as well in some form. For some applications, adding a capsule or channel

to hold the electrolyte is acceptable. For many applications, however, it is advantageous to have an actuator that is encapsulated in a way that preserves more of the actuator's properties, or advantages, like its compactness and mechanical flexibility. Some limited investigation of possible encapsulation methods was undertaken.

One promising encapsulation material is silicone. Silicone can be made very leak proof, and it comes in a variety of formats and durometers. It can also be molded in place, into a desirable shape, or made to adhere to another material. One promising moldable encapsulant is Loctite Superflex Blue RTV Silicone Adhesive Sealant 30560 [61]. This silicone based material has an elastic modulus much less than that of polypyrrole and would not impede the actuation of the polymer if incased inside. Figure 3-16 shows a gold backed polypyrrole ribbon encapsulated in this material. For actuation, a nylon mesh spacer would be used to separate the working and counter electrodes, a technique that appears in some the devices in Chapter 5.

Experimentation was also done on silicone elastomers with durometers in the 10 to 20 Shore A range. It is envisioned that these could provide backing for one or both sides of an encapsulated system. These elastomers can also be used to provide force. A ribbon of this material is used to produce the restoring preload force in an application described in Section 6.5.

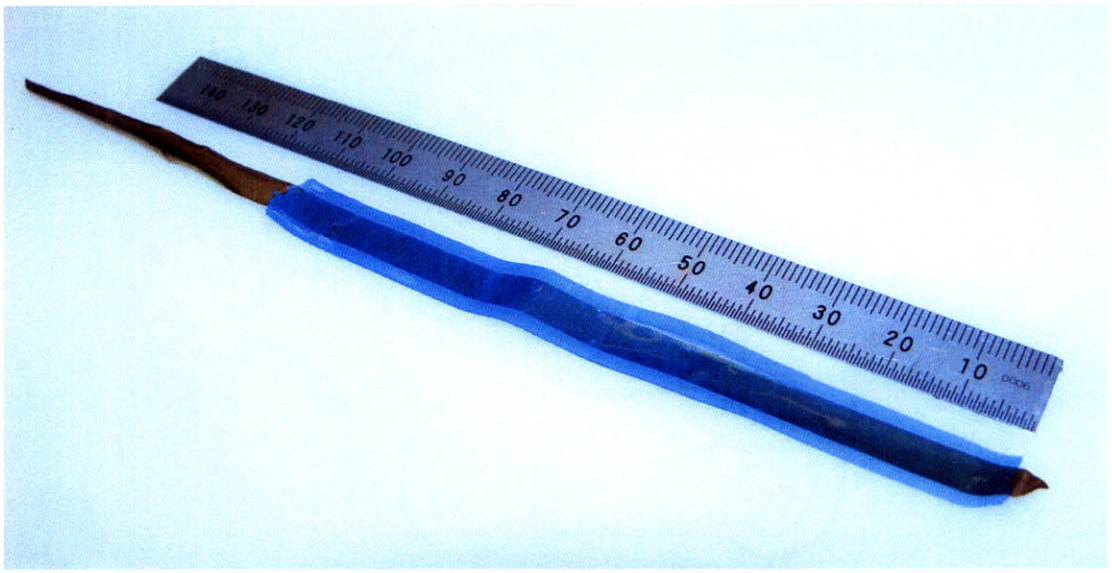

Figure 3-16: A gold backed polypyrrole ribbon is shown encapsulated in a molded silicone sheath.

Chapter 4

Actuator characterization

4.1 Introduction

Although conducting polymers undergo a change in volume as a result of ingressing and egressing ions, when loaded uniaxially they can be considered a translational actuator. Conducting polymer linear actuators are characterized by their generated active stress, active strain, strain rate, work capacity, and efficiency [7]. Characterization is generally performed in a two input two output system. Either the voltage is controlled and the current is measured, or the current is controlled and the voltage is measured. And likewise, either the stress on the actuator is held constant and the strain is measured, or the strain is held constant and the stress is measured. Because of the simultaneous control required, characterizing of conducting polymer films is best done with precise, specially designed instrumentation.

4.2 Basic film characterization

4.2.1 Dimension measurements

Although determining length is perhaps the most basic of measurements, it is not so simple with conducting polymer based materials. In fact, it can potentially be a large source of error. Conducting polymers, such as polypyrrole swell, shrink, shrivel,

and stretch depending on moisture content, ion content, oxidation state, and loading. All three linear dimensions can be problematic, and unfortunately the accuracy of these measurements are reflected directly in the calculated actuation properties. For example, the measurements of width and thickness will effect the cross sectional area of the polymer, and therefore the calculated passive stress imposed on the polymer as well as the active stress exhibited by it during actuation. Similarly, the measured length of the actuator forms the basis of the calculated active strain.

4.2.2 Conductivity measurements

Conductivity measurements are normally performed with a four point measurements system. N. Vandesteeg has a thorough review of four point measurement techniques in his PhD thesis [7].

4.3 The EDMA

The EDMA, or electrochemical dynamic mechanical analyzer, is an invaluable tool in the characterization of electroactive materials, including conducting polymer actuators. A typical DMA, or dynamic mechanical analyser, allows one to perform a variety of experiments in order to obtain stress-strain curves for materials, while the additional electrochemical component allows one to investigate a material's electroactive response given controlled electrical inputs.

The EDMA used to perform the characterization in this chapter was fabricated by N. Vandesteeg and B. Schmid of the MIT BioInstrumentation Laboratory [7, 22]. The instrument, shown in Figure 4-1, has been used extensively in the investigation of materials at the BioInstrumentation Lab [7, 6, 62]. The EDMA consists of an array of instruments which are simultaneously controlled by custom software to bestow electrical and mechanical inputs on a material, while outputs are measured on the materials. All of the information is logged for later study and analysis. For example, one is able to hold a material at a given stress

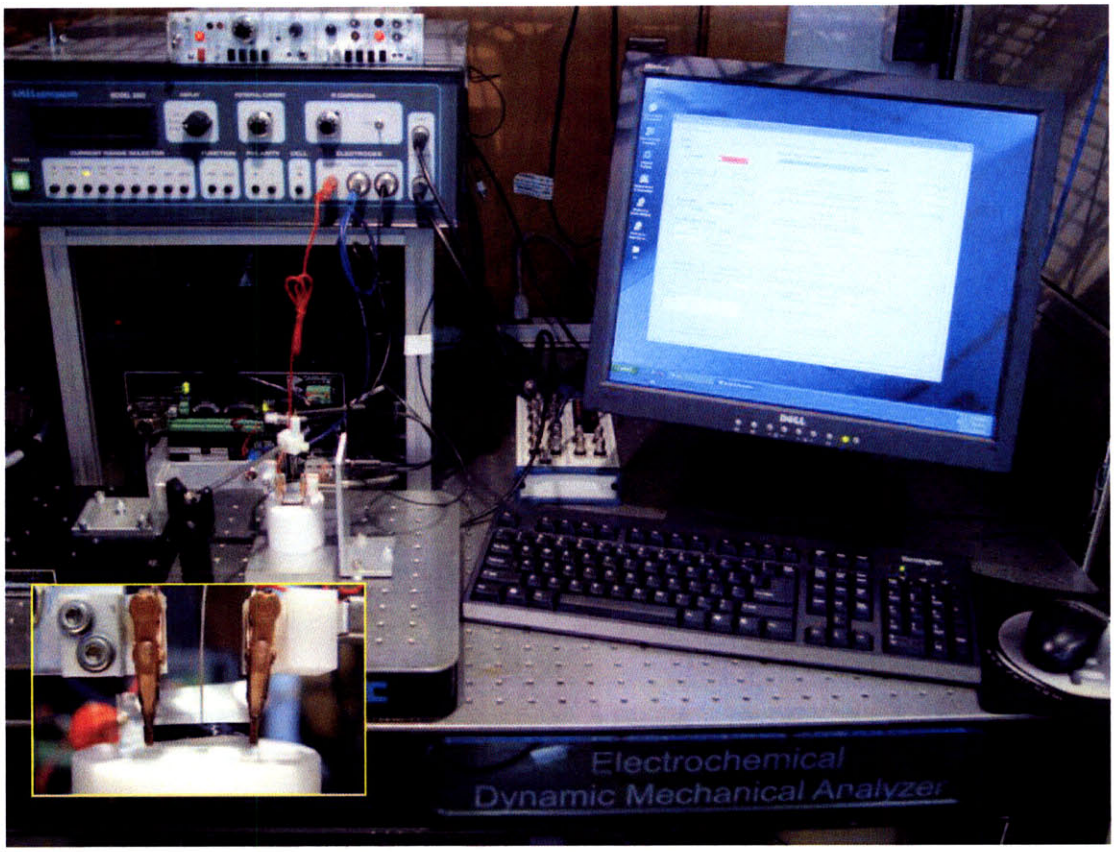

Figure 4-1: The electrochemical dynamic mechanical analyzer (EDMA) used for characterizing conducting polymer actuators (from [7]).

4.3.1 The potentiostat

As shown in the schematic in Figure 4-2, the potentiostat utilizes three electrodes: a working electrode consisting of the polypyrrole film held by and electrically to gold coated claps, a reference electrode consisting of a silver wire, and a counter electrode, most often consisting of a stainless steel film. All three electrodes are connected by copper wire to their corresponding potentiostat terminals. The function of the reference electrode is to reduce the resistance drop related to the solution.

Often overlooked is the potential that is occurring at the counter electrode. The use of a reference electrode lets one largely neglect the effect of the bath geometry, including the shape, size, and location of the counter electrode. These are important parameters, however, especially when considering the design of a stand alone device.

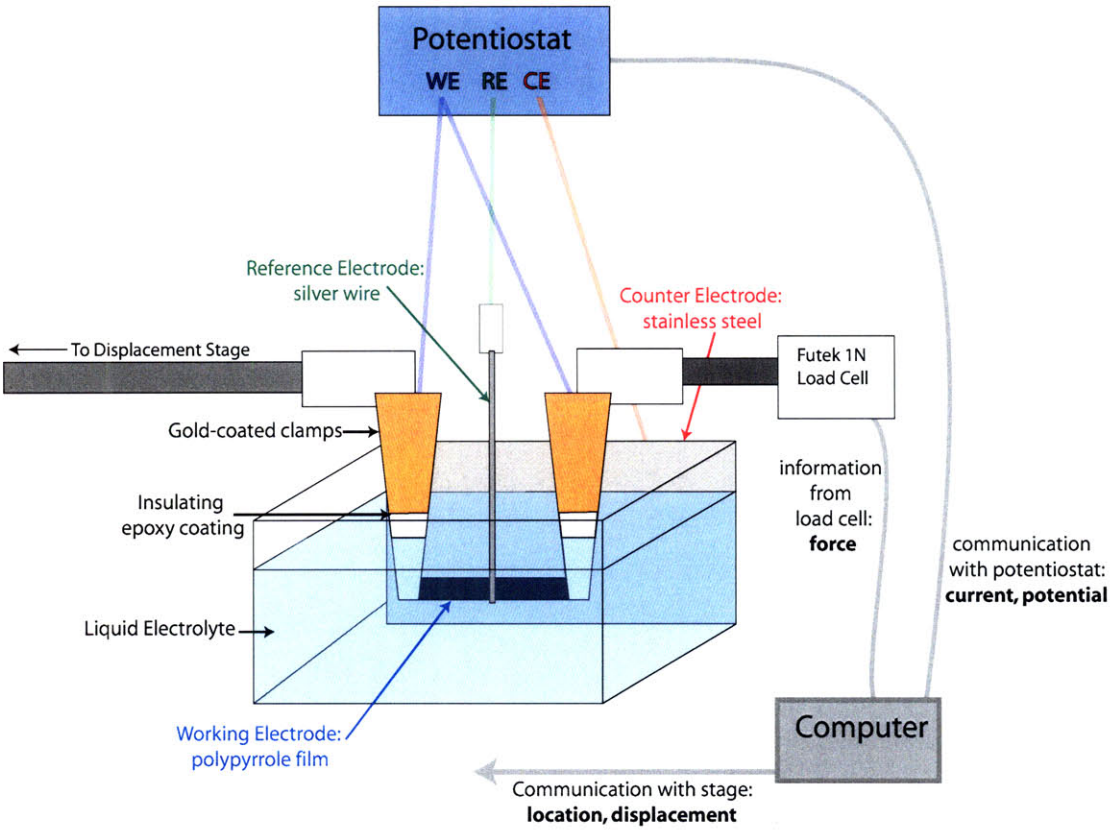

Figure 4-2: Schematic of the electrochemical dynamic analyzer (EDMA) used for characterizing conducting polymer actuators (from [6]).

4.3.2 Preloading the actuator

The EDMA includes a Futek load cell in line with the polymer film under test. As mentioned above, the EDMA can be used in isotonic or isometric mode.

For a conducting polymer actuator under constant load, the active stress, ϵ, produced as a result of ion movement is given by

$$\epsilon = \alpha \rho, \tag{4.1}$$

where α is the strain to charge density ratio and ρ is the charge density of the material. The above equation shows that monitoring the charge flowing in and out of the system (the electrical current) one can indirectly measure the polymer's strain.

By preloading the actuator isotonically, this becomes

$$\epsilon = \sigma/E + \alpha\rho, \tag{4.2}$$

where σ is the stress imposed on the film, and E is the elastic modulus of the polymer.

4.3.3 Typical operation

Conducting polymers require *warmup* cycles in order to ensure that their measured properties can be accurately compared [6]. Failure to adequately warm up a conducting polymer film can lead to misleading data. This procedure normally consists of cycling the film slack with a 0.1 V/s, ±1 V triangle wave. Figure 4-3 shows a 28 mm gold backed film subjected to 15 cycles. The warmup in Figure 4-3 is shown to be incomplete. Figure 4-4 shows the completion of the warmup cycling. The plot follows a repetitive pattern.

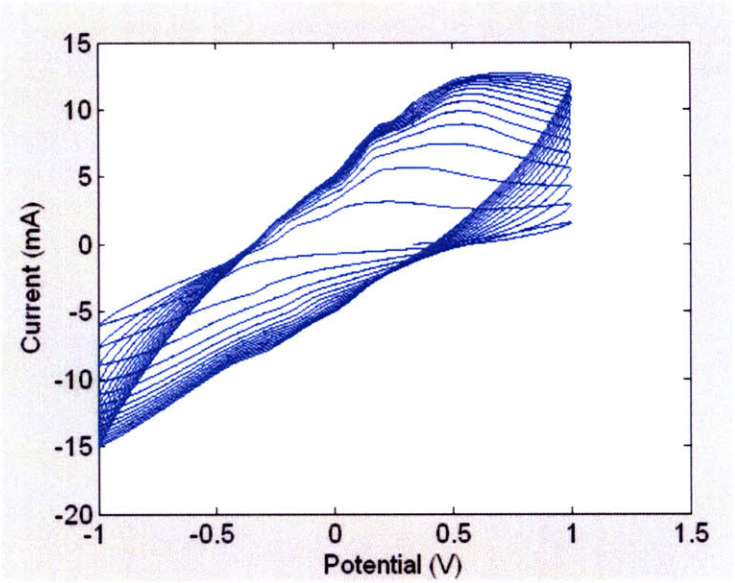

Figure 4-3: Data showing a a 28 mm gold backed polypyrrole subjected to a 0.1 V/s, ±1 V triangle wave warmup. This data shows incomplete warmup cycling.

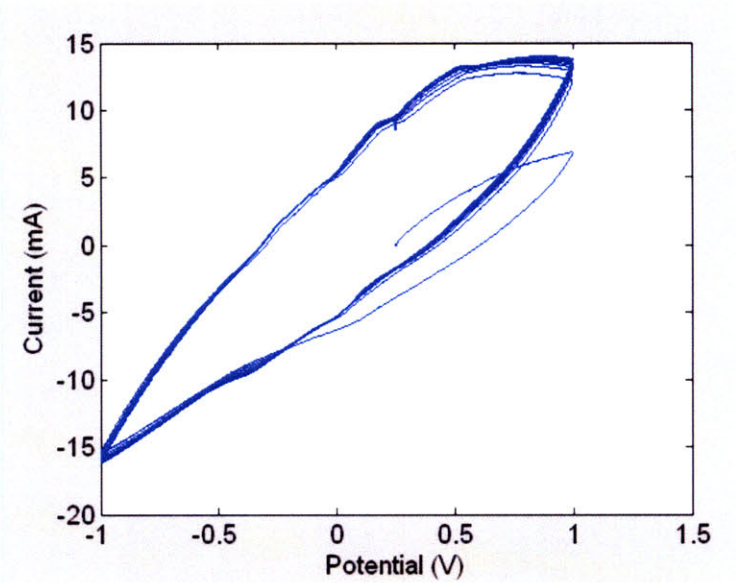

Figure 4-4: Data showing a a 28 mm gold backed polypyrrole subjected to a 0.1 V/s, ±1 V triangle wave warmup. This data shows complete warmup cycling.

4.4 Actuator electroactive response

A typical electroactive response obtained with the EDMA is shown in Figure 4-5. The preload in this data is compensating a little slowly due to chosen settings relating to the EDMA force feedback, but significant strain is demonstrated nonetheless. The actuation was performed in a $BMIMPF_6$ bath with a silver wire reference electrode. In this experiment, a voltage square wave, referenced to the silver reference electrode, was inputted on the two clamped ends of a gold backed polypyrrole film held under tension at approximately 2 MPa. The current, charge, and strain were recorded along with the voltage and the stress imposed on the film.

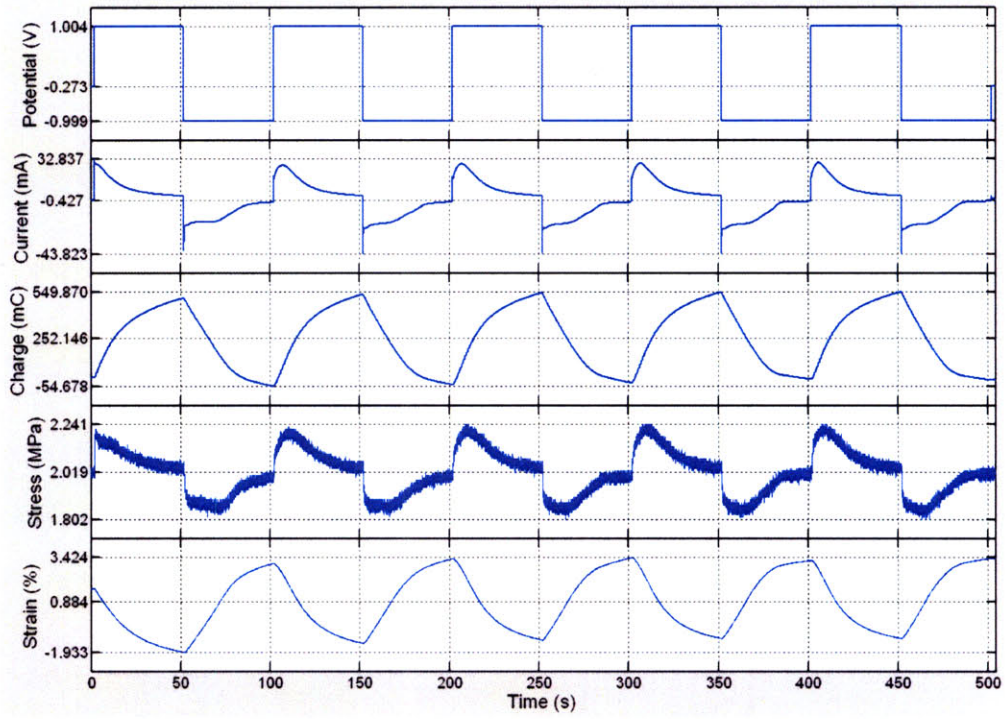

Figure 4-5: Electroactive response of a 28 mm gold backed polypyrrole linear actuator measured with the EDMA in isotonic mode.

Chapter 5

Actuator advancements

As mentioned in Chapter 2, scaling conducting polymer linear actuators to macroscale devices comes with a set of challenges. This chapter explores these challenges in more detail. First, the differences in reporting material properties and actuator capabilities are discussed. Next, the challenges of scaling these actuators are discussed in detail. The significance of the material's finite conductivity is explored and characterized. A multipoint measurement apparatus developed for this task is described. Experiments and results performed on polypyrrole and gold backed polypyrrole ribbons are then discussed. Attention is then brought to key improvements in actuator performance: Increased displacement output, increased actuation speed, and increased force output. Several testing platforms and example devices are described in order to support this discussion.

5.1 Introduction

The characterization techniques highlighted in the previous chapter provide valuable tools for evaluating new conducting polymer based materials for use as actuators. Additionally, they allow one to hone in on qualities of the films that are beneficial for actuation, as well as parameters that allow those films to be used to their fullest potential. Just as these techniques prove valuable for the characterization of smaller films, so do they in the characterization of larger *macroscale* actuators. That is,

actuators that exhibit actuation discernable by direct human measurement such as the naked eye. The ability to simultaneously and accurately measure and control the electrical inputs to the actuated material, as well as its position, or strain, and its preloaded force, or stress, is invaluable in constructing larger systems that use or are made up of these materials. Additionally, the force feedback system of an instrument like the EDMA allows one to use an ideal load for initial testing, and by using a high performance stage, friction is effectively eliminated from the system. Friction, preload, and other challenges common in stand alone devices are discussed in Chapter 6.

A goal of the work reported in this thesis is to increase the performance of linear conducting polymer actuators. Of particular interest are improvements in the outputted force, displacement, and speed of the actuators. These outputs relate to corresponding actuator and material properties reported in the literature as active stress, active strain, and strain rate. Normally, material properties are measured using specialized or custom instruments like the EDMA described in Section 4.3. If one assumes a uniform material that behaves identically throughout, one can move from these material properties to the more directly measurable values with size dependant units. For example, the displacement output or stroke of an actuator, d, is related to the material's active strain ϵ and its length, l, by

$$d = \epsilon\, l. \tag{5.1}$$

Likewise, the force outputted by a conducting polymer actuator, f, is related to its active strain, σ, and its cross sectional area, A, by

$$f = \sigma\, A, \tag{5.2}$$

where its cross sectional area is calculated from its width, w, and thickness, t, using

$$A = w\, t. \tag{5.3}$$

Interestingly, the dimensionless material and actuator properties more often reported are calculated from the physical measurements made using a load cell or a linear encoder, for example, by programmed instrumentation software. Equations for the active strain, ϵ, and active stress. σ are

$$\epsilon = \frac{d}{l}, \tag{5.4}$$

and

$$\sigma = \frac{f}{A} = \frac{f}{w\,t}. \tag{5.5}$$

In practice, approximations are often made in obtaining and using these values. For example, active stress is often calculated using Equation 5.4 with a cross sectional area calculated from the width and thickness values measured when the film was dry and unloaded. Similarly, active strain is often calculated using Equation 5.5, where the length of the polymer is taken at the beginning of its stroke, perhaps at its most contracted position. Additionally, these calculations are dependant on the measured sample dimensions, which, as discussed in Section 4.2, can be somewhat difficult to obtain accurately and edge effects are effectively averaged into these calculations. For example, if the clamping of the ends of the sample under test restricts actuation in the region around the mechanical clamps, the overall displacement upon actuation is reduced. This would lead to calculated strain value that is less than is produced away from the mechanical clamps.

It is important to distinguish between two important challenges: to improve the material properties of conducting polymer actuators, and to increase the output potential of the fabricated actuators. Although related, the former challenge does not include a context of scale, and challenges that will need to be addressed upon applying the actuators are not included, while the later challenge confronts the limitations of the materials and actuators head on. The difficulties in their application at the macroscale are effectively included in the measured data. Because of this, and because the physical measurement data (displacement, force, and speed) can be considered more accurate than the derived material properties, it is these data that are empha-

sized below. And, above all, it is these physical output capabilities that are of primary concern for the engineer planning to use these actuators in a target application.

5.2 Scaling challenges

Increasing the useable dimensions of manufactured conducting polymer films is a significant advance toward their widespread use. Even with very high degree of material uniformity, challenges exist in applying these longer actors in physical devices. When approaching an application where linear conducting polymer actuators are being considered, it is easy to fall into the trap of extrapolating a finding, such as a measured or reported active strain of say 2% or a strain rate of 2%/s derived from a small sample under test, to a desirable larger actuator more suitable for the particular application. Although applying Equation 5.1 and Equation 5.2 can give a first approximation, the reality is scaling conducing polymer actuators is not so simple, and these calculations can be misleading, especially as longer and longer actuators are considered.

In increasing the size of the actuators, several significant issues become more pronounced and must be considered. For example, if an electrical connection is made at a single end of a polymer strip, the sizeable resistance of the polymer causes an ohmic potential drop along the length of the polymer which impacts its performance as an actuator [3, 12, 23, 26, 11]. This effect is of increased importance for longer films. Additionally, as an actuator is made wider, nonlinear effects such as rippling across a ribbon in tension are increased. Also, because strain rate is related to the diffusion of the ions into and out of the polymer, it is impacted by the thickness of the polymer [3, 12, 4, 1]. Thicker films tend to move more slowly. The ability to tension and manually adjust the polymer in response to swelling and creep also plays a larger role at the macroscale, although it is a problem that must be addressed whenever applying a conducting polymer based actuator. In order for polypyrrole and similar actuating polymers to be readily used as macroscale engineering components, the above issues need to be addressed. The remainder of this chapter focuses on improving the output properties of polypyrrole based linear actuators by focusing on

shortening two limiting time constants: One related to the actuator's length, and one related to the actuator's thickness.

5.3 Finite conductivity

Although polypyrrole is considered conductive, its conductivity is of course finite. A typical conductivity measured for polypyrrole is 5×10^4 S/m [6], corresponding to a resistivity of 2×10^{-5} Ωm. For comparison, gold has a conductivity of 4.5×10^7 S/m, corresponding to a resistivity of 2.2×10^{-8} Ωm [63]. When a conducting polymer, such as polypyrrole, is used as a linear actuator, it is loaded along its length by means of two mechanical connections. Electrical connection is normally made at one or both ends of the polymer ribbon. Upon actuation, the finite conductivity has the effect of creating a voltage drop along the film.

The diffusive elastic model (DEM) [24, 46, 3, 12], reviewed in Section 2.2, has been shown to work well in predicting actuation of smaller linear actuators [24, 46], or perhaps more correctly for actuators of an appropriate aspect ratio and actuation time scale. Am important assumption made in the DEM is that an identical electrical potential exists throughout the polymer film. That is, the entire polymer bulk will see the driving potential simultaneously. This assumption no longer holds as the conducting polymer actuator's aspect ratio is increased; that is, as its length is made significantly longer than its width. This lengthening of the polymer film has the effect of increasing the its resistance.

The resistance, R, at location x along a homogeneous polymer ribbon is given by

$$R(x) = \int \frac{1}{A\sigma} dx, \tag{5.6}$$

where A is again the cross sectional area, and σ here refers to the polymer's conductivity. It follows therefore that the resistance along the length of a linear actuator connected at one end is given by

$$R = \frac{l}{A\sigma}, \tag{5.7}$$

or

$$R = \frac{l}{w\,t\,\sigma}, \tag{5.8}$$

where w, t, and l are again the actuator width, thickness, and length, respectively. Note that the resistance can also be expressed using the polymer's resistivity, ρ, by

$$R = \frac{\rho}{A}, \tag{5.9}$$

or

$$R = \frac{\rho}{w\,t}. \tag{5.10}$$

Note that in the above equations, the resistance is measured from the polymer's electrical connection point along its length. During actuation, current flows into or out of the polymer, and this resistance will lead to a voltage drop, V, at distance x along the actuator [3] given by

$$V_{Drop}(x) = \int \frac{I(x)}{A\,\sigma} dx. \tag{5.11}$$

Upon inspection of Equation 5.11, one sees that the voltage drop can be reduced by either increasing the conductivity of the film (or equivalently reducing its resistivity), by increasing the cross sectional area of the film, by decreasing the film's length, or by reducing the current required of the film. Changing any of these variables, however, will have an effect on actuation, and tradeoffs will invariably need to be considered. For example, if the cross sectional area is increased by adding to the actuator's thickness, the time constant relating to the diffusion of ions into the polymer will be made longer and at some point will dominate. Likewise, the current and length of the actuator are normally chosen in order to produce a required maximum output, in which case the driving voltage, and therefore the required current can be considered a requirement. Increasing the conductivity of the actuator is certainly of interest, but in doing so one must consider the effects on the actuator's stain to charge density ratio, as well as its elastic modulus and overall morphology.

The voltage drop along longer conducting polymer films is significant because it

limits actuation speed. For a conducting polymer actuator, charging rate is directly related to actuation rate. And, as was discussed in Section 2.2, the charging rate of a conducting polymer is controlled by the diffusion of ions into the bulk polymer. This diffusion is governed by a concentration gradient through the polymer bulk, and is ultimately determined by the concentration of ions at the polymer double layer. The concentration of ions at the double layer (or at the polymer/electrolyte interface) is dictated by the voltage potential at the double layer at that location. The net effect of the voltage drop mentioned above is that the concentration at the double layer is proportionally reduced with this voltage, thus reducing the charging rate and actuation rate of the polymer. For longer conducting polymer linear actuators, the effect of this voltage drop can be quite limiting. For example, Della Santa *et al.* reported that only the first 30 mm of their conducting polymer actuators contracted [26, 11].

5.4 Multipoint measurement experiment

5.4.1 Introduction

Experiments were performed in order to characterize linear actuators manufactured using the methods of Chapter 3, including ribbon actuators fabricated to include an incorporated gold conducting layer. In characterizing conducting polymer free standing films, even when using specialized instrumentation such as the EDMA, it is rare that one measures (or at least reports) voltages other than the waveform used to stimulate the film via the potentiostat. In this case, however, a series of measurements were made along the polymer films in order to investigate how the inputted voltage potential is propagated along conducting polymer films of significant length. These experiments are similar to some performed by P. Madden and reported in his PhD thesis [3], but they build substantially on his procedure by utilizing a larger and more precise testing apparatus, by simultaneously measuring more points along the films, and by running experiments over longer time frames and voltage ranges.

5.4.2 Experimental setup

An experimental apparatus was created in order to perform 16 simultaneous measurements along conducting polymer ribbons as they are subjected to controlled voltage waveforms. The apparatus uses sixteen 0.250 mm diameter titanium wires (99.7%, metals basis, Alfa Aesar [64]) to sense voltages at an even spacing of 12.5 mm along a polymer ribbon as a waveform is applied at one or more of the wires via the EDMA potentiostat (AMEL Model 2053) mentioned in Section 4.3. The experimental setup is shown dismantled in Figure 5-1 and assembled in Figure 5-2. The base of the apparatus is a fabricated acrylic bath, created by laser cutting a acrylic plate to achieve the two desired pieces and then bonding them together by epoxy. The top plate is similarly fabricated of acrylic and has groves cut into the sides that are used for aligning the titanium wires. The wires are held in place with polyimide tape. A stainless steel (316L) ribbon is positioned at the base of the rectangular bath, and is used as the counter electrode for the experiment. Above this sits a 1.5 mm thick silicone rubber spacer, also fabricated by laser cutting. The silicone spacer serves both to distance the conducting polymer working electrode from the stainless steel counter electrode, and to provide a semicompliant or absorbing backstop which serves to evenly distribute the force placed for the titanium sensing wires positioned along the top plate and pressed into the polypyrrole ribbon. A preload pressure is then placed on the top plate by tightening a nylon screw in contact with the top plate, thus creating a preload force distributed between the interfaces of the sixteen titanium wires and the polymer ribbon on top of the silicone spacer. A silver wire is used as a reference electrode in the experiments that follow. The preloading nylon screw and silver wire reference electrode can be seen in Figure 5-2. The experiments were performed in neat $BMIMPF_6$.

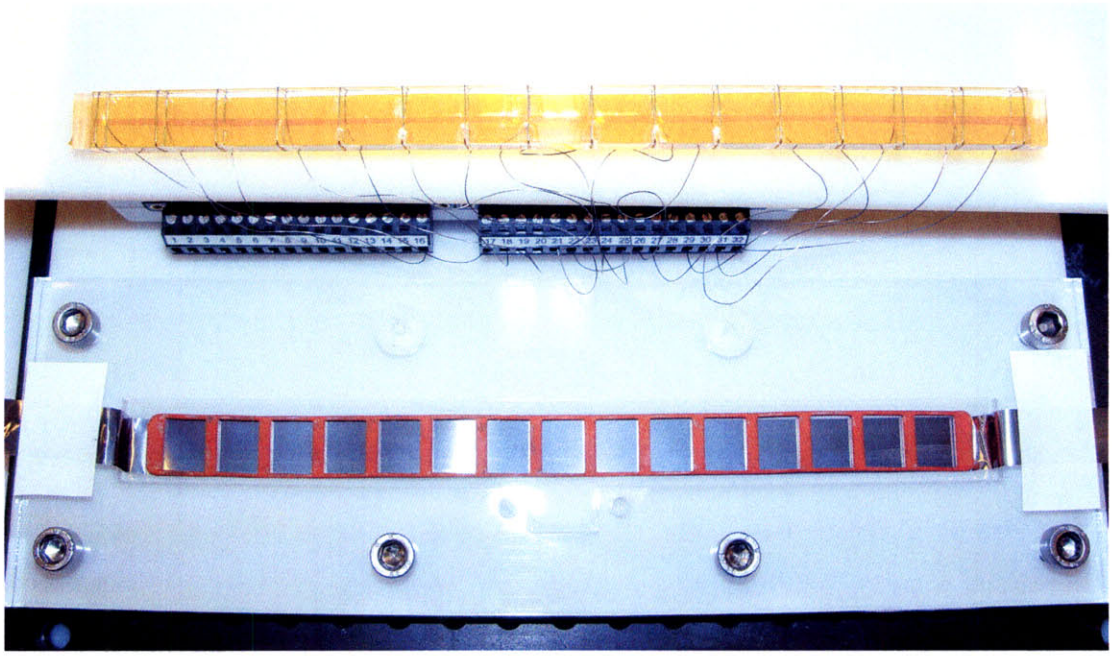

Figure 5-1: Experimental setup used for recording a series of voltage measurements along a conducting polymer ribbon. The apparatus is shown dismantled with the top plate flipped upward.

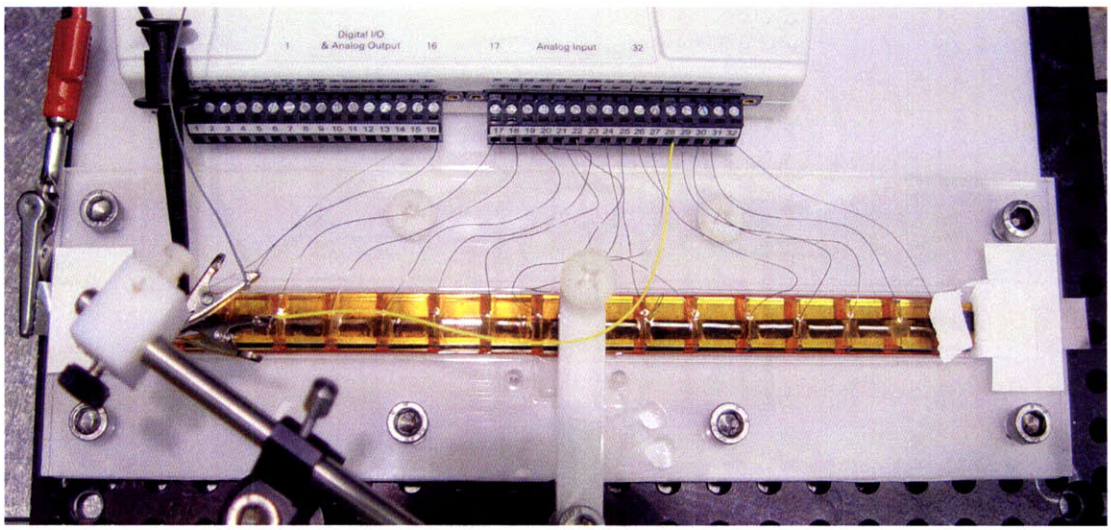

Figure 5-2: Experimental setup used for recording a series of voltage measurements along a conducting polymer ribbon. The apparatus is shown in use and a gold backed polypyrrole ribbon can be seen sandwiched between the titanium wires of the top plate and the silicone spacer in the bath of neat $BMIMPF_6$. A silver wire reference electrode protruded from below a PTFE mount can be seen towards the left side of the bath.

5.4.3 Polymer synthesis

Two PF_6^- doped polypyrrole ribbons were prepared using the procedures described in Chapter 3. Both films were deposited using the procedure described in Section 3.2 and one ribbon was fabricated to incorporate a gold conductive layer as described in Section 3.4. The thicknesses of the films were measured with a micrometer at eight points along each ribbon and averaged, giving an average thickness of 16.75 μm for each of the ribbons. This identical measured average thickness for the two polymer films is helpful in that it lets one draw more direct comparisons in the results presented below.

5.4.4 Polypyrrole ribbon experiments

A series of experiments were performed on the polypyrrole ribbon without the gold layer in order to investigate the limiting effects of longer conducting polymer ribbons on voltage propagation, and indirectly actuation. The ribbon was *warmed up* (see Section 4.3.3) in the neat $BMIMPF_6$ liquid salt bath in order to bring the film to a state as it would be used for repetitive actuation [6]. During this electrochemical warmup, the ions flow in and out of the polymer, effectively *wetting* the film. A 0.1 V/s $\pm$1 V triangle wave was used for the warmup cycles.

Following the warmup, the polypyrrole film was subjected to square waves in potential with respect to a silver counter electrode using the potentiostat, a setup very similar to the standard use of the EDMA described in Section 4.3. A range of square wave frequencies and magnitudes were used to stimulate the film by electrically connecting to one or both of the titanium wires at either end of the series of measurement wires. Waveforms of interest are shown below.

Figure 5-3 shows the result of a 0 V to 1 V step in potential imposed on the polypyrrole ribbon in neat $BMIMPF_6$ with respect to a silver reference electrode. The single electrical connection point corresponds to the 0 mm position in the figure.

When actuated, the active stress and active strain produced by a conducting polymer film (depending if it is run in isometric or isotonic mode, for example) are

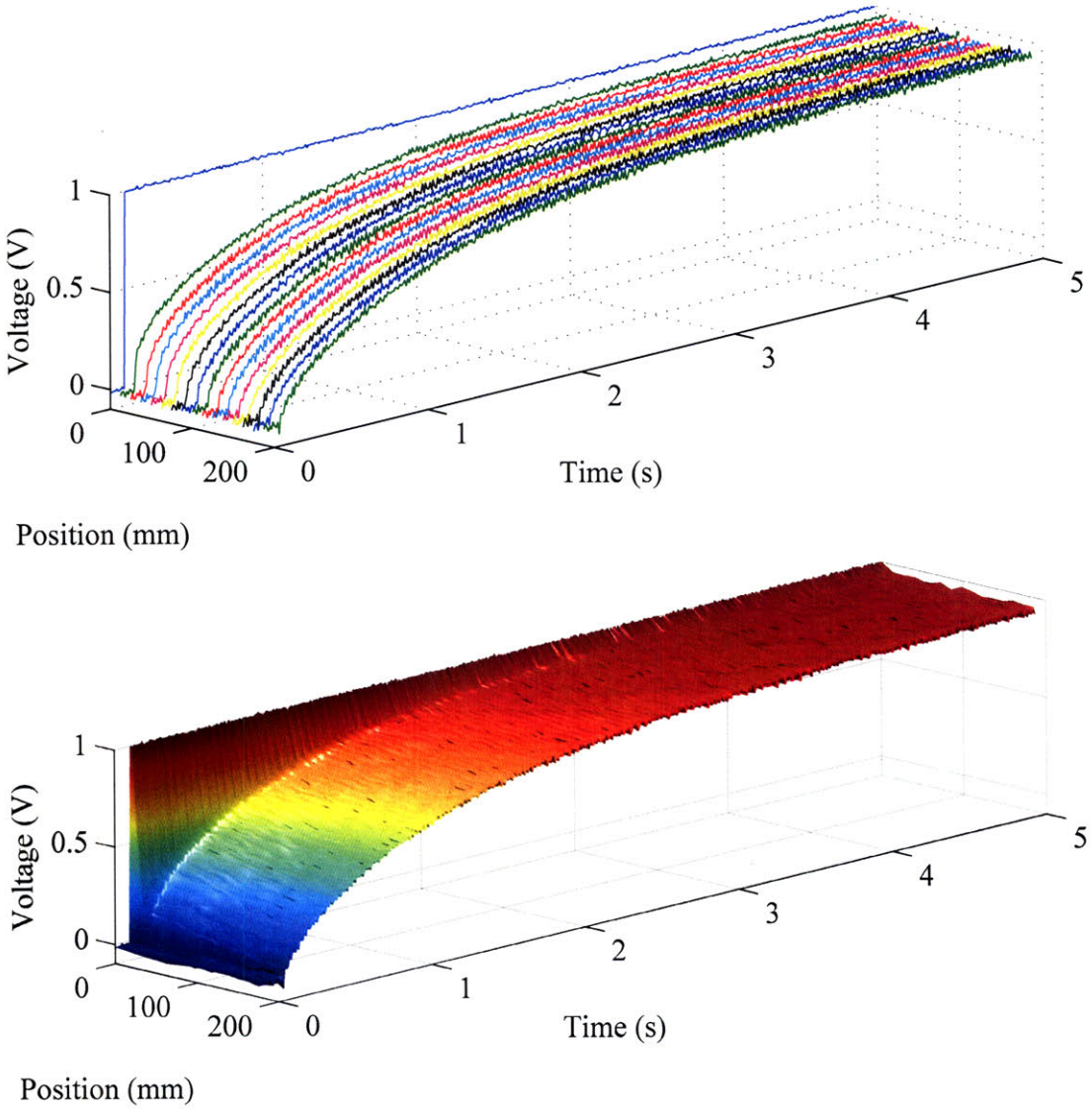

Figure 5-3: Line and surface plots showing the propagation of an inputted voltage step along a polypyrrole ribbon. Voltage potentials were measured along the ribbon at intervals of 12.5 mm. The electrical connection point corresponds to the 0 mm position on these plots. Measurements were made with respect to a silver wire reference electrode in an electrolyte of neat $BMIMPF_6$ liquid salt.

directly related to the uptake and expulsion of ions. This ion movement is generally increased as the driving voltage used for actuation is increased, thus providing a higher voltage potential and ion concentration at the polymer/electrolyte interface. This resulting higher ion concentration will generally drive faster ion movement [12].

The notion of a repeated cycle is helpful in expressing the requirements for an

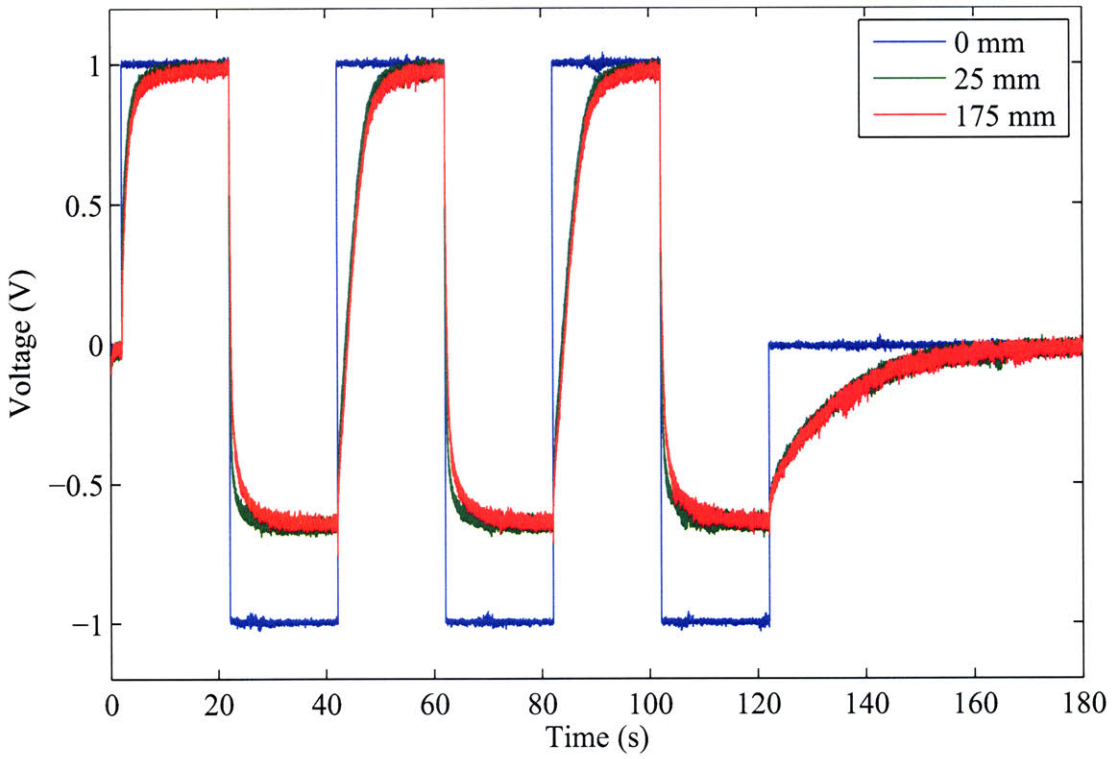

Figure 5-4: Data recorded 25 mm and 175 mm along a polypyrrole ribbon driven with a ±1 V square wave input at the 0 mm position.

actuator. In practical use, whether creating a motion similar to that produced by a fish fin ray or driving a mechanical ratchet, repetitive cycles are likely to occur. Also, these cycles capture the output performance of the actuator, delivering a force at a velocity, thus making this motion a good way to compare actuators of potentially different composition. In order to achieve a repeated action from a linear conducting polymer actuator, a waveform is applied to the polymer at its electrical connection point(s).

The polymer ribbon was cycled with a ±1 V square wave, measured versus a silver reference electrode. This output is displayed in Figure 5-4. Note, that these are the same data shown in Figure 5-3, but with the time axis extended. In this 2D plot, data are shown for three of sixteen measurement positions for clarity, since the plots tend to significantly overlap at this scale. The three displayed waveforms correspond to data recorded at positions 0 mm (location of the driving potential), position 25 mm, and position 175 mm.

Two behaviors are readily apparent in Figure 5-4. First, when driven with the -1 V potential, the voltage along the polymer hits a threshold and does not approach -1 V. Second, the shape of the measured voltage waveform changes with subsequent cycles. These behaviors both stem from the same cause: The measured voltages are representative of ions flowing into and out of the polymer bulk.

From electrochemistry, and as discussed in Section 4.4, there is a concept of an electrochemical window in which the electrochemistry can occur. Outside this window other reactions will dominate. No matter how low the driving voltage is brought, the polymer will not be further reduced. It is essentially quenched. It can no longer accept any new electrons. This effect, observed in the measured voltages and current, has an appreciable impact on the actuation. With less of a voltage difference at the film, ions ingress at a slower rate, and less actuation is observed. Figure 5-5 shows plots of the polymer ribbon subjected to a ± 1.5 V square wave, measured with respect to a silver reference electrode. Note that, just like in Figure 5-4, the negative voltage plateaus. Additionally, it can be seen that the voltage slows considerably in the positive components of the waveform. Although the data in Figure 5-5 show the measured voltage rising well beyond the 1 V input shown in the plots in the Figure 5-4 case, it does not fully reach 1.5 V within the cycle period. This substantial slowing in the rise of measured voltage may be due to the near expulsion of the $BMIM^+$ cations as the film is brought more positive. If held high for a long enough period, one might start bringing in more of the slower PF_6^- anions [7]. Figure 5-6 shows a surface plot analogous to the one in Figure 5-3, but for a cycle of the ± 1.5 V data shown in Figure 5-5.

The second behavior mentioned above, the decrease in rise time from one cycle to the next for positions some distance away from the inputted potential, is evident in the plots shown in both Figure 5-4 and Figure 5-5. This behavior can be explained by two factors. First, a conducting polymer's conductivity is dependant upon its oxidative state. Most significantly, its conductivity drops substantially as it is reduced. With this in mind, it is not surprising that the voltage rise observed some distance from the connection point will be be slower when commencing from a lower potential, as seen

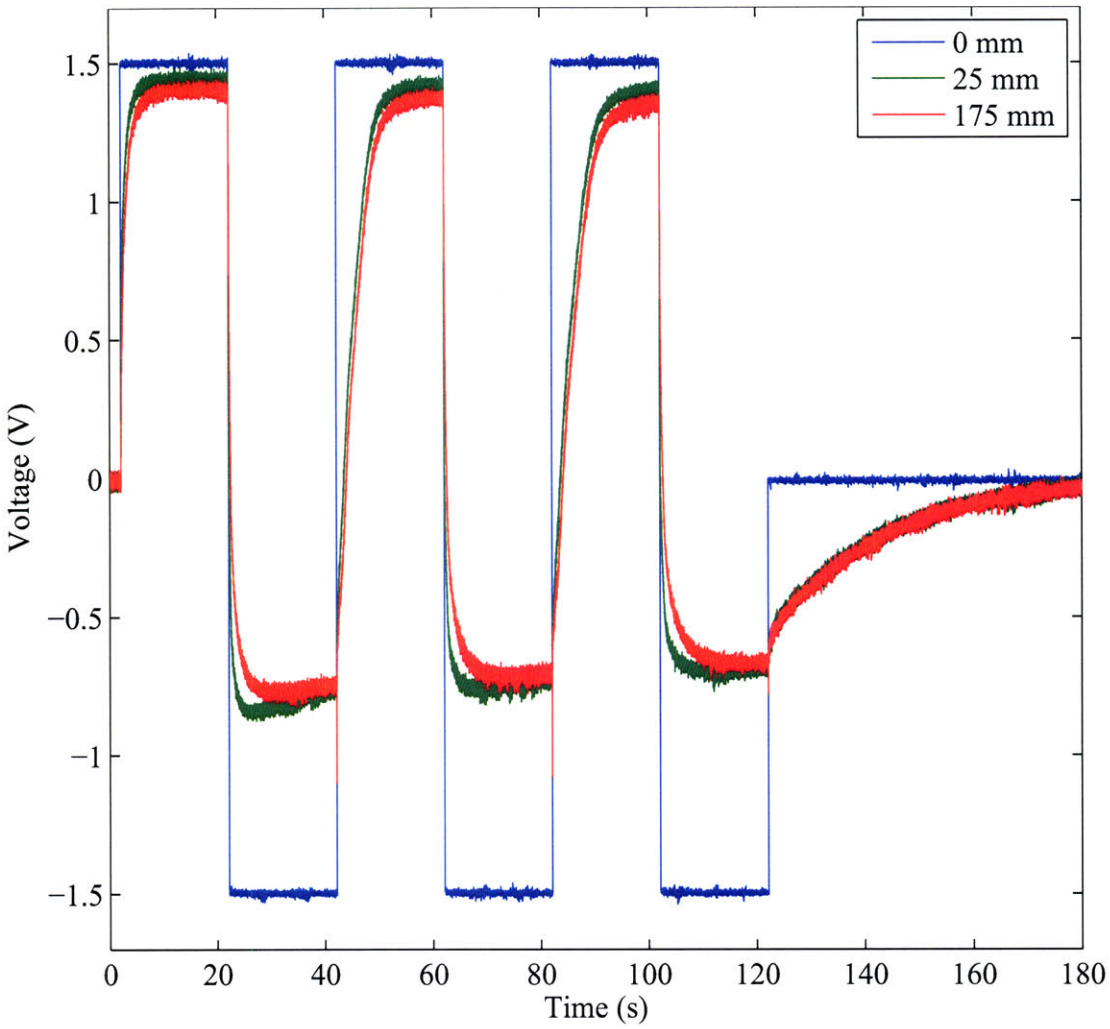

Figure 5-5: Data recorded 25 mm and 175 mm along a polypyrrole ribbon driven with a ±1.5 V square wave input at the 0 mm position.

in comparing Figure 5-3 and Figure 5-6. Second, it is possible to drive charge in and out of the polymer film at a rate that does not allow the charge to fully equalize by ion movement throughout the bulk polymer. Different segments of the film may be at varying ionic concentrations, as well as oxidative states, even in a localized polymer volume. And, even when the film is driven slowly, it takes significant time for the film to equalize after it is no longer driven by a potential, a result of its significant volumetric capacitance [24, 3, 7]. This is evident when observing the resting potential of the film after the cell voltage is disconnected. When uniaxially loaded as a linear actuator, this effects the material's strain, or the actuator's position, as well as its

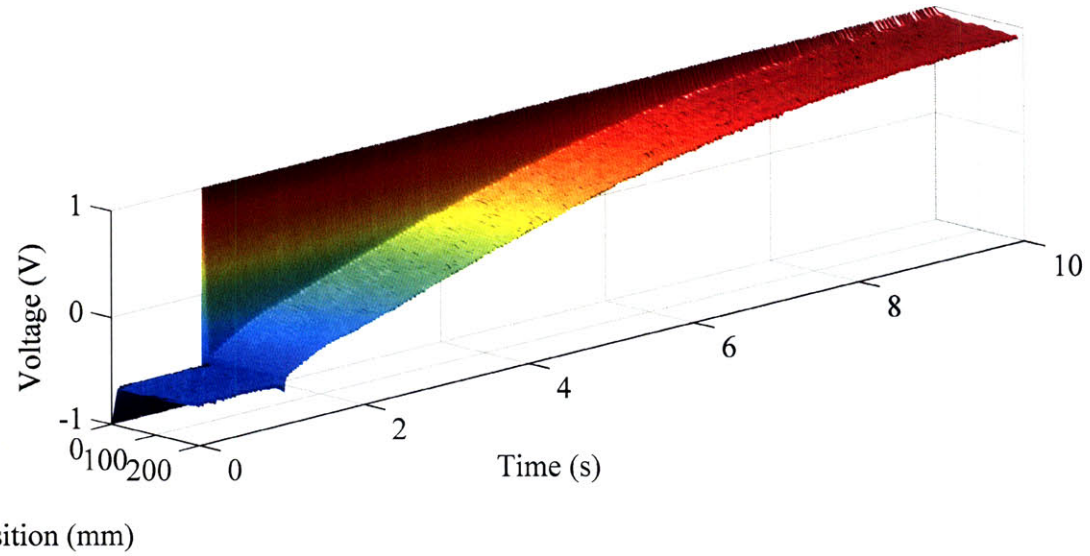

Figure 5-6: Surface plot showing the propagation of an inputted voltage step along a polypyrrole ribbon. Voltage potentials were measured along the ribbon at intervals of 12.5 mm. Electrical connection was made at the 0 mm position.

voltage. This placement of a conducting polymer into a state that effects subsequent inputted waveforms can be referred to as a memory effect.

5.4.5 Actuator memory

It is possible to bring a polymer back to equilibrium and a controlled oxidative state after it has been subjected to rigorous (but not material degrading) testing. One way found to be effective is to hold the film at a known potential before running a test. 0 V with respect to the reference electrode is often used. The open circuit voltage initially measured between the the polymer working electrode and the reference electrode is also sometimes used if it is desirable not to move the voltage before driving it to chosen value. A second way is to impose a repeated waveform on the polymer. When the polymer working electrode voltage is cycled around the reference potential, for example, the waveforms recorded at positions along the polymer settle into a repeated pattern. This settling effect is evident at faster cycle times as demonstrated by the data shown in Figure 5-7 and Figure 5-8. A similar effect is also observed during actuation, as shown in Figure 5-15 and Figure 5-16 in Section 5.6.

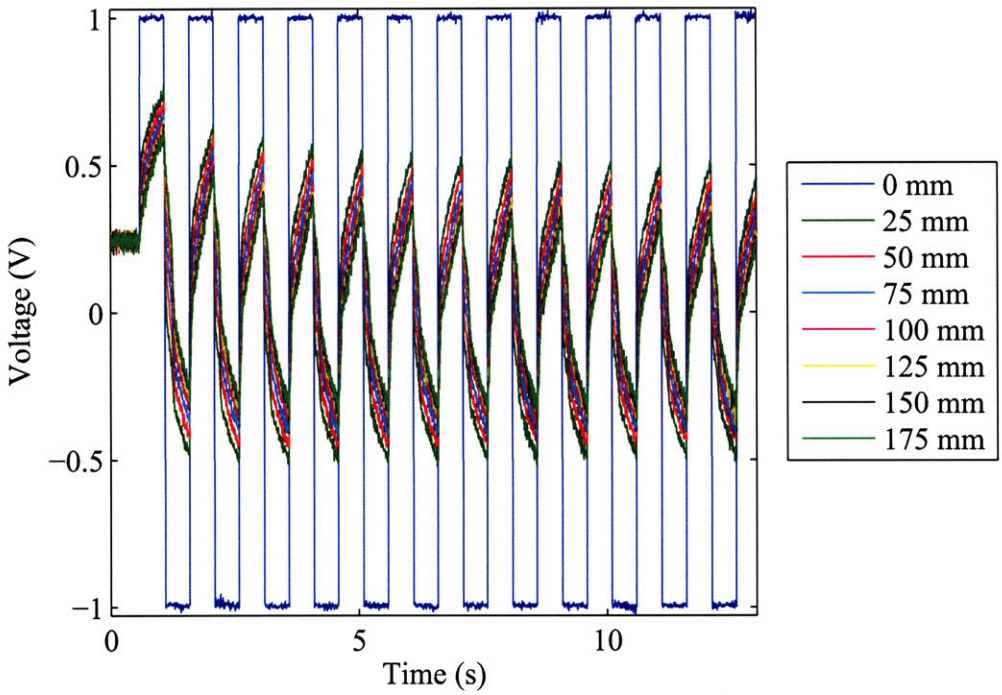

Figure 5-7: A polypyrrole ribbon is cycled with ±1 V 1 Hz square wave inputted at one end of the film (0 mm). The voltages at eight positions along the film are shown over time. In this case, the voltage oscillations were started from the polymer's resting potential.

By examining two trials performed under nearly identical conditions on the same film, Figure 5-7 and Figure 5-8, one can observe the differences in magnitudes achieved as a result of starting voltage, or polymer state. In Figure 5-7, a ±1 V 1 Hz square wave is imposed at the 0 mm end of the 187.5 mm polypyrrole film. The voltages at eight equally spaced positions are shown for clarity. This trial began from the resting potential of the film. In Figure 5-8, a similar test is run, but the voltage is held at 0 V with respect to the reference electrode prior to imposing the voltage oscillations at the 0 mm end of the polymer ribbon. One observes that the plots in Figure 5-7 initially go higher, but the oscillations settle out in both cases.

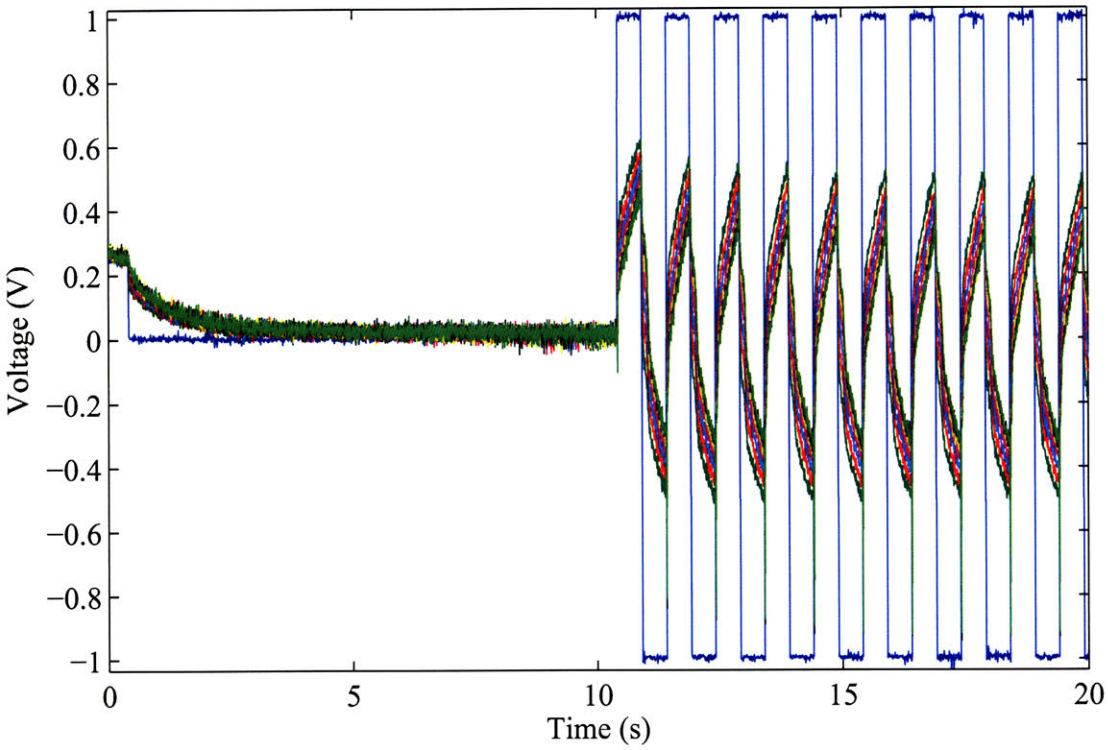

Figure 5-8: A polypyrrole ribbon is cycled with ±1 V 1 Hz square wave inputted at one end of the film (0 mm). The voltages at eight positions along the film are shown over time. In this case, the voltage at 0 mm was held at 0 V for 10 s before the voltage oscillations were started. The legend shown in Figure 5-7 applies to this figure as well.

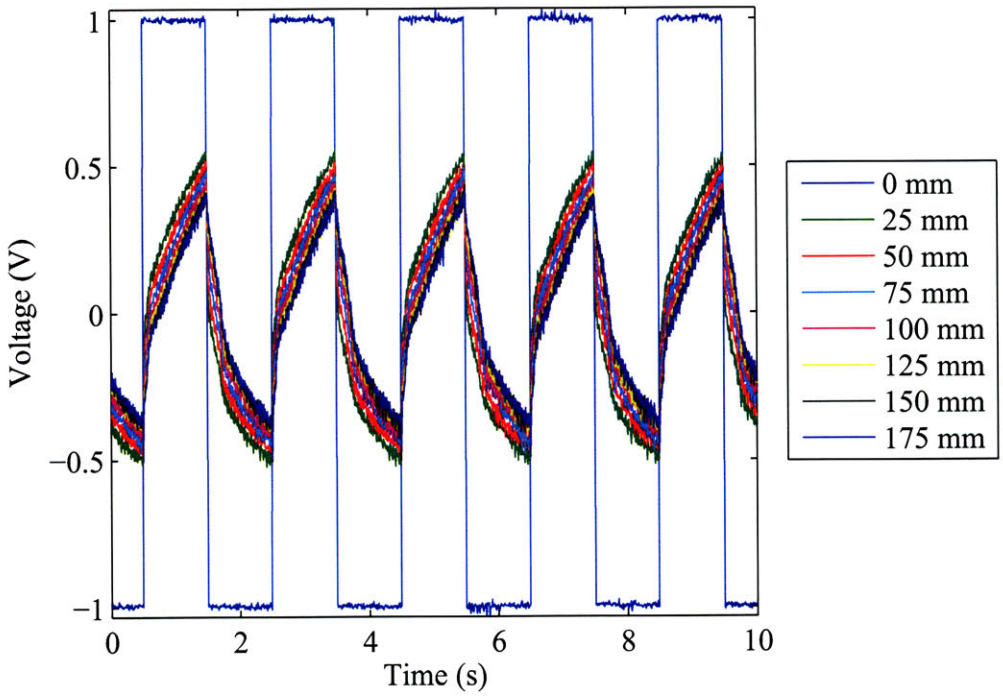

Figure 5-9: A polypyrrole ribbon is cycled with a ±1 V 0.5 Hz square wave inputted at one end of the film (0 mm). The voltages at eight positions along the film are shown over time.

An enlarged view of settled cycles of a ±1 V 0.5 Hz square wave is shown in Figure 5-9. As will be demonstrated below, the addition of a nonreactive conducting layer to the polymer ribbon has a positive effect on these waveforms.

5.4.6 Gold backed polypyrrole ribbon experiments

The ultimate goal of adding a nonreactive conductive layer to electroactive polymers is to increase their actuation speed. The hope is to achieve this by mitigating the voltage drop that occurs along conducting polymers of substantial length, or aspect ratio, as a result of their finite conductivity, as discussed in Section 5.3. Here, voltage propagation along gold backed polymer ribbons, manufactured using the methods described in Chapter 3, are examined and compared with the non-gold case. This comparison will reveal the advantages of adding this conducting layer.

The plots shown in Figure 5-10 offer a direct comparison to those found in Figure 5-3 of Section 5.4.4. Just a quick inspection reveals that the voltage rises much more quickly in the gold backed polymer case. Also, in the case of the gold backed film, a gradient in voltage along the film moving away from the electrical connection point is observed immediately after the voltage step is applied, and the voltages measured along the film rise together over time. This is in contrast with the polypyrrole only case of Figure 5-3, where a dominating voltage drop is observed between the measurements taken at 0 mm and 12.5 mm. In this case, the voltages measured along the film also rise together over time, but with a smaller observed gradient moving away from the connection point, and at a much slower rate.

Figure 5-11 shows plots for a gold backed polymer ribbon cycled with a ± 1 V 0.5 Hz square wave inputted at one end of the film. The voltages at eight positions along the film are shown over time. These plots are analogous to those previously shown in Figure 5-9. When compared, one observes a sizeable gain in the voltages measured at a given time period at points away from the driving waveform. Similarly to the step input, the gold backed polymer case of Figure 5-11 shows an observable gradient in the voltage measured along the film moving away from the electrical connection point. And, the polymer only case of Figure 5-9 again shows a much smaller gradient and a dominating voltage drop is again observed at or near the connection point.

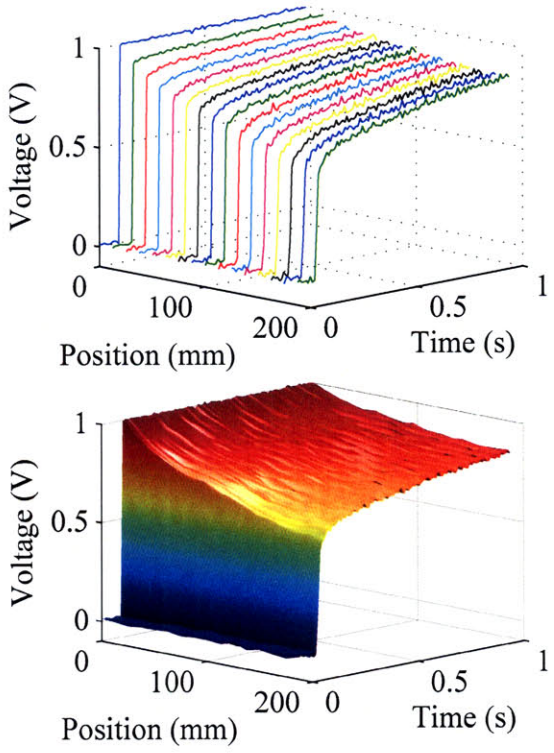

Figure 5-10: Line and surface plots showing the propagation of an inputted voltage step along a gold backed polypyrrole ribbon. Voltage potentials were measured along the ribbon at intervals of 12.5 mm. The electrical connection point corresponds to the 0 mm position on these plots. Measurements were made with respect to a silver wire reference electrode in a $BMIMPF_6$ liquid salt bath.

5.4.7 More connection points

Although comparing the plots of Section 5.4.4 with Section 5.4.6 shows the gold layer has a positive effect on the voltage drop measured at points along the film, it is still present. Like polypyrrole, gold also has a finite conductivity, and as a very thin layer, its resistance can be appreciable. The conductive layer can be thickened to a point, but it is anticipated that this thickening of the gold layer will eventually influence the actuation of the polymer due to an increase in stiffness. It is of interest, therefore, to examine the effect of adding additional electrical connections to the polymer ribbon.

Figure 5-12 show the effect of adding a second electrical connection to a polypyrrole ribbon without a gold layer. Electrical connection is made at one end (0 mm) and at 187.5 mm along the film. Figure 5-13 similarly shows the effect of adding a

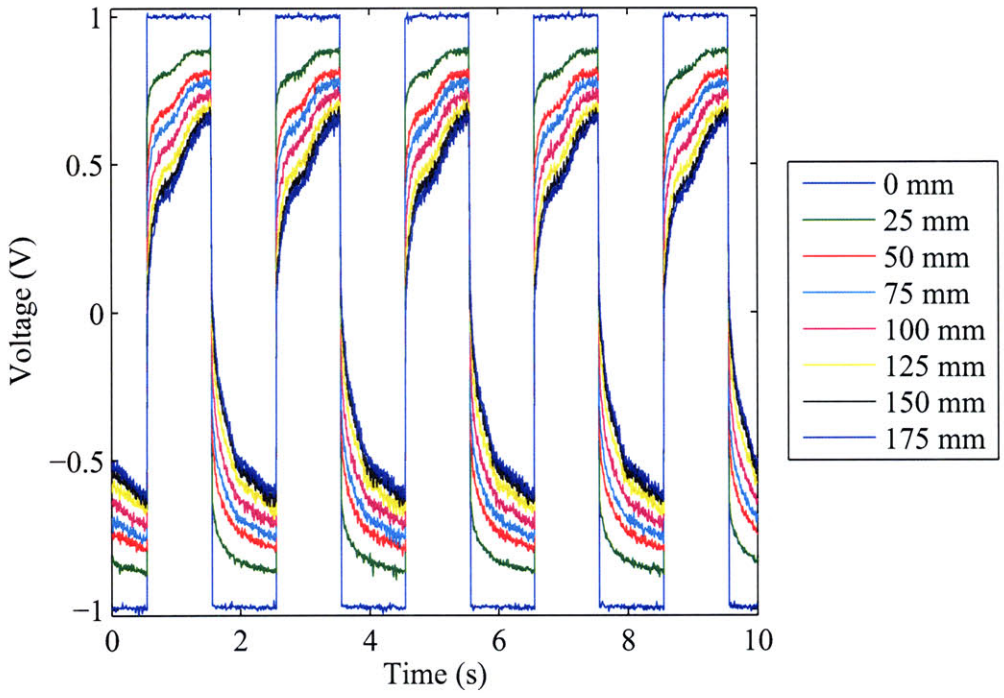

Figure 5-11: A gold backed polypyrrole ribbon is cycled with a ±1 V 0.5 Hz square wave inputted at one end of the film (0 mm). The voltages at eight positions along the film are shown over time.

second connection point, again at 187.5 mm, in the case of a gold backed polypyrrole ribbon. For clarity, data is shown for points 0 mm, 25 mm, 50 mm, and 75 mm along the films. This allows the single connection point cases to be readily compared with the double connection cases, where the voltage will climb back up as one approached the 187.5 mm point. A second connection point is found to provide a positive effect in both the polymer alone and gold backed polymer cases. That is, it allowed the voltages to climb quicker at points measured along the film. Charge inputted at the 187.5 mm end of the film was observed at the points near the close to the 0 mm end, even after a short time. It is clear, however, that the net effect of adding the second connection point is small when compared to the addition of the gold layer. That is, the two plots shown in Figure 5-12 (or Figure 5-13) are much more similar to each other, in shape and magnitude, that when comparing the plots of one figure to those of the other figure.

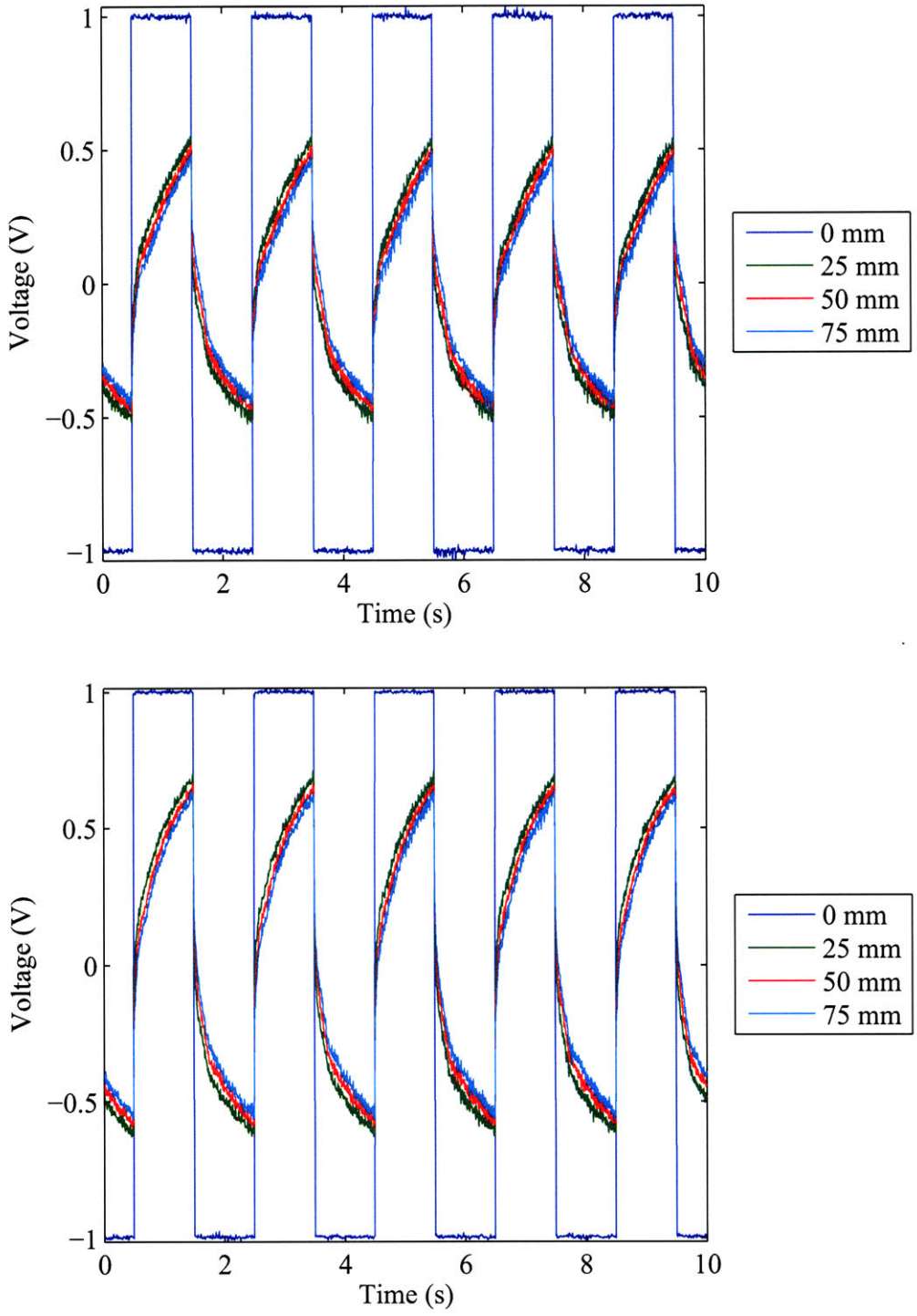

Figure 5-12: Polypyrrole ribbon cycled with a ±1 V square wave with one electrical connection at the 0 mm position (above) and with two electrical connections: one at 0 mm and one at 187.5 mm (below).

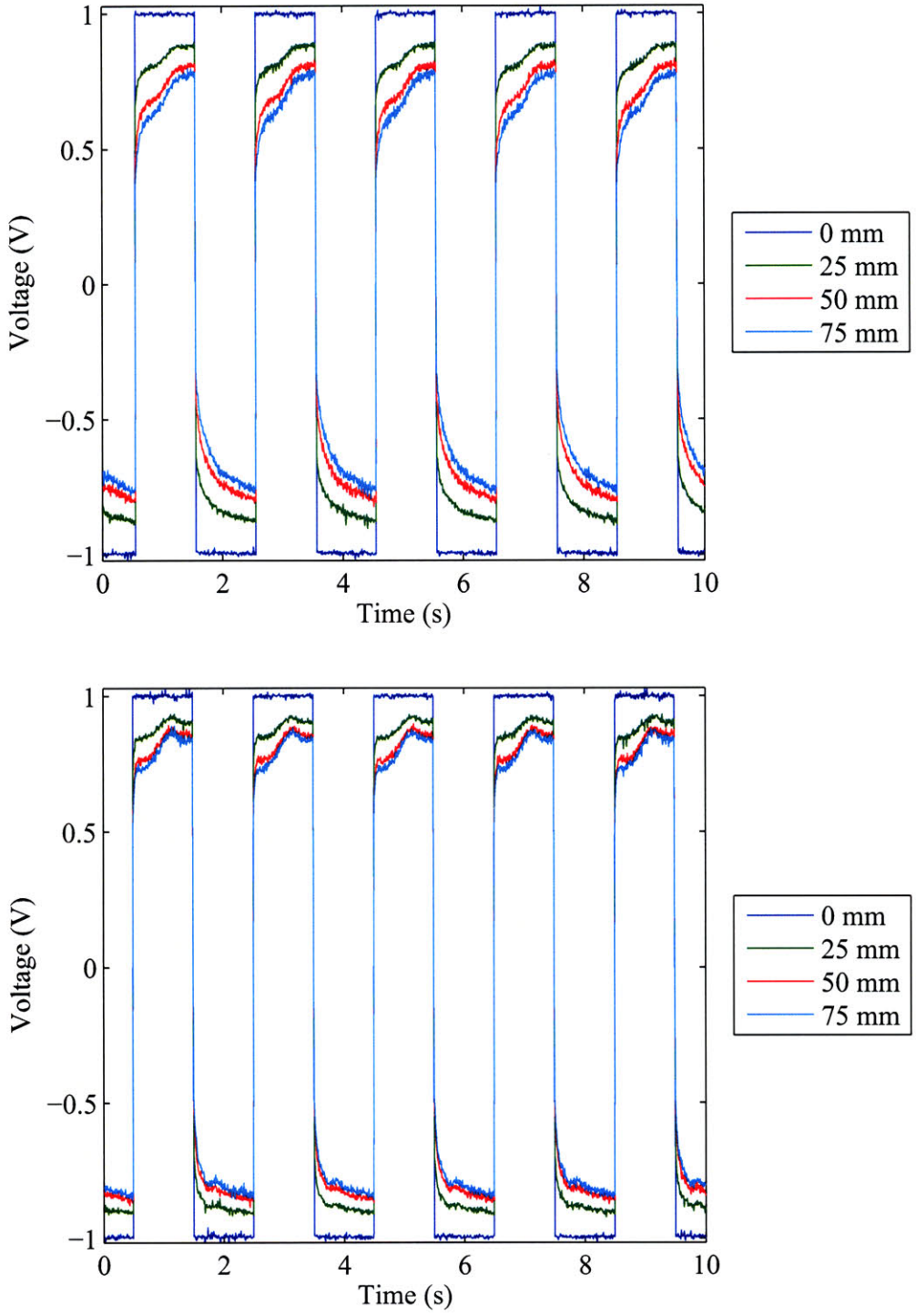

Figure 5-13: Gold backed polypyrrole ribbon cycled with a ±1 V square wave with one electrical connection at the 0 mm position (above) and with two electrical connections: one at 0 mm and one at 187.5 mm (below).

5.4.8 Experiment conclusions

Experiments were performed in order to better understand the losses that occur as a result of polypyrrole's finite conductivity, an effect of great importance to the development of longer linear conducting polymer actuators. Additionally, experiments were made to characterize the effect of incorporating a conducting layer into the polymer film.

An apparatus was designed and fabricated to simultaneously measure sixteen points along a 187.5 mm conducting polymer ribbon. The use of titanium wires preloaded onto the film under test and backstopped by silicone rubber was found to perform very well. From the trends in the data, one can deduce that the connections were secure and the contact resistances at the wire/film interface were uniform from wire to wire.

It is clear that conductor incorporation is beneficial for faster propagation of charge along the conducting polymer films. This is evidenced by a substantial increase in rise time between in comparing the gold backed to the non gold backed films when driven at one or two ends by step or square waveforms in potential. It is anticipated that the addition of this layer will have a similar effect on actuation speed and will be examined in Section 5.6.

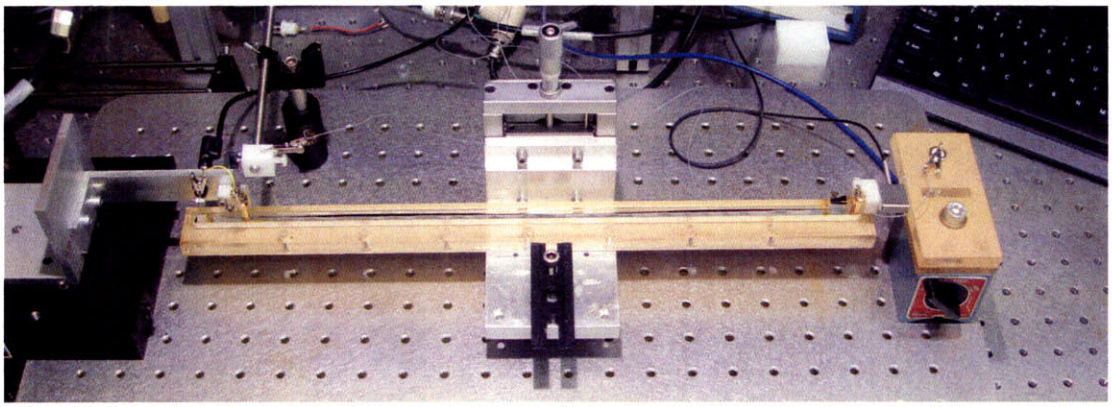

Figure 5-14: A setup created to test long conducting polymer actuators in the EDMA.

5.5 Increased output displacement

Free standing electroactive conducting polymer testing and characterization is typically performed using small film samples (e.g. 5 mm $\times$ 2 mm $\times$ 20 μm) [24, 6, 7]. Many applications, however, will require output displacements much larger in magnitude. This increase in actuation stroke can be accomplished in three ways: by increasing the size of the polymer actuator, by using mechanisms to create a mechanical amplification at the expense of produced force, or using mechanisms to ratchet a larger displacement with repeated cycles. The first approach is discussed here, and the other two approaches are outlined in Chapter 6.

Figure 5-14 shows one of several setups created to test long actuators in the EDMA. The setup consists of an acrylic bath, a nylon mesh separator, and a carbon fiber paper counter electrode. The acrylic bath was fabricated by a combination of laser machining and milling, and the separator and counter electrode were cut from larger stock by laser machining. The separator electrically isolates the polypyrrole ribbon working electrode from the carbon fiber paper counter electrode. Electrical connection is made via two gold coated clips at either end of the bath, and a silver wire, shown on the left, is used as a reference electrode. This setup allows one to use the EDMA to characterize films of up to 400 mm in length.

5.6 Improved actuation speed

As discussed in Section 5.3, adding a nonreactive conducting layer to polypyrrole linear actuators has a beneficial effect on voltage and charge propagation along longer films. It is anticipated that the addition of this layer will have a similar effect on actuation speed. In this section, the effect of this layer on actuation is studied.

Two time constants are central to the challenge of increasing the actuation speed, or the strain rate, of conducting polymer based actuators [24, 65, 7]. The charging time constant τ_{RC}, is given by

$$\tau_{RC} = R_S C_V, \tag{5.12}$$

where R_S is the solution resistance and C_V is the volumetric capacitance of the polymer film. This time constant relates to the charging time that results from electrical properties of the polymer. The diffusion based time constant, τ_D, is given by

$$\tau_D = \frac{a^2}{4D}, \tag{5.13}$$

where D is the diffusion constant and a is the film thickness. This time constant relates to the moving of ions into or out of the film as a result of an applied potential.

Which constant dominates for a given situation depends on the geometry of the system. For longer thin films, the charging time constant will tend to dominate [7]. The diffusion time constant will be revisited in Section 5.7.

Figure 5-15 shows plots for two separate isotonic tests conducted on two polypyrrole actuators, one with an incorporated gold layer, and one without. Both tests were run under similar conditions. The films are loaded uniaxially in a bath similar to the one shown in Figure 5-14 and electrical connections were made at both ends of the films. The data in Figure 5-15 shows that the gold backing indeed does affect actuation. A decrease in the rise time is apparent for the gold backed case, as well as an increase in the overall strain observed. It is anticipated that this difference could be made more dramatic by thickening the gold layer on the ribbon actuator.

As was discussed in Section 5.4.7, even with a layer of gold on the polymer ribbon,

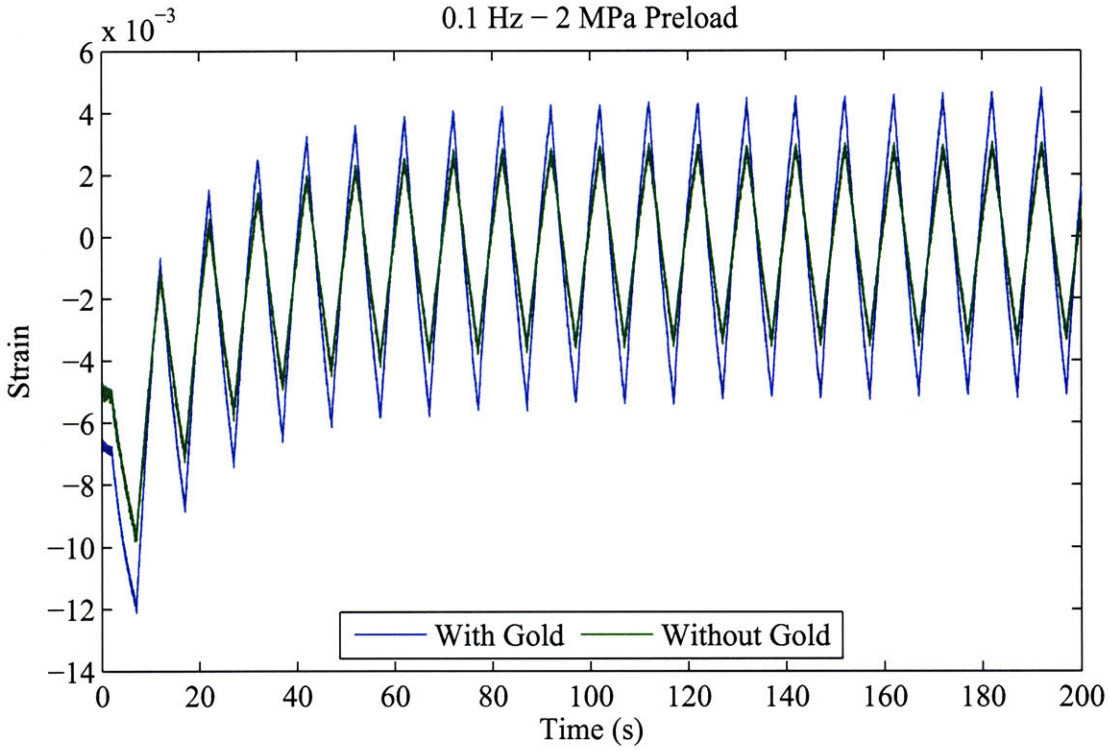

Figure 5-15: Plots comparing the outputs of gold backed and non gold backed polymer films actuated at 0.1 Hz and preloaded isotonically at 2 MPa.

there exists a voltage drop along the actuator. Figure 5-16 shows the effect of adding a third connection point in the center of a 216 mm gold backed actuator. The connection was made with a gold plated clip similar to those used in the EDMA instrument to secure the polymer ends. Care was taken to suspend the clip by its wire in order to minimize its effect on actuation. The film was subjected to a ± 1 V 20 mHz square wave, measured with respect to a silver reference electrode in a $BMIMPF_6$ liquid salt bath with stainless steel counter electrode.

The plot in Figure 5-16 shows that further advantage may be made by thickening the gold layer. The waveform corresponding to the three electrical connection case shows faster actuation, or a faster strain rate. This results in a larger observed strain (or displacement) for a given time period, here 25 s. Note that when driven by a repeated waveform, the observed strain or displacement is limited by the frequency of the driving frequency waveform, as well as the material properties of the film, the physical dimensions of the film, and other factors such as the choice of electrolyte and

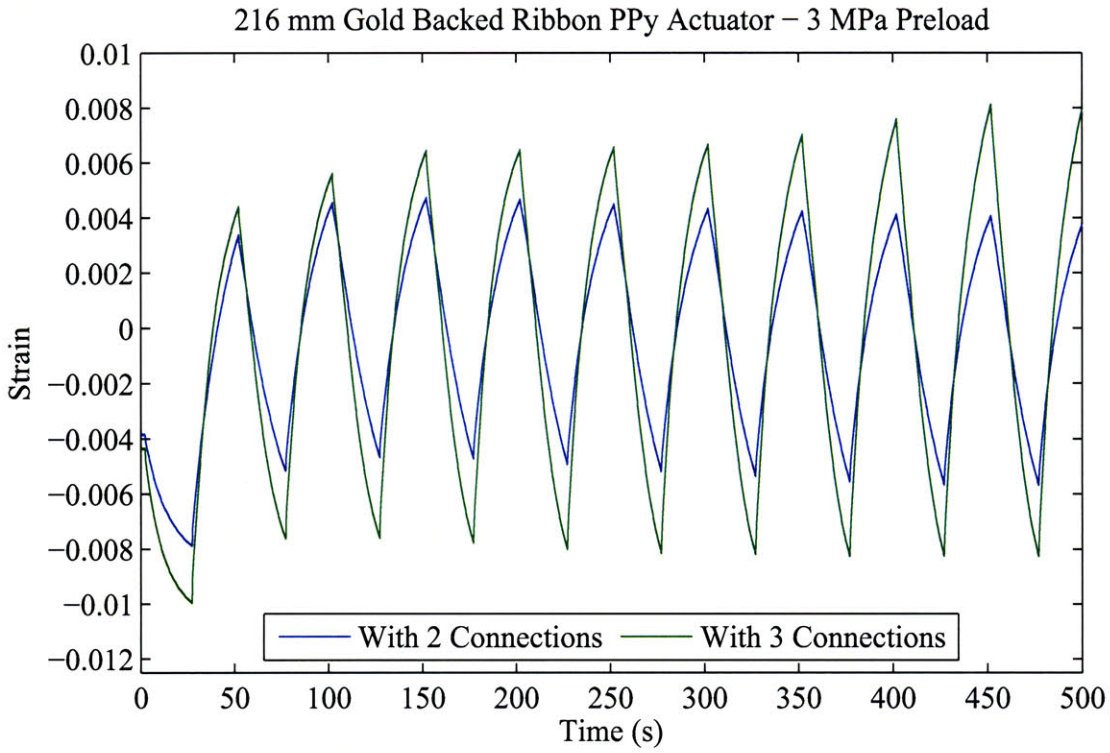

Figure 5-16: Plot of a 216 mm gold backed polypyrrole linear actuator preloaded isotonically at 3 MPa and actuated with a ±1 V square wave at 20 mHz.

ions used [6] and the operating temperature [7].

5.7 Increased output force

The significance of the diffusion based time constant, given by Equation 5.13 in Section 5.6, is that a single conducting polymer sample thick enough to generate Newtons of force would actuate too slowly to be of use in many applications. That is, its power output would be limited. Additionally, electrodeposited polymers begin to exhibit less desirable morphologies after their deposited thicknesses approaches 40 μm [6].

Creating a single thin but wide actuator is another option, but because the actuator is uniaxially preloaded and because it contracts volumetrically, edge effects can be very limiting. Additionally, it has historically been difficult to produce polymer films at larger scales that are uniform enough to be evenly loaded. These difficulties largely arise from the challenges of manually removing polymer films from their substrates after electrodeposition without temporarily or permanently deforming it, but are accentuated by large volume changes that occur in the polymer films once removed. For example, ripples and wrinkles are more often observed in larger films making them difficult to mechanically clamp and preload uniformly. As mentioned in Chapter 3, the incorporation of a conducting layer helps to mitigate these difficulties.

As mentioned in Chapter 2, one potential way to improve force without sacrificing speed is to use several parallel ribbon lengths and actuate them simultaneously in order to achieve a large net output. Figure 5-17 shows a schematic depicting basic parallel actuation applied to conducting polymer actuators. The basic unit consists of a conducting polymer working electrode, a suitable metal, carbon fiber paper, or conducting polymer counter electrode, and an isolating layer made of a mesh, fine paper, or gel. This layer electrically separates the working and counter electrodes, but allows ions to flow relatively freely. Actuation occurs in an electrochemical bath, but the system could be encapsulated as mentioned in Section 3.5.4. Several of these units are then mounted together in order to achieve a combined power output between the two mechanical attachment points.

As mentioned in Section 2.3, a key challenge in achieving effective parallel actu-

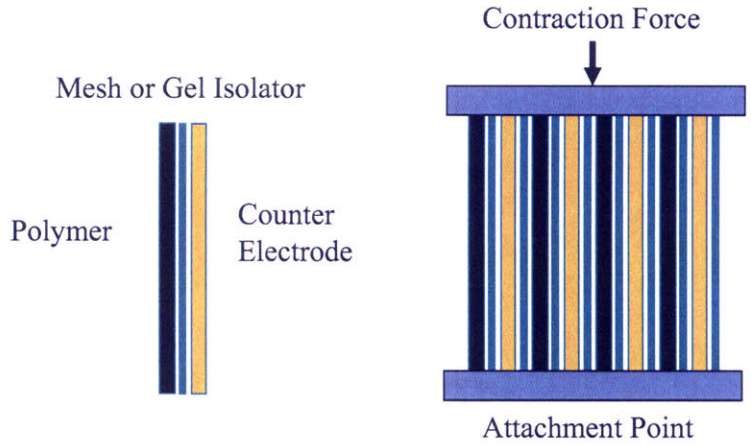

Figure 5-17: A schematic showing the concept of parallel actuation. On the left is an actuator unit, and on the right is a collection of those units working together to generate a combined output.

ation is uniformly tensioning the polymer ribbons or actuator units, thus allowing them to equally contribute to the net outputted force or generated stress over the system's range of motion. One approach taken to confront this challenge is to use a single polymer ribbon, manufactured using the methods discussed in Chapter 3, that is snaked around a series of posts, rollers, or pulleys in order to achieve a series of active lengths of conducting polymer. The polymer ribbon is woven so that the tension is evenly distributed when a preload is applied between two sets of mechanical attachment points. If friction is adequately controlled, a single tension is achieved throughout the ribbon when a preload force is applied between the two sets of connection points. If completely averaged, the resulting actuation force is a sum of the force outputs from the individual polymer actuator lengths, or the active stress in the polymer ribbon, multiplied by its cross section and the number of parallel lengths in tension.

Figure 5-18 shows a CAD rendering of an early attempt at parallel actuation. Figure 5-19 shows the realized version of the design. This device was designed to mechanically connect to the electrochemical dynamic mechanical analyzer (EDMA) described in Section 4.3, allowing for the use of the EDMA's control and logging capabilities. The hardware added to the EDMA consists of bath that incorporates a

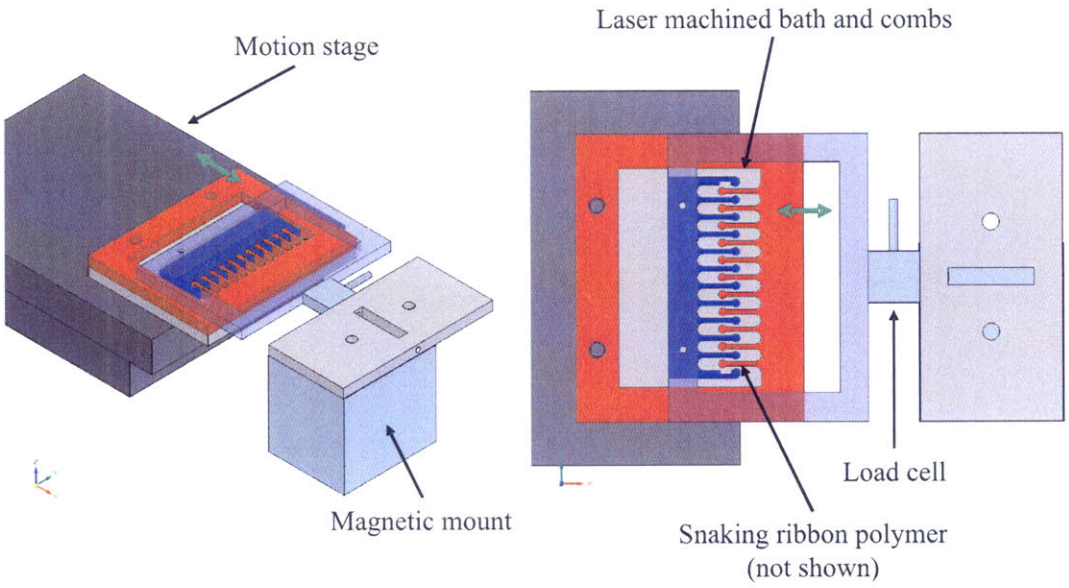

Figure 5-18: A device utilizing a snaking gold backed polypyrrole ribbon actuator to provide parallel actuation and a larger force output.

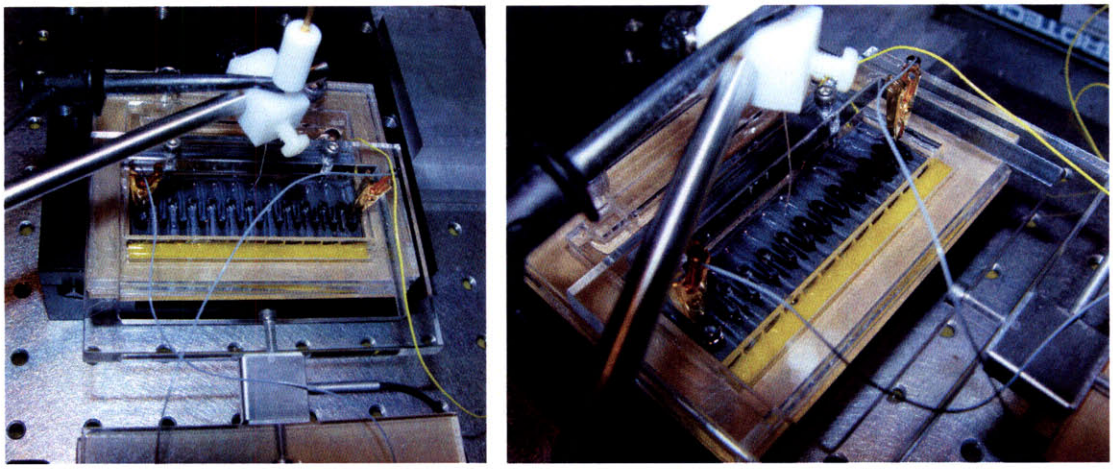

Figure 5-19: A device utilizing a snaking gold backed polypyrrole ribbon actuator to provide parallel actuation and a larger force output.

comb-like structure to provide one set of posts onto which a snaking polymer ribbon applies stress, and an arm-like structure that supports a second similar comb-like structure. In this device, the bath is mounted on the precision stage and moves under the control of the EDMA. The EDMA load cell is mounted inline between the arm-like structure and a magnetic mount which is secured to the optical table. Carbon fiber paper serves as the counter electrode in this device, and a nylon mesh

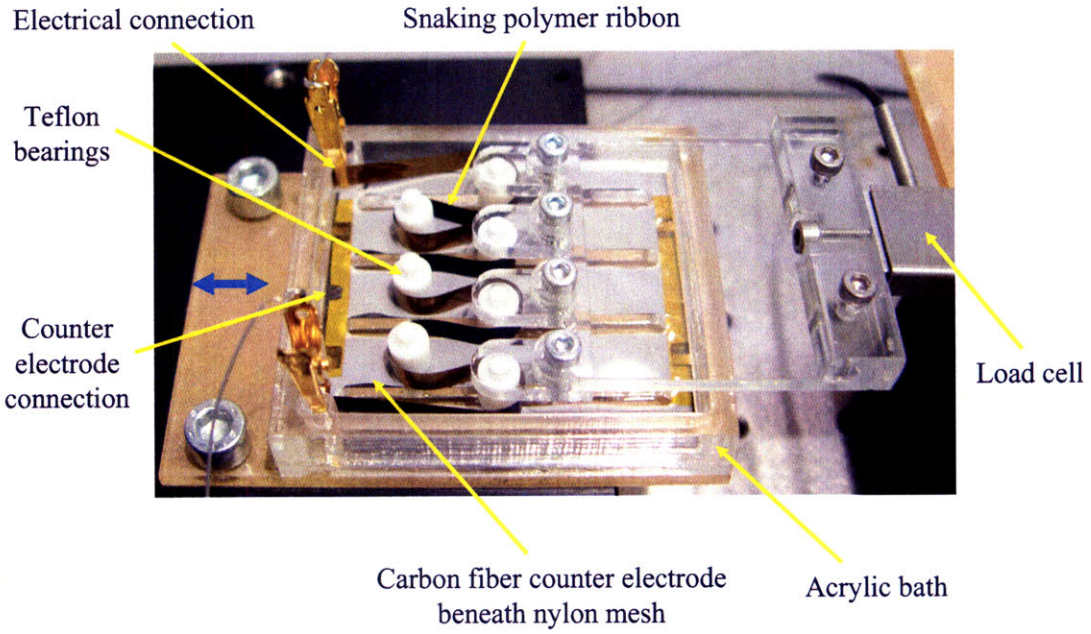

Figure 5-20: A device utilizing a snaking gold backed polypyrrole ribbon actuator to provide parallel actuation and a larger force output. The device is shown unloaded.

electrically separates the working and counter electrodes without impeding ion flow. Gold plated clips are used to secure the two ends of the conducting polymer ribbon actuator as well as connect to the ribbon electrically. A silver wire is used as the reference electrode.

Unfortunately, friction was an issue with the system shown in Figure 5-18 and Figure 5-19. Although the parallel ribbon lengths are of identical size and should actuate at the same rate, eliminating the need for the ribbon to move across the posts during actuation, initially achieving identical tension on the lengths proved to be very difficult. The setup was therefore evolved in order to more easily tension the parallel polymer ribbon lengths.

Figure 5-20 shows a device designed to provide parallel actuation where PTFE (Teflon) rollers, mounted on PTFE posts, were used to reduce friction and allow tension to be averaged more easily between neighboring parallel lengths of the snaking polymer ribbon. Like the device of Figure 5-18 and Figure 5-19, this setup connects to the EDMA in order to utilize its control and logging capabilities. In this setup, the acrylic bath, nylon mesh separator, and carbon fiber paper counter were all fabricated

using laser machining, with the acrylic bath subsequently assembled using epoxy. Mounting and tensioning the polymer ribbon actuator proved to be much easier with this device. The device utilizes eight parallel lengths of conducting polymer ribbon, where the two outside lengths are slightly longer than the inner six lengths.

Figure 5-21 shows data gathered using the device shown in Figure 5-20. In this experiment, the device was preloaded isotonically at 2 N and a gold backed polymer film was actuated in $BMIMPF_6$ liquid salt. Warm up cycling, as described in Section 4.3.3, was used in order to get the ions flowing in a reliable way. The first plot shows the +/-1.5 V square wave that was imposed on the polypyrrole working electrode with respect to a silver reference electrode. The second and third plots show the corresponding current and charge outputs, respectively. The fourth plot shows the active strain output from the polymer, pulling successfully against the 2 N load. The 0.7% recorded strain shown in this plot is larger than the highest reported output at 2 N (0.5% [23]), as discussed in Section 2.3.

Figure 5-22 shows plots of a similar test repeated for 180 cycles. Significantly, no creep is observed during this actuation and the resulting motion is shown to be repeatable. This is in stark contrast to the output of many previous devices, as well as polymer films simply mounted in the EDMA. This stability can be attributed to the incorporated gold layer, which, although it yields to point, likely also supports the polymer under stress. The exhibited stability also requires the polymer film to not be actuated too aggressively in driving voltage or in stress preload.

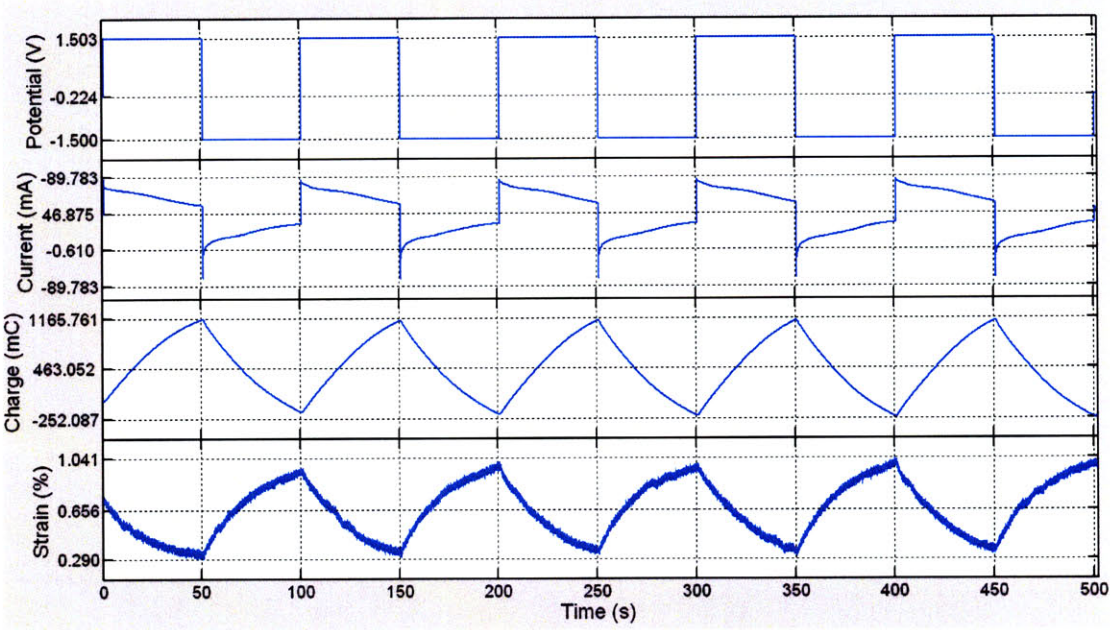

Figure 5-21: Plots showing resultant current, charge, and strain outputs for the parallel actuator shown in Figure 5-20 when driven with a square wave in potential. A force feedback system was used to isotonically hold the actuator at 2 N for the duration of the experiments.

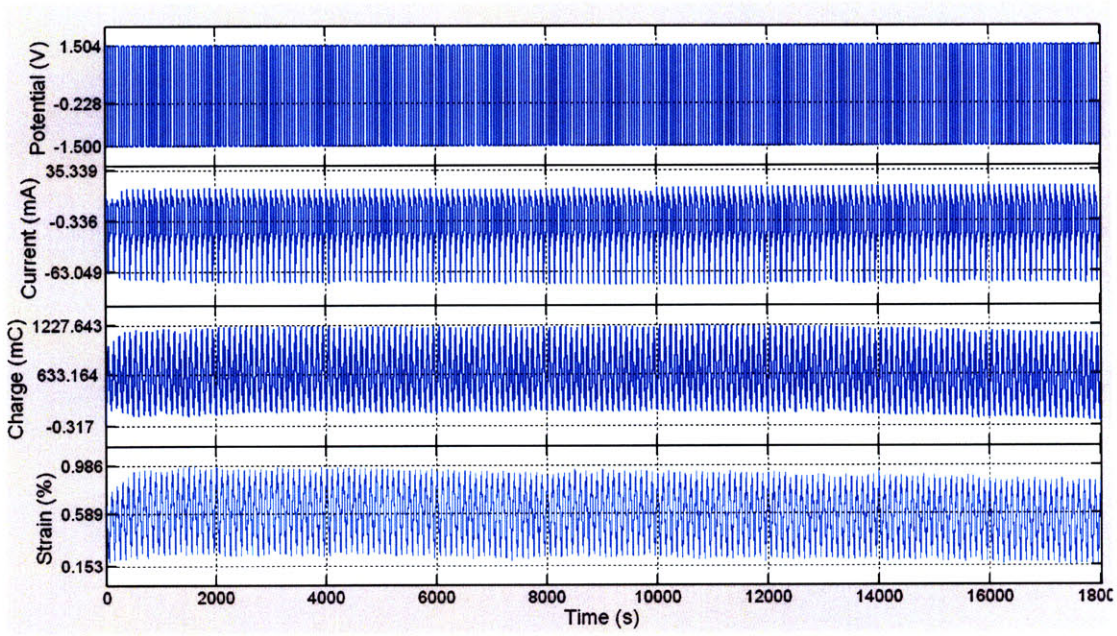

Figure 5-22: Plots showing data obtained while running the parallel actuator shown in Figure 5-20 over several hours.

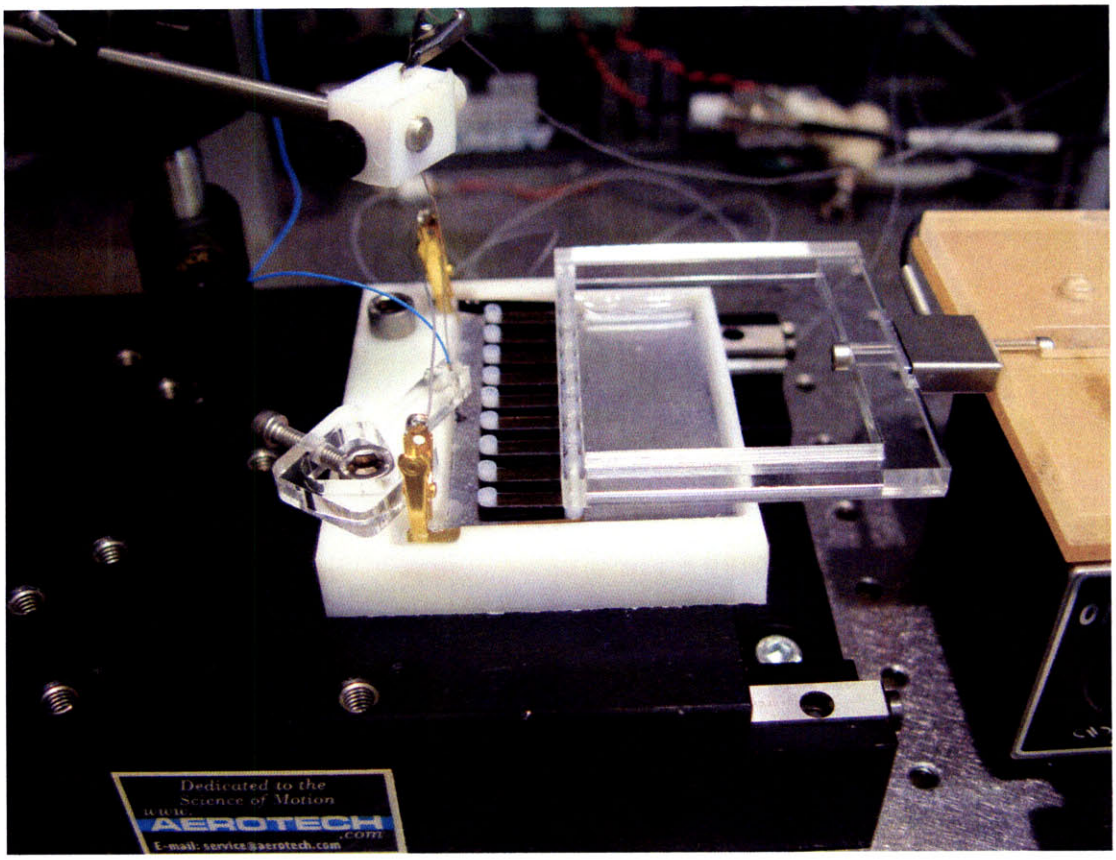

Figure 5-23: A device utilizing a snaking gold backed polypyrrole ribbon actuator to provide 20 parallel active ribbons.

The system of Figure 5-20 was scaled up to utilize twenty parallel conducting polymer ribbon lengths, again by weaving a single polymer linear actuator around a series of rollers. This larger device is shown in Figure 5-23. Smaller PTFE rollers and dowels were incorporated in this device, and were also found to successfully distribute the polymer ribbon tension between the parallel lengths. The bath structure in this case was machined from polyacetal (Delrin). A carbon fiber paper counter electrode and a mesh separator were again employed. This system demonstrated the ability of pulling 10 N over a strain of 1.5%. These values far exceed the largest output published to date (0.5% strain with a 2 N preload [23]).

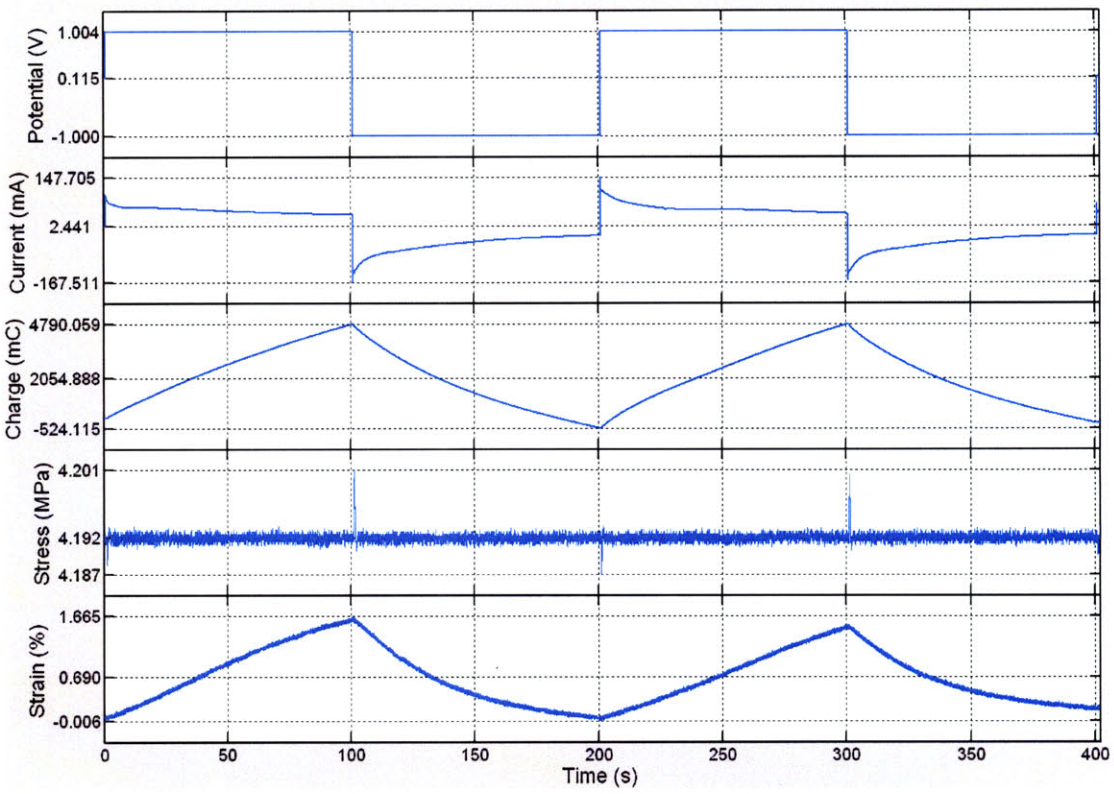

Figure 5-24: Plot showing data collected from the 20 segment device when preloaded at 10 N.

Chapter 6

Actuator application

Throughout the work presented in this thesis, stand alone demonstration devices (operated independently from the EDMA) were routinely designed and constructed. In addition to these setups offering simple demonstrations of polymer ribbon actuators in action, they also served as platforms for investigating the application of conducting polymer linear actuators in general. In this chapter, several devices are presented. These include setups designed to show conducting polymers lifting hanging masses, deflecting beams, and pulling against flexure based motion stages. Also, an approach is presented for the application of conducting polymer linear actuators to a biomimetic system.

6.1 Introduction

Chapter 5 highlighted the challenges in increasing the output performance of linear conducting polymer actuators. Substantial increases in displacement, force, and speed were demonstrated for polypyrrole based actuators created using the manufacturing methods of Chapter 3, by recording the actuators' output using the EDMA. Although these improvements are big steps forward in applying conducting polymer actuators to macroscale devices, they are by no means the end of the story. A large part of the difficulty in applying conducting polymers to real systems and engineering problems is how the actuators are connected, supported, and controlled. By incorporating the

new format polymer ribbons into stand alone devices, the engineering challenges of mechanical and electrical connection, preload, actuator tensioning and adjustment, electrical control, and friction are confronted head on.

6.2 Moving a mass

Moving or lifting a mass is a fundamental task asked of nearly all actuators. Figure 6-1 shows an experimental setup that was constructed in order to test conducting polymer linear actuators. A machined gold plated brass bath serves as the system counter electrode and the base of the system. Two parallel stainless steel rods are suspended by machined polyacetal fixtures mounted on stainless steel posts. A sliding shuttle, made of PTFE and mounted with Rulon plain bearings for low friction, is mounted on the parallel rods. The shuttle is connected by a thread to the hanging mass slung over a low friction pulley. The shuttle and one of the polyacetal fixtures house press fit capstan clamps. The clamps, wire electrical discharge machining (wire EDM) from copper and electroplated with gold, have slits machined into them lengthwise that serve as mounting points for the ribbon actuator. A conducting polymer ribbon is positioned in the slits, and the clamps are rotated so that the ribbon is wrapped about the clamps in order to increase friction via the capstan effect, thus holding the polymer in place.

This setup was found to produce a low enough level of friction to allow the polymer to lift the mass. A ruler was added to more easily monitor the actuation. The capstan clamps were found to work fine, but mounting the film was made easier by utilizing small pieces of polyimide tape to keep the polymer ribbon in the slits of the capstan clamps when the ribbon was unloaded and slack. Neat $BMIMPF_6$ was used as the electrolyte, and actuation was controlled using a potentiostat.

Figure 6-2 shows a second setup designed to lift a suspended mass. In this setup, the mass is suspended in the bath. The mass is selected by adding or removing screws in the hanging polyacetal structure. Here, electrical connection is made via aluminum crimps, fabricated by wire EDM. The crimps serve to mechanically join ribbon ends

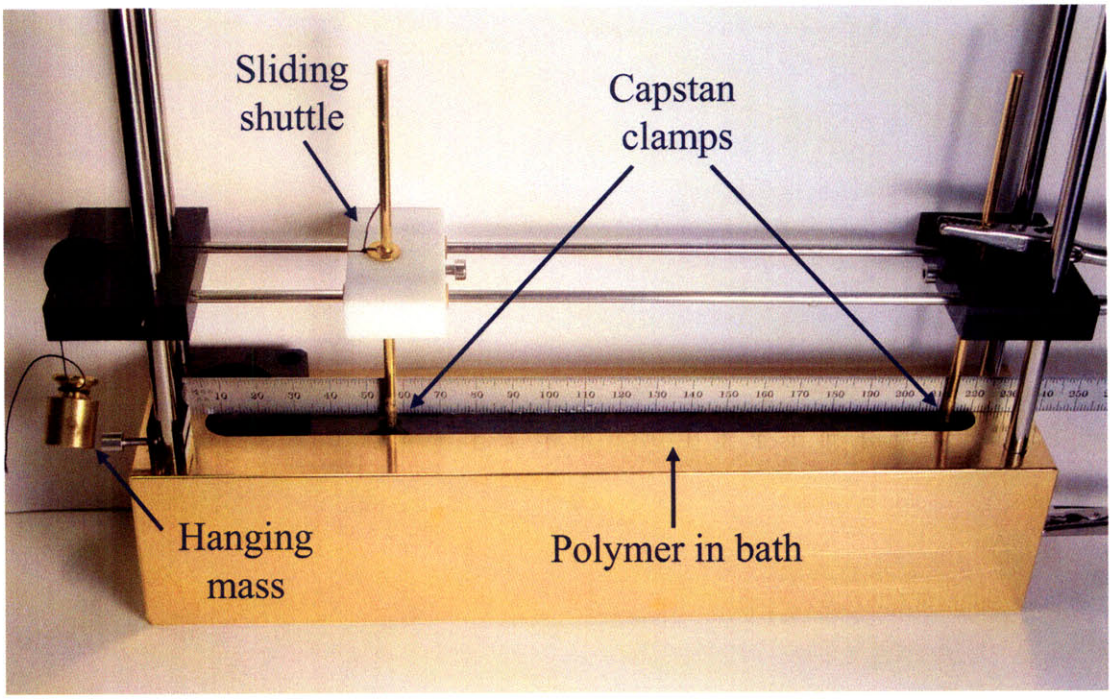

Figure 6-1: A hanging mass testing platform (from [1]).

together. The crimps are initially in the shape of a U, and the electrical wire and the polymer ends are placed in its groove. Force is then applied to close the crimp. A close up a closed crimp is shown in Figure 6-2. This method was found to provide a very good electrical and mechanical connection, more solid and robust than the rotated capstan clamps shown in Figure 6-1. It is a technique that can be applied to the connection of conducting polymer linear actuators in general. Although the crimps shown here were custom manufactured, off the shelf connectors, such as ring terminals, may provide a quick solution. An electroplating step may be required to ensure that they are nonreactive when the polymer actuator is electrochemically cycled.

6.3 Deflecting a beam

Using beam deflection to serve as an actuator preload has one large advantage: It can support the actuator with next to no friction, a large source of inefficiency in many machines and mechanisms. With no contact or rubbing surfaces, a suspended

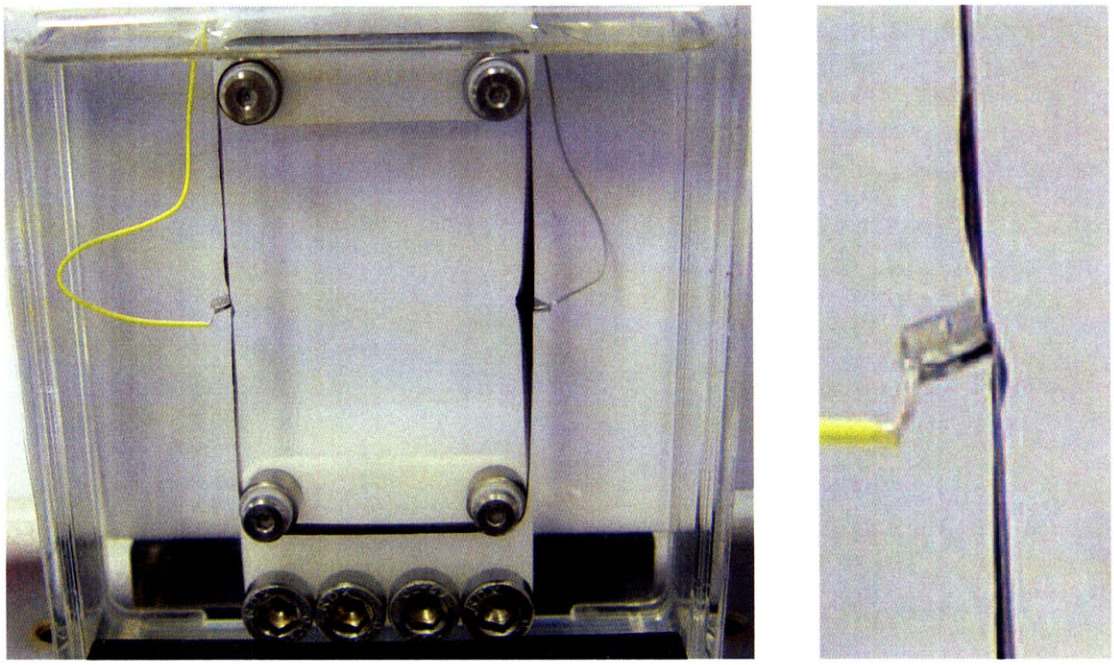

Figure 6-2: A hanging mass is suspended in an electrolyte bath. Metal crimps are used to connect the electrical wires as well as the polymer ribbon ends together.

beam will simply bend in response to a load. And, that bending is normally linear and predictable within some limited range.

Figure 6-3 shows a setup that was created where a polypyrrole based linear actuator is made to pull against a suspended beam. Two beams are shown in the figure, one constrained, and the other allowed to move. A camera was included in the setup to record the movement. The beam length was chosen to provide a suitable preloading stress on the polymer ribbon, about 2 MPa. Electrical connection is made via the beams, as can be seen in the image of the upper left. Capstan clamps, identical to those used in the setup of Figure 6-1, were used to connect the polymer ribbon actuator.

The setup shown in Figure 6-3, which is similar to that depicted in Figure 6-1, demonstrates a method of preloading a conducting polymer ribbon actuator that is essentially friction free. The images on the right in Figure 6-3 show measured contraction that resulted from the actuation of a 200 mm long, 10 mm wide gold backed conducting polymer actuator submerged in neat $BMIMPF_6$ and subjected to

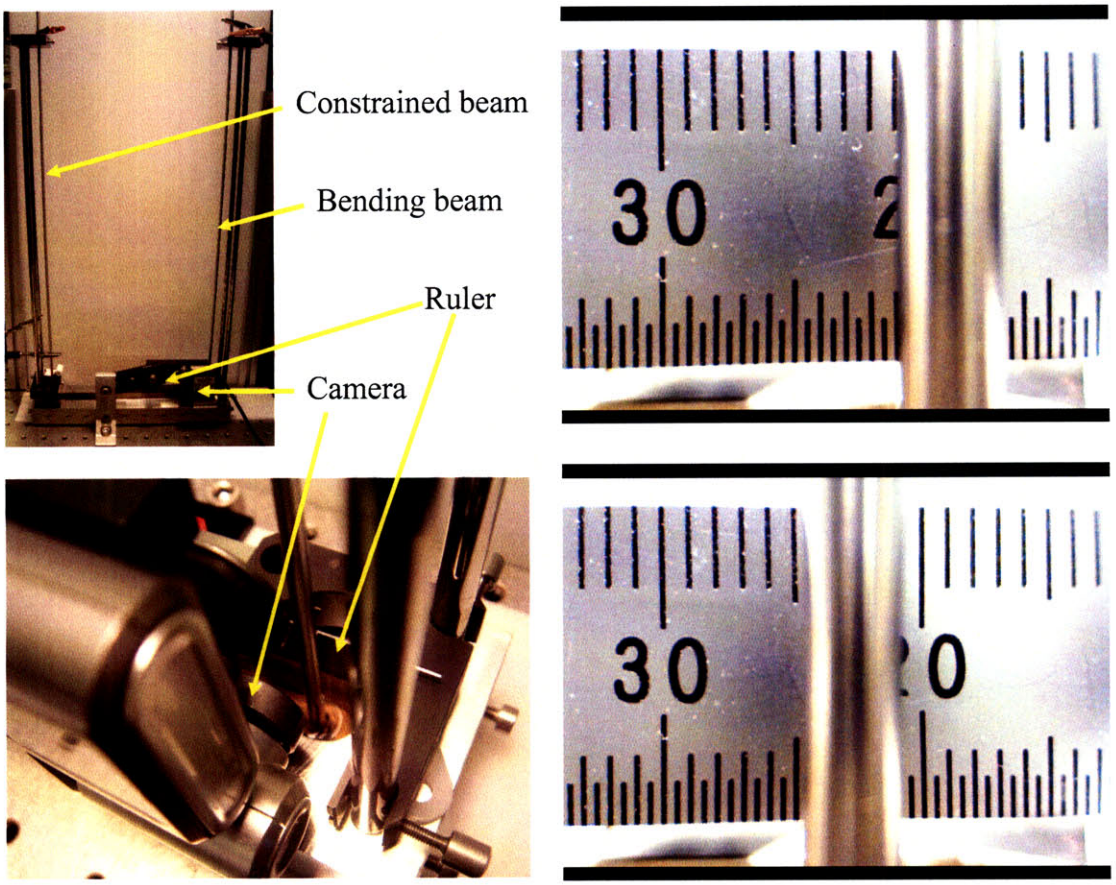

Figure 6-3: A stainless steel rod is deflected by a polypyrrole ribbon actuator and recorded by a camera.

a ± 1 V square wave input with respect to a silver reference electrode. About 4 mm of deflection is shown, which corresponds to a 2% strain.

6.4 Flexures and motion stages

Like the beam deflection described above, flexures are great mechanisms for supporting controlled movement while all but eliminating friction and hysteresis [66, 67, 68, 69]. Several flexure based stages were constructed in order to provide passive testing platforms for preloading polypyrrole based linear actuators and for investigating these actuators' incorporation into stand alone devices. Analytical models, ANSYS finite element analysis (FEA) software, and Solid Edge CAD software were utilized in order to refine these designs [67, 70, 71].

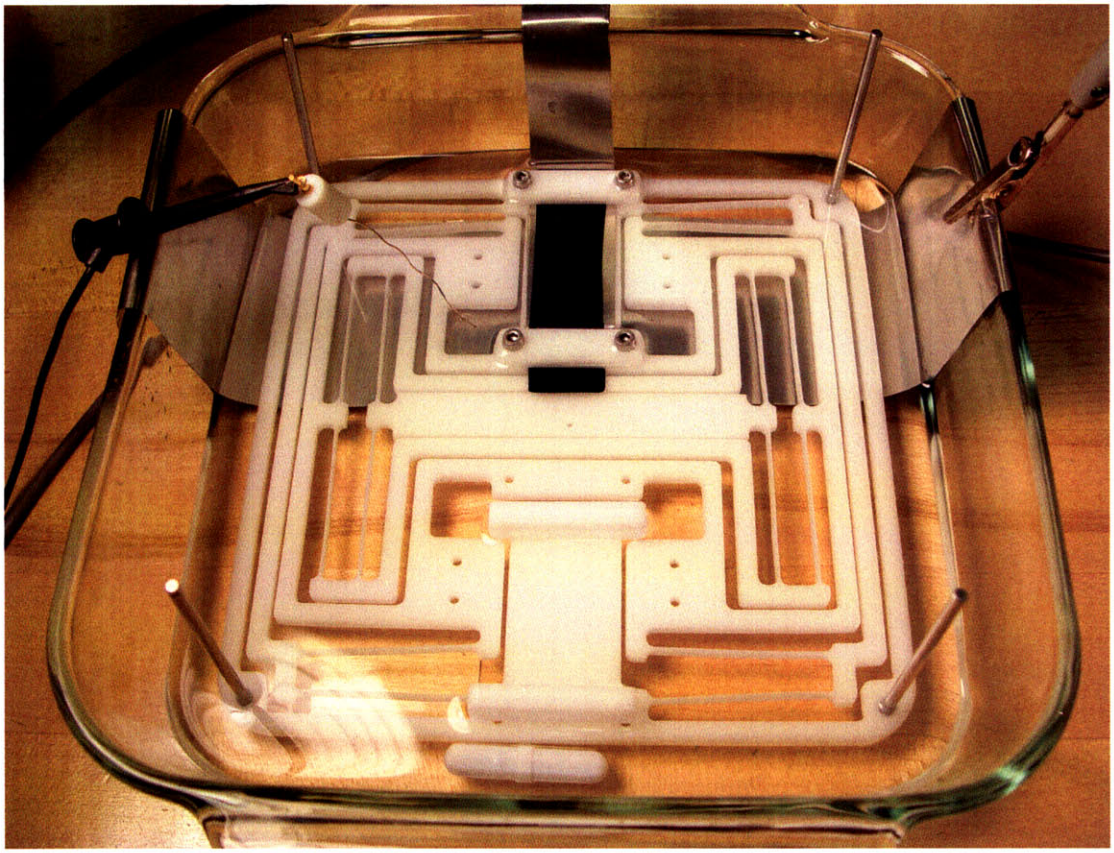

Figure 6-4: An early flexure based device incorporating a polypyrrole linear actuator. For scale, the holes and rods incorporated in the device are 3 mm in diameter.

The flexures were created by laser machining sheets of polymethyl methacrylate (Acrylic) or polyacetal (Delrin) using a Trotec Speedy 300 laser cutter [72]. The process was found to work well in producing these structures due to its ability to machine detailed and delicate structures with suitable accuracy. The use of laser machining, where no significant force is produced on the workpiece, allowed flexure designs to move beyond the use of simpler notch flexure hinges to more detailed monolithic shapes. The flexure incorporating structures could also be produced comparatively quickly, which allowed designs to be iterated and refined in a manner not possible using slower methods.

Figure 6-4 shows an early flexure based device that incorporated a polypyrrole linear actuator. A double compound flexure based design was utilized in order to create a motion stage that delivers motion along one single translational direction.

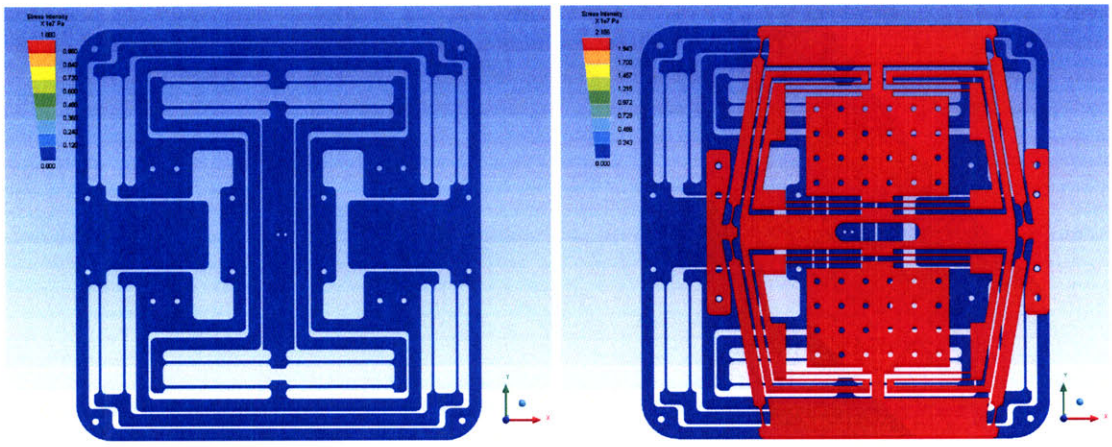

Figure 6-5: Schematic showing a flexure based motion amplifier.

This design creates controlled motion in one direction, while providing significant stiffness in the other two translational directions, as well as in rotation. Additionally, the flexures were designed so that they provide a suitable preload force on the mounted polypyrrole linear actuator. A second set of double compound flexures is included in this motion stage in order to allow for a rigid connection that can move freely in the transverse direction. For example, this scheme allows a second motion stage to be mounted on top of the first. By coupling the stages together with a rod, two dimensional motion can be achieved, where each stage is responsible for producing motion in one orthogonal direction. This idea is explored in greater detail later in this section.

The stage shown in Figure 6-4 utilized stainless steel foil for electrical connection to the polypyrrole working electrode as well as for the basis of the counter electrode. A silver wire was used as a reference electrode during actuation. Although effort was made to utilize a sizable volume of polymer in this device, output displacement was very limited. This let to a focus on increasing the amount of polymer incorporated into the motion stages and devices in general, especially by increasing the length of the ribbon actuators.

Mechanical amplification can provide an additional way of increasing actuator displacement. Flexures incorporating linkages can be designed in order to provide displacement amplification [68, 69, 70]. When it comes to power output, linear con-

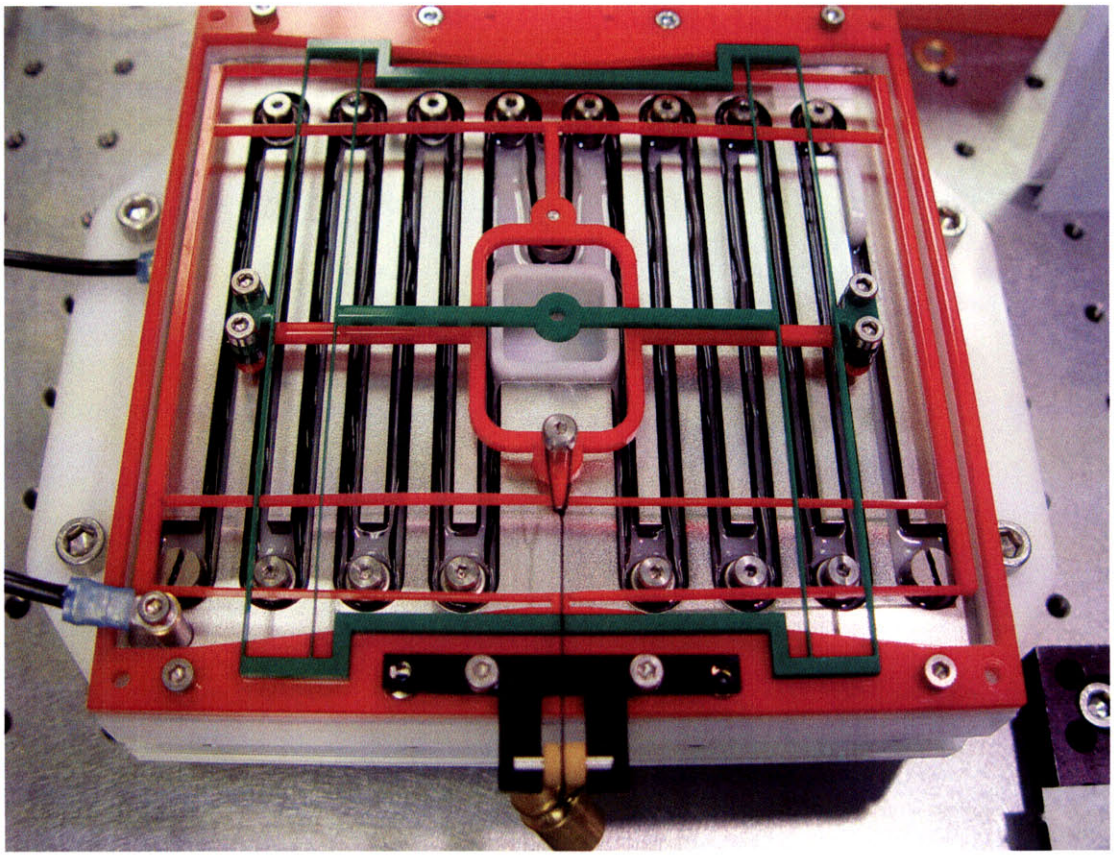

Figure 6-6: A flexure based motion stage actuated by a snaking polypyrrole ribbon actuator.

ducting polymer actuators often produce more force output and less displacement than is best suited for many applications. One can use leverage in order to increase displacement, or the actuator stroke, at a cost in force output. Figure 6-5 shows a set of flexure stages that were designed in order to increase actuator displacement by 5 times. For example, when a conducting polymer linear actuator, mounted between the hole filed plates of the upper structure, contracts by 1 mm, the lower stage moves by 5 mm. Again, ANSYS was used as a tool for creating flexures with an appropriate stiffness. This stage was fabricated by laser machining and yielded a product similar to that depicted in Figure 6-4. Although the device was not tested thoroughly, the fabricated stage did provide the expected displacement amplification and the design was validated.

The motion stage depicted in Figure 6-4 was evolved significantly in order to incor-

porate significantly longer polypyrrole ribbon actuators. Figure 6-6 shows a flexure based motion stage actuated by a 1.5 m snaking polypyrrole ribbon actuator. The stage consists of a electrolyte bath, a polypyrrole ribbon actuator, a counter electrode, tensioning mechanisms, and a set of flexures to control the motion. The bath was machined from polyacetal and incorporates a central hole through which a connecting rod can pass. The ribbon actuator in each stage is 1.5 m long, 5 mm wide and 22 μm thick. The ribbon layout was designed to enable a 15 mm range of travel with actuator strains of less than 2%, a value typically achievable from this actuator [73]. The polymer is snaked around pulleys that consist of either stainless steel bushings sitting on stainless steel dowels press fit into the acetal bath, or needle bearings sitting on shoulder screws, as depicted in Figure 6-6. The dowels are connected electrically beneath the bath in order to provide charge injection at multiple points along the actuator, thus reducing ohmic potential drop effects. A central pulley is mounted on the flexure system and moves upon actuation, thus giving an effective actuator cross section of twice the polymer ribbon cross section. The stainless steel counter electrode, manufactured by wire EDM, was designed to be equidistant from the snaking polymer actuator at all points. Tension control is required in order to preload the actuators and to allow for swelling and creep effects. Stainless steel snug fit dowels at each end of the actuator, used analogously to a violin string tuning peg, were incorporated for this task.

The flexures were designed to meet the preload requirements of the polymer ribbon actuator. Double compound flexures were again used in order to achieve linear motion. The flexures where designed using analytical calculations in conjunction with FEA to provide a restoring force corresponding to a stress of 2 MPa on the polymer actuator at 15 mm of displacement. Each flexure is actuated by twice the ribbon cross section, or 2.2×10^{-7} m^2, which corresponds to a force of 0.44 N. The flexures were machined from 3 mm acrylic sheet using a Trotec Speedy 300 laser cutter [72]. An additional adjustable preload force is applied to the actuator via a hanging mass as shown in Figure 6-9.

In addition to using analytical and FEA tools to predict and study flexure behav-

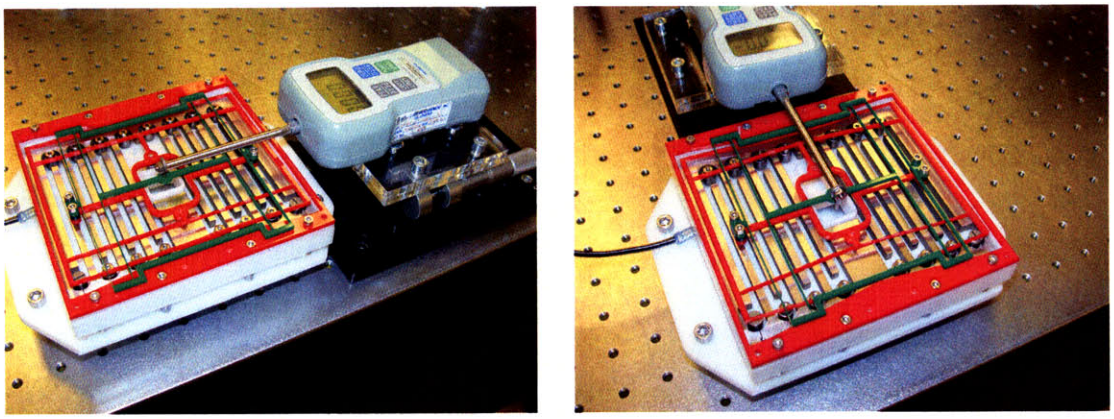

Figure 6-7: A flexure based stage is characterized with a force gauge mounted on a precision stage indexable by a micrometer. The left image shows the upper flexure being characterized, and the right image shows the lower flexure being characterized.

ior, physical tests were conducted. Figure 6-7 shows flexure stages being characterized using a force gauge mounted on a precision stage indexable by a micrometer. Data collected using these instruments is shown in Figure 6-8. As can be readily seen in these plots, flexure deflection can be very linear with applied force. This characterization validated FEA as a useful tool in predicting the behavior of flexures created to deliver a given preload stiffness.

The motion stages shown in Figure 6-4 and Figure 6-6 were both designed to be stackable at 90 degrees in order to achieve motion in an X-Y plane, where each stage is responsible for motion in one orthogonal direction. The stages are joined together via a connecting rod that attaches to the upper flexure on each stage. In keeping the motion delivered by each stage along a single rectilinear axis, the motion stages are effectively decoupled and each actuator completely determines the rod position in one rectilinear direction, in this case within a 15 mm $\times$ 15 mm X-Y plane. This allows the rod position to be more easily controlled and the performance of each actuator to be more easily monitored.

Although conducting polymer based rotary motors have been proposed [22], a low voltage conducting polymer powered continuously rotating device has not yet been achieved. A modification to the X-Y stage concept was made in order to achieve rotary motion of a rotational platform actuated via the connecting rod joining the

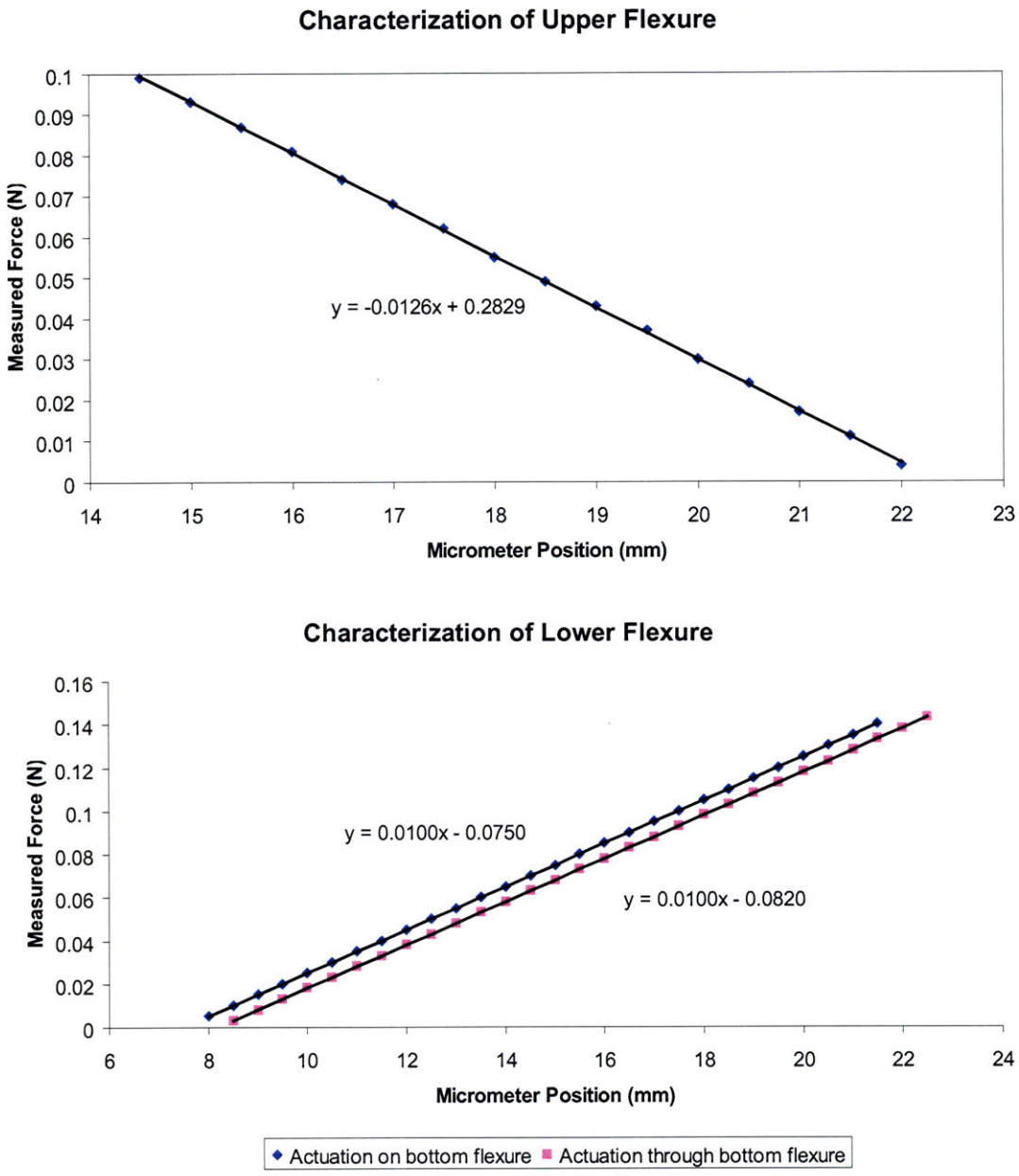

Figure 6-8: Data showing the characterization of the flexure based stage.

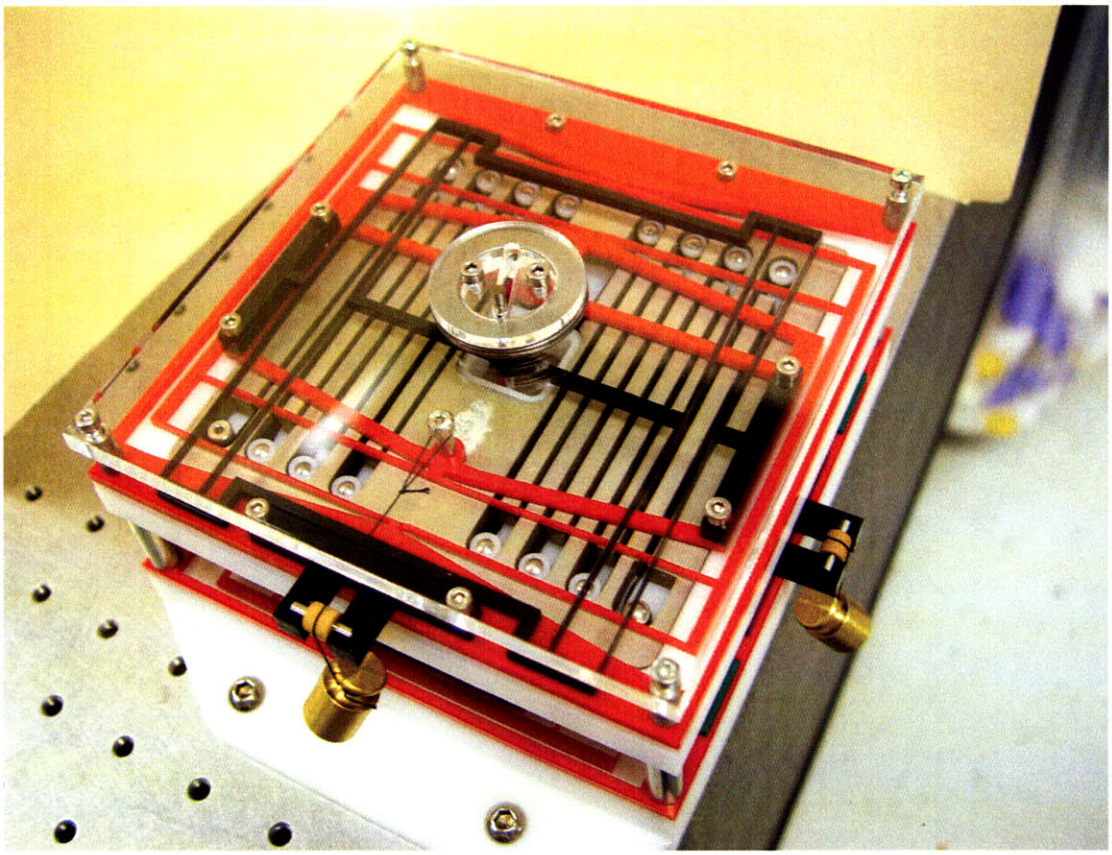

Figure 6-9: Image of a rotary motor utilizing two polypyrrole ribbon actuators. The system is comprised of two motion stages as shown in Figure 6-6, offset by 90 degrees.

two orthogonal stages. The connecting rod provides the eccentric required to turn a rotary platform that rests on a needle thrust bearing. The rotary platform has a 3 mm groove machined in it which allows the connecting rod the freedom to move radially. By stacking a second double compound flexure on top of the first in each stage, the connecting rod is constrained in a vertical orientation.

Rotary motion is achieved by actuating the polymer ribbons with periodic waveforms 90 degrees out of phase which moves the connecting rod through a circular path and turns the rotational platform via the developed eccentric. An assembled rotary motor is shown in Figure 6-9. The device is comprised of two motion stages similar to that depicted in Figure 6-6.

Throughout this work, the pairing of flexures with conducting polymer actuators appeared logical and promising, although the rollers or pulleys used at the time

suffered from friction problems and reduced the outputted motion. Laser cutting monolithic acrylic flexures proved to be a reliable and relatively simple method for achieving the forces and motions required for the motion stages. Friction at the stainless steel bushing/dowel interface was significant, however, and investigation into alternative bearing options is warranted. It is important to note that this work was performed before the methods for incorporating the gold conducting layer onto the polypyrrole ribbon actuators were devised, and in fact helped show that the development was needed.

6.5 Fish fin studies

The motion of a swimming fish's fins are of particular interest to biologists, fluid dynamicists, and engineers [74, 75, 8, 76, 1]. There is a lot that can be learned by observing, studying, and even mimicking nature. As part of a larger collaboration [74, 75, 8, 76], the MIT BioInstrumentation Laboratory has been involved with a project to create a biorobotic fish fin that uses conducting polymer actuators [77, 1]. It is envisioned that key motions and behaviors of a pectoral fin like that of the bluegill sunfish *Lepomis macrochirus*, shown in Figure 6-10, can be mimicked using a fin utilizing conducting polymer actuators.

The fin is being developed to have linear dimensions approximately four times that of the biological fin. In order to maintain similarity, the fin must be flapped at 0.4 to 0.8 Hz, and a 1 to 5 N force is required over a displacement of 1 to 2 mm. Conventional actuator technologies were applied to this project first, but a goal of this work is to move conducting polymer actuator based systems to a point where they can be applied to an application such as this. The fabrication of long, uniform actuators with conductors incorporated for increased speed and overall displacement brings this application within reach. It is anticipated that some form of mechanical amplification, parallel actuation, or both will additionally be required in order to achieve the desired motions.

Figure 6-11 shows a schematic of how conducting polymer based actuators could

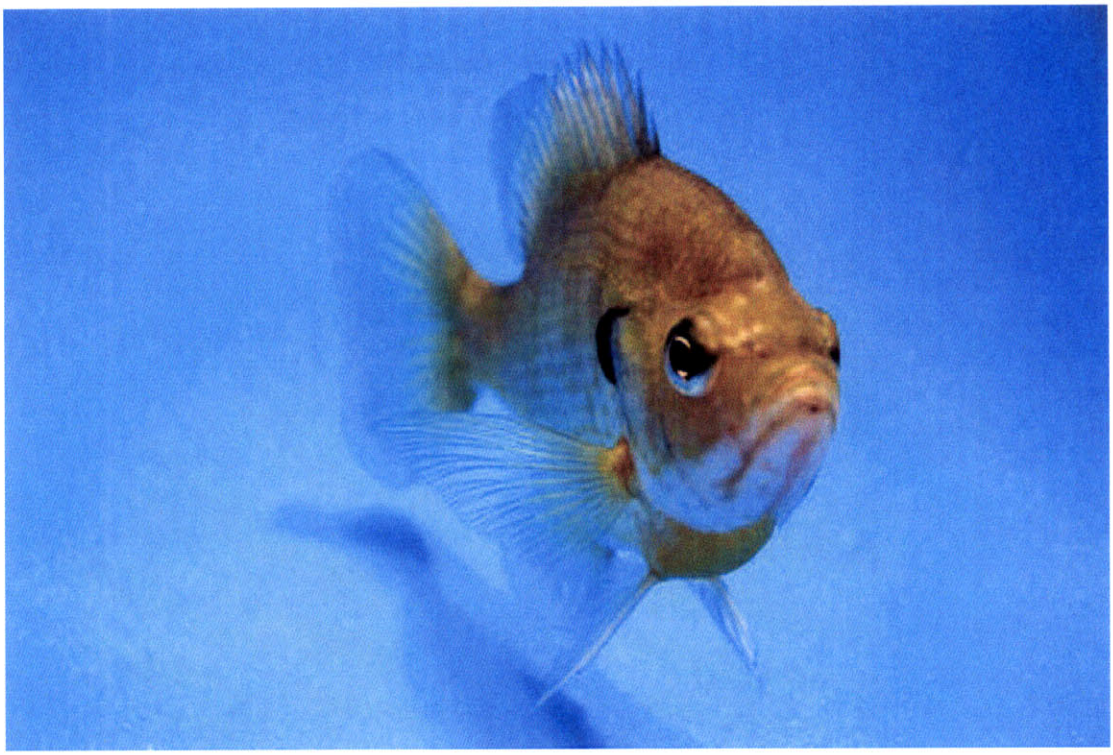

Figure 6-10: A bluegill sunfish's right pectoral fin is shown extended from its body (from [8]).

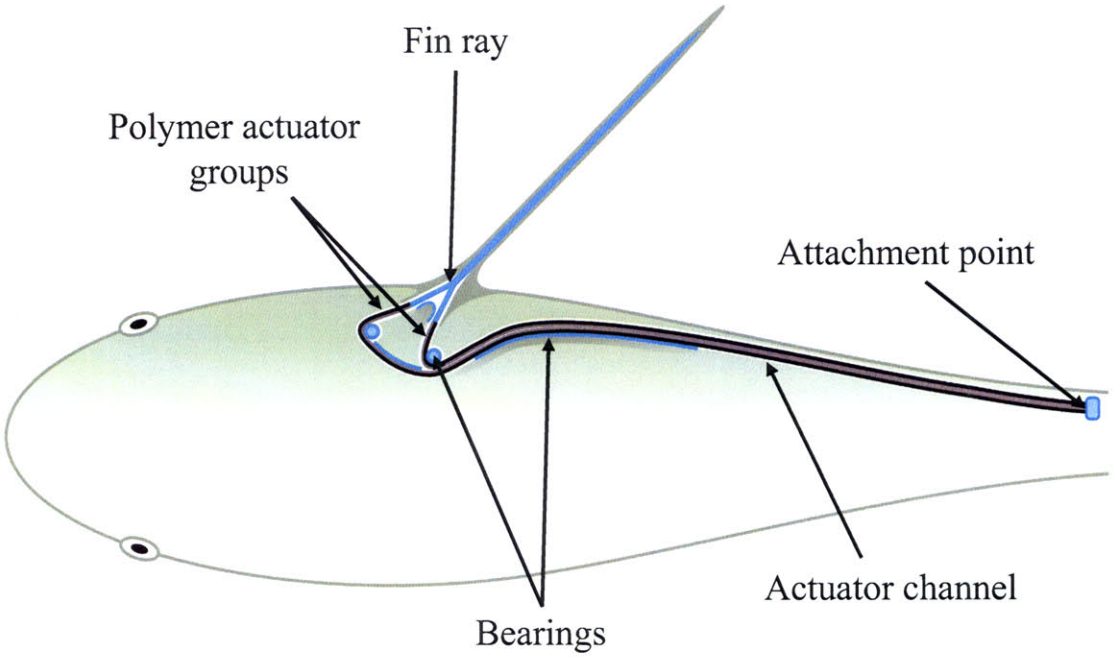

Figure 6-11: Schematic showing how conducting polymer actuators could be applied to a biorobotic fish in order to control the movement and stiffness of the pectoral fin [1].

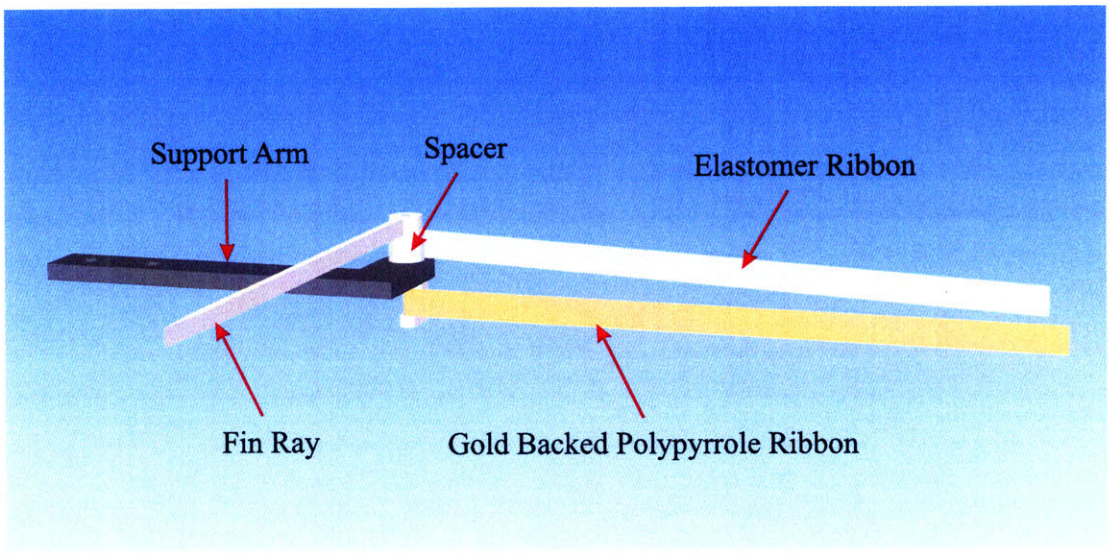

Figure 6-12: Front view of a design for rotationally actuating a fin ray.

be applied to drive a pectoral fish fin. In this depiction layered bilayer or trilayer actuators are incorporated into the fins in order to control curvature and stiffness (as demonstrated in Figure 1-2), and linear conducting polymer actuators are used to provide the larger rotational motions. As shown in Figure 6-11, bearings could be applied in order to guide or constrain the linear actuators within suitable actuator channels incorporated into the artificial fish.

Figure 6-12, Figure 6-13, and Figure 6-14 show a design for creating rotary motion of an artificial pectoral fin ray. A gold backed polypyrrole ribbon actuator is wrapped about dowel protruding from a low friction bearing fixtured in a support arm. The ribbon actuator is mechanically fixtured at the far end, and upon actuation, the force is transferred around the dowel to the local fixture point. A preload force is applied using a stretched elastomer similarly attached to a spacer attached around the suspended dowel. When the actuator contracts, the force is applied through a lever arm equal to the radius of the dowel, thus potentially achieving a high degree of leverage and a significant angular rotation of the fin ray.

Figure 6-15 shows an image of a fin ray actuated by a gold backed polypyrrole ribbon actuator in the design depicted in Figure 6-12, Figure 6-13, and Figure 6-14. The fin ray rotates on an ball bearing encased in the machined acrylic mount. An

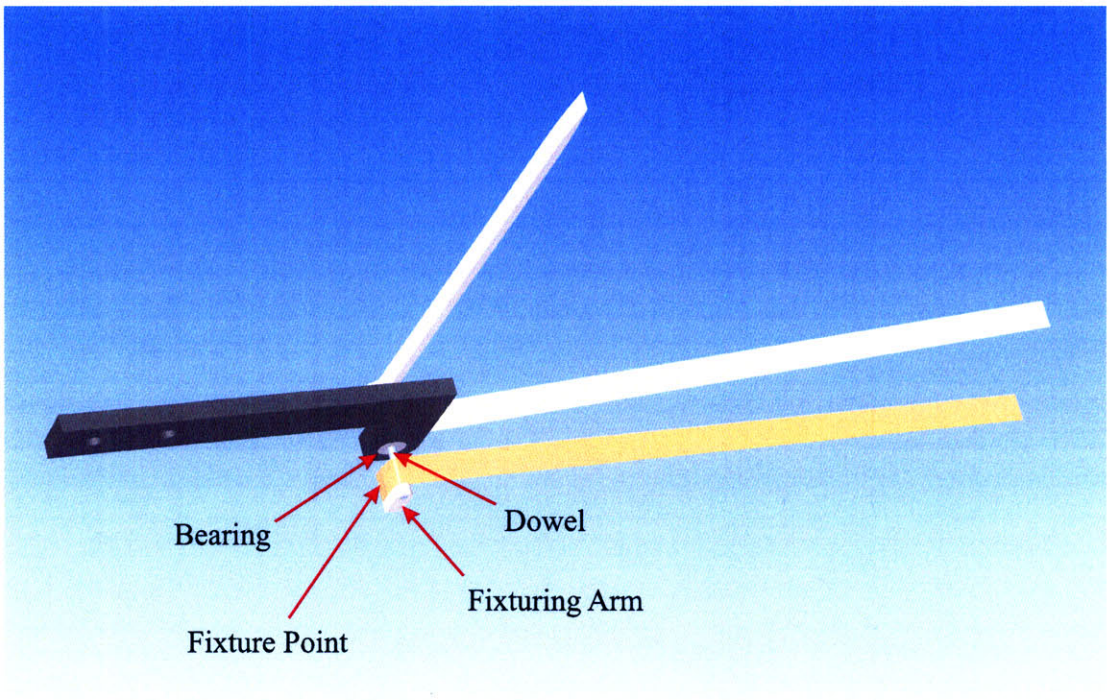

Figure 6-13: Bottom view of a design for rotationally actuating a fin ray.

elastomer is used for the restoring force and a 1.6 mm diameter dowel was used. This fin ray demonstrated tip displacements of over 50 mm at 0.2 Hz and 10 mm at 2 Hz.

It is envisioned that fin rays of this design could be stacked and joined together with a webbing in order to create a fin. The rays could then be actuated in and out of phase as needed in order to achieve a variety of motions. Actuation in fluid rather than air presents a number of challenges, however. These include a larger requirement for force or torque output and sealing of the actuator system.

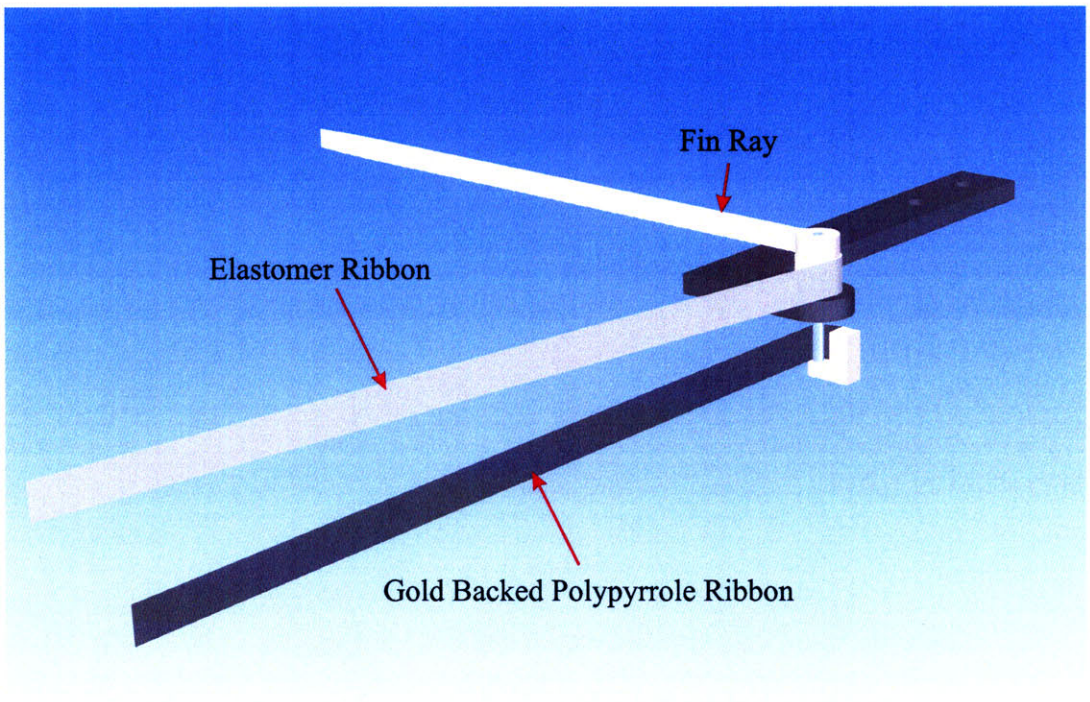

Figure 6-14: Back view of a design for rotationally actuating a fin ray.

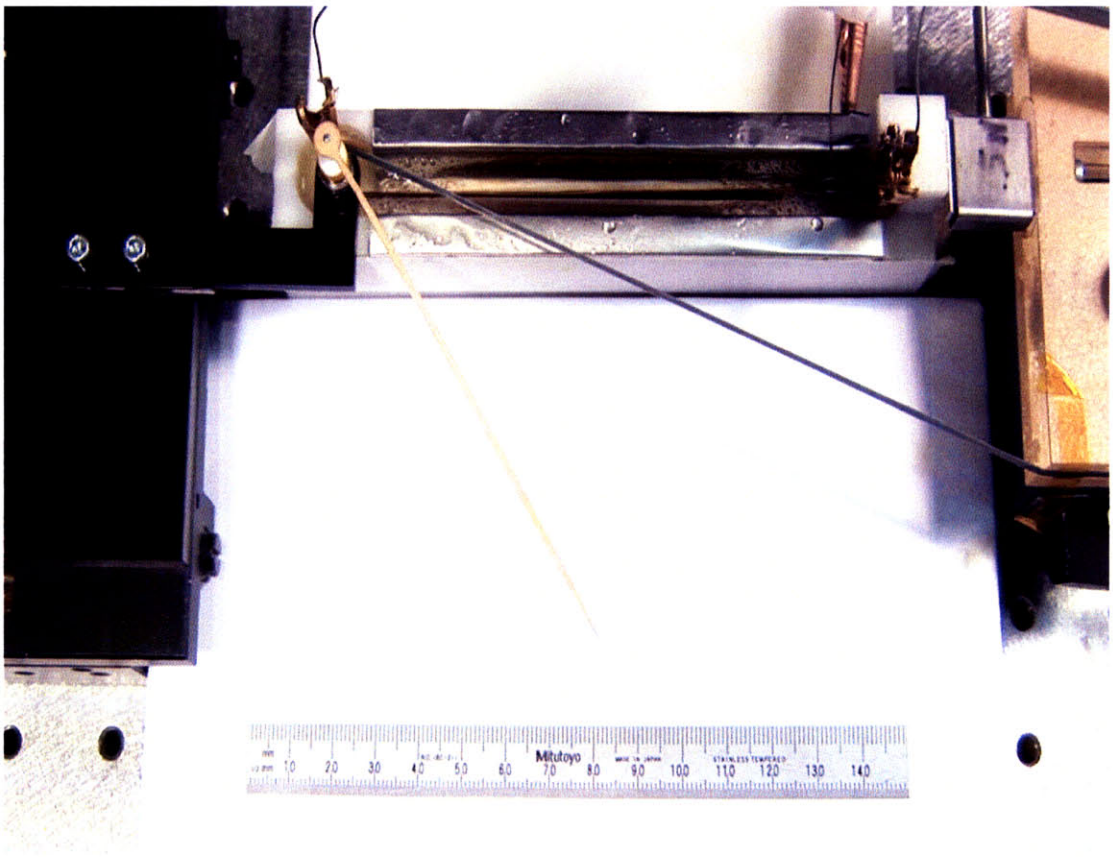

Figure 6-15: Image of a fin ray actuated by a gold backed polypyrrole ribbon actuator preloaded by an elastomer ribbon. This is a realization of the design depicted in Figure 6-12, Figure 6-13, and Figure 6-14.

Chapter 7

Conclusions

This thesis presents work undertaken with a general goal of moving conducting polymer linear actuators closer to use as viable and convincing engineering materials. Of particular interest is the application of these materials to biomimetic devices, where the actuators could be used as *artificial muscles.* Biomimetic systems would benefit from the incorporation of actuators with combinations of properties common to biological systems, for example low density, controllable mechanical flexibility, and compact size. Several technologies exist today that are often classified as artificial muscles. A key component separating an artificial muscle from a conventional actuator is its ability to directly generate sizeable strains at reasonable stresses. This leads to the possibility of directly driving a load without a gearbox or other mechanisms that would add size, increase complexity, and reduce efficiency.

Chapter 1 listed a number of technologies often touted as artificial muscles. Of these, conducting polymer actuators were selected as the basis of this work. Because of a desire to explore macroscale actuation, conducting polymer linear actuators were selected over layered actuators. Layered actuators are limited in their configurability in that they generally produce one single bending motion, and it is difficult to configure and attach a layered actuator so that its curving motion is able to deliver a sizable and consistent force. Linear polymer actuators are always used preloaded, which is generally easier to work with when designing complementary hardware. Linear actuators can also be scaled more easily than layered actuators.

A conducting polymer linear actuator, in its simplest form, consists of a ribbon of polymer film connected at its two ends. Normally, one or both of these connections also serve as the electrical connection used to charge and discharge the film with respect to a counter electrode, thus causing an expansion or contraction. A preload force is applied by means of a carefully devised instrument, as described in Chapter 4, or by a hanging mass or a stretched elastomer, as described in Chapter 6.

The mechanisms of conducting polymer actuation and the state of the art in conducting polymer actuator performance were reviewed in Chapter 2. Before this work, conducting polymer linear actuators were produced primarily with small physical dimensions, and their output was generally limited to displacements of less than 0.5 mm, forces of less than 1 N, and cycle frequencies of less than 0.1 Hz. Conducting polymer linear actuators were rarely tested on a length scale of more than a few millimeters, and their incorporation into real applications was limited. It was a goal of this work, therefore, to make strides in improving the magnitudes of these outputs. With this in mind, effort was made on two fronts: To develop and refine manufacturing techniques that could reliably produce conducting polymer linear actuators at scales never achieved before. And, to develop approaches, techniques, and hardware that would allow these actuators to be used reliably in stand alone devices, possibly utilizing some degree of mechanical leverage.

As mentioned in Chapter 2, scaling conducting polymer linear actuators for use in macroscale devices comes with a set of challenges. In increasing the size of the actuators, several significant issues become more pronounced. For example, if an electrical connection is made at a single end of a polymer strip, the sizeable resistance of the polymer film causes an ohmic potential drop along the length of the polymer which impacts its performance as an actuator. Also, because strain rate is related to the diffusion of the ions into and out of the polymer, it is impacted by the film thickness. Thicker films actuate more slowly. Focus was placed on improving the output properties of polypyrrole based linear actuators by shortening two limiting time constants: One related to the actuator's length, and one related to the actuator's thickness.

7.1 Major contributions

Measurable improvements in conducting polymer based actuation were achieved through this work. These improvements were a result of new and novel manufacturing procedures that improved the actuator composition and of the development of supporting hardware that leveraged the actuators'capabilities. Numerous devices and experiments were designed, built, and performed in order to characterize and demonstrate the newly created ribbon actuators. The major contributions within this work are summarized below.

New manufacturing methods were devised in order to fabricate long ribbon-like conducting polymer linear actuators. These methods were presented in Chapter 3. A custom slicing tool was designed and built for use in a CNC turning center. A procedure utilizing this tool was then developed, and it enabled polypyrrole actuators to be constructed on scales never before realized. Polymer ribbons were created with uniform thicknesses of 10 to 30 μm, widths of 20 μm to 20 mm, and lengths exceeding 5 m, for example. A second method was devised where a conductive gold layer is incorporated into the ribbons using an electroplating procedure. These fabrication techniques are generally scalable. For the generation of larger quantities of film, batch processing could be applied to the slower processes. For example, several crucibles could be utilized and electrodeposited with conducting polymer simultaneously. Faster steps, like slicing and removing the polymer ribbons, could be performed one at a time while another array of crucibles are coated with polymer.

These new manufacturing methods enabled significant improvements in actuator output. Chapter 4 described the techniques utilized in characterizing conducting polymer linear actuators. Those techniques were expanded and applied to the macroscale actuators, as described in Chapter 5. A multipoint measurement apparatus was developed for this task and was found to perform well. The conductive layer was found to enhance the electrical response of the polypyrrole based ribbons. Increases were made to the key actuator output metrics of displacement, actuation speed, and force output. Generally, gains were made by utilizing longer lengths of conducting polymer

made available using the new manufacturing techniques. Additionally, the increased uniformity and added conductivity of these ribbon actuators were found to have a positive impact on their performance. Displacements of 4 mm and usable cycle speeds of 2 Hz were demonstrated. The gold layer also showed a positive effect on creep, allowing the actuators to be repeatedly cycled with little adjustment over time.

Parallel actuation was explored as a method of achieving greater forces without compromising actuation speed. For example, a device utilizing twenty parallel conducting polymer ribbon lengths demonstrated the ability of pulling 10 N over a strain of 1.5%, multiplying the previously reported maximum displaced isotonic load by five. This device, described in Chapter 5, utilized a single polymer linear actuator that was snaked around a series of PTFE rollers and dowels in order distribute the polymer ribbon tension between the parallel lengths. The rollers were found to perform well in averaging the tension. The new longer actuator form factor, measured in meters rather than millimeters, enabled new approaches to familiar problems. For example, the use of a single long ribbon that woven back and forth around rollers eliminated the need to individually tension the contributing members - a large source of lost output in previously reported systems.

The integration of these actuators into stand alone systems that include joints and flexures has yielded novel techniques in amplifying motion while minimizing friction, improving electrical connection, and increasing actuator lifetime. Much like a gear ratio is selected to bring the output of a given motor into a desirable range, an analogous mechanical design can be applied to a conducting polymer actuator in order to achieve an output that best matches the capabilities necessary for a given application. This was demonstrated with the flexure based stages and fin ray devices of Chapter 6.

The challenges of incorporating conducting polymer actuators into a biomimetic system were discussed and an approach was introduced in Chapter 6. The realized device incorporated a highly mechanically leveraged system based on a gold backed conducting polymer linear actuator. The device was found to demonstrate suitable output motion in air, and the design is scalable to an array of fin rays, each similarly

actuated. The improvements realized through this work move polypyrrole linear actuators, and conducting polymers in general, closer in fit to application in stand alone devices and biomimetic devices.

7.2 Future work

In order for conducting polymer to properly compete with more conventional linear actuator technologies for use in macroscale applications, connection, encapsulation, and control issues need to be further addressed. Electroactive polymers, such as polypyrrole, require an ionic reservoir to supply the ions required for actuation. When these actuators are applied to a system, the bath must be incorporated as well in some form. For some applications, adding a capsule or channel to hold the electrolyte is acceptable. For many applications, however, it would be advantageous to have an actuator that is encapsulated in a way that preserves more of the actuator's advantages, like its compactness and its mechanical flexibility. One approach is to encapsulate the conducting polymer linear actuator in an elastomer along with a counter electrode, a permeable nonconductive separator, and an ionic reservoir. The nonactuating components should be made as compliant as possible in order to achieve a true ribbon-like stand alone actuator system usable in a variety of mediums, including air. Silicone was investigated as an encapsulant for this purpose, as described in Chapter 3, and it proved promising, although more investigation and a refinement of application techniques are required.

It may be advantageous to eventually hide many of the actuator subtleties from the end user. Much like typical battery cells can be used today with no knowledge of their chemical interworkings, one can imagine a conducting polymer actuator system being analogously manufactured. The system would certainly include an encapsulating outer skin to hold the required ionic reservoir, but it could also potentially include driving electronics, sensors to monitor electrical and mechanical states and properties, and a control system specific to the technology that would simplify the actuator's use in practise.

New materials are continuously under development by many groups focused on actuator development. Relating to conducting polymers, of particular interest is the prospect of incorporating or blending conductive materials such as carbon nanotubes into the polymer actuator as it is electrodeposited. This additive could be made to display order at a number of possible scales, or even layered between layers of conducting polymer. Or, it could be simply uniformly distributed. In any case, these additives are expected to provide a beneficial effect, perhaps like the electroplated gold layer, on the ohmic drop observed along longer films, as well as on creep displayed by the actuators as they are used.

Appendix A

Polymer slicing using the Mazak turning center

As discussed in Chapter 3, polypyrrole ribbons were sliced from polypyrrole films previously electrodeposited onto glassy carbon crucibles. This was accomplished using a custom built tool mounted in a Mazak Super Quick Turn 15MS turning center. Included below is a sample of G Code used to cut a threadlike spiral pattern through the film. The G Code was generated using FeatureCAM software [59] with a postprocessor suitable for the Mazak turning center. It should be noted that several alterations could be made to this code that would lead to a similar or even identical result. This program brings the custom tool, described in Chapter 3, to position 10 mm off of the mounted glassy carbon crucible, lowers it by 20 mm, thus preloading it 10 mm into the tool's incorporated springs. It then performs a threading pattern, here at a pitch of 20 μm, and then removes the tool straight out from the crucible and then back to the resting position.

```
%
N20 G18 G21 G40
N25 G50 S4000
N30 G53
N35 G99 M202
N40 G13.1 G18
N45 M01
N50 G28 U0. W0.
N55 G53
N60 T0404
N65 G99 G97 S120 M04
N70 G00 X94.998 Z0.M8
N75 X54.975
N80 G32 Z-2.0 E0.02
N85 G00 X115.0
N90 M09
N95 M05 M205
N100 G28 U0. W0.
N105 G53
N110 M30
%
```

Table A.1: Example G Code used to cut the spiralling slicing pattern on the Masak turning center.

Bibliography

[1] J. Tangorra, P. Anquetil, T. Fofonoff, A. Chen, M. Del Zio, and I. Hunter. The application of conducting polymers to a biorobotic fin propulsor. *Bioinspiration & Biomimetics*, 2(2):S6–S17, 2007.

[2] P. Anquetil. *Large Contraction Conducting Polymer Molecular Actuators.* PhD Thesis, Massachusetts Institute of Technology, 2004.

[3] P. G. A. Madden. *Development and Modeling of Conducting Polymer Actuators and the Fabrication of a Conducting Polymer Based Feedback Loop.* PhD Thesis, Massachusetts Institute of Technology, 2003.

[4] M. Del Zio. *Conducting Polymer Actuators: Temperature Effects.* Masters Thesis, Massachusetts Institute of Technology, 2006.

[5] J. Ding, L. Liu, G. M. Spinks, D. Z. Zhou, G. G. Wallace, and J. Gillespie. High performance conducting polymer actuators utilising a tubular geometry and helical wire interconnects. *Synthetic Metals*, 138(3):391–398, 2003.

[6] R. Z. Pytel. *Artificial Muscle Morphology - Structure/Property Relationships in Polypyrrole Actuators.* PhD Thesis, Massachusetts Institute of Technology, 2007.

[7] N. Vandesteeg. *Synthesis and Characterization of Conducting Polymer Actuators.* PhD Thesis, Massachusetts Institute of Technology, 2007.

[8] R. Mittal, H. Dong, M. Bozkurttas, G. V. Lauder, and P. Madden. Locomotion with flexible propulsors: II. Computational modeling of pectoral fin swimming in sunfish. *Bioinspiration & Biomimetics*, 1(4):S35–S41, 2006.

[9] J. D. W. Madden, N. A. Vandesteeg, P. A. Anquetil, P. G. A. Madden, A. Takshi, R. Z. Pytel, S. R. Lafontaine, P. A. Wieringa, and I. W. Hunter. Artificial muscle technology: Physical principles and naval prospects. *IEEE Journal of Oceanic Engineering*, 29(3):706–728, 2004.

[10] I. Hunter and S. Lafontaine. A comparison of muscle with artificial actuators. In *5th Technical Digest, IEEE Solid State Sensors and Actuators Workshop*, pages 178–185, Hilton Head Island, SC, 1992.

[11] A. Della Santa, D. De Rossi, and A. Mazzoldi. Characterization and modelling of a conducting polymer muscle-like linear actuator. *Smart Materials & Structures*, 6(1):23–34, 1997.

[12] P. G. A. Madden, J. D. W. Madden, P. A. Anquetil, N. A. Vandesteeg, and I. W. Hunter. The relation of conducting polymer actuator material properties to performance. *IEEE Journal of Oceanic Engineering*, 29(3):696–705, 2004.

[13] A. S. Hutchison and Wallace. Development of polypyrrole-based electromechanical actuators. *Synthetic Metals*, 113:121–127, 2000.

[14] L. Bay, K. West, P. Sommer-Larsen, S. Skaarup, and M. Benslimane. A conducting polymer artificial muscle with 12% linear strain. *Advanced Materials*, 15(4):310–313, 2003.

[15] J. D. Madden, R. A. Cush, T. S. Kanigan, and I. W. Hunter. Fast contracting polypyrrole actuators. *Synthetic Metals*, 113(1-2):185–192, 2000.

[16] S. Pei and O. Inganas. Electrochemical applications of the bending beam method. 1. Mass transport and volume changes in polypyrrole during redox. *Journal of Physical Chemistry*, 96:10507–10514, 1992.

[17] Q. Pei and O. Inganas. Electrochemical applications of the bending beam method. 2. Electroshrinking and slow relaxation in polypyrrole. *Journal of Physical Chemistry*, 97:6034–6041, 1993.

[18] E. Smela, M. Kallenbach, and J. Holdenried. Electrochemically driven polypyrrole bilayers for moving and positioning bulk micromachined silicon plates. *Journal of Microelectromechanical Systems*, 8(4):373–383, 1999.

[19] E. Smela, O. Inganas, and I. Lundstrom. Controlled folding of micrometer-size structures. *Science*, 23:1735–1738, 1995.

[20] J. D. Madden, R. A. Cush, T. S. Kanigan, C. J. Brenan, and I. W. Hunter. Encapsulated polypyrrole actuators. *Synthetic Metals*, 105(1):61–64, 1999.

[21] M. K. Andrews, M. L. Jansen, G. M. Spinks, D. Z. Zhou, and G. G. Wallace. An integrated electrochemical sensor-actuator system. *Sensors and Actuators a-Physical*, 114(1):65–72, 2004.

[22] B. Schmid. *Characterization of Macro-Length Conducting Polymers and the Development of a Conducting Polymer Rotary Motor.* Masters Thesis, Massachusetts Institute of Technology, 2005.

[23] G. M. Spinks, T. E. Campbell, and G. G. Wallace. Force generation from polypyrrole actuators. *Smart Materials & Structures*, 14(2):406–412, 2005.

[24] J. D. Madden. *Conducting Polymer Actuators.* PhD Thesis, Massachusetts Institute of Technology, 2000.

[25] S. Roth. *One-Dimensional Metals.* VCH, New York, 1995.

[26] A. Della Santa, D. De Rossi, and A. Mazzoldi. Performance and work capacity of a polypyrrole conducting polymer linear actuator. *Synthetic Metals*, 90(2):93–100, 1997.

[27] C. O. Chiang, C. R. Fincher, Y. W. Park, A. J. Heeger, H. Shirakawa, E. J. Louis, S. C. Gau, and A. G. MacDiarmid. Electrical conductivity in doped polyacetylene. *Physical Review Letters*, 39(17):1098–1101, 1977.

[28] A. Heeger. Semiconducting and metallic polymers: The fourth generation of polymeric materials. *Synthetic Metals*, 125:23–42, 2002.

[29] T. Herod and J. Schlenoff. Doping-induced strain in polyaniline: Stretchoelectrochemistry. *Chemistry of Materials*, 5:951–955, 1993.

[30] B. Dufour, P. Rannou, D. Djurado, M. Zagorska, I. Kulszewicz-Bajer, and A. Pron. The role of chain and dopant engineering in the preparation of processable conducting polymers with desired properties. *Synthetic Metals*, 135-136:63–68, 2003.

[31] B. Dufour, P. Rannou, D. Djurado, M. Bee, and A. Pron. Doping-induced stretchability of metallic poly(aniline). *Synthetic Metals*, 135-136:323–324, 2003.

[32] E. Smela, W. Lu, and B. Mattes. Polyaniline actuators part 1. PANI(AMPS) in HCl. *Synthetic Metals*, 151:25–42, 2005.

[33] E. Smela and B. Mattes. Polyaniline actuators part 2. PANI(AMPS) in methanesulfonic acid. *Synthetic Metals*, 151:43–48, 2005.

[34] M. R. Gandhi, P. Murray, G. M. Spinks, and G. G. Wallace. Mechanism of electromechanical actuation in polypyrrole. *Synthetic Metals*, 73(3):247–256, 1995.

[35] E. Smela and N. Gadegaard. Surprising volume change in PPy(DBS): An atomic force microscopy study. *Advanced Materials*, 11(11):953, 1999.

[36] E. Smela and N. Gadegaard. Volume change in polypyrrole studied by atomic force microscopy. *Journal of Physical Chemistry B*, 105(39):9395–9405, 2001.

[37] J. Reynolds, C. Baker, C. Jolly, P. Poropatic, and J. Ruiz. Electrically conductive polymers. In *Conductive Polymers and Plastics*, pages 1–40. J. Margolis, editor, Chapman and Hall, New York, 1989.

[38] A. Malinauskas. Chemical deposition of conducting polymers. *Polymer*, 42:3957–3972, 2001.

[39] M. Yamaura, T. Hagiwara, and K. Iwata. Enhancement of electrical conductivity of polypyrrole film by stretching: Counter ion effect. *Synthetic Metals*, 20:209–224, 1988.

[40] M. Yamaura, K. Sato, T. Hagiwara, and K. Iwata. Memory effect of electrical conductivity upon the counter-anion exchange of polypyrrole films. *Synthetic Metals*, 48:337–354, 1992.

[41] S. Sadki, P. Schottland, N. Brodie, and G. Sabouraund. The mechanisms of pyrrole electropolymerization. *Chemical Society Reviews*, 29:283–293, 2000.

[42] R. H. Baughman. Conducting polymers in redox devices and intelligent materials systems. *Makromolekulare Chemie - Macromolecular Symposia*, 51:193–215, 1991.

[43] T. F. Otero and H. Grande. Electrochemomechanical devices: Artificial muscles based on conducting polymers. In *Handbook of Conducting Polymers.* T. A. Skotheirm, R. L. Elsenbaumer, J. R. Reynolds, and M. Dekker, editors, Marcel Dekker, New York, 1997.

[44] R. H. Baughman, R. L. Shacklette, and R. Elsenbaumer. Micro electromechanical actuators based on conducting polymers. In *Molecular Electronics: Materials and Methods*, volume 7 of *Topics in Molecular Organization and Engineering.* R. I. Lazarev, editor, Kluwer Academic Publishers, Boston, 1991.

[45] T. F. Otero. Electrochemical devices based on conducting polymers. In *Polymer Sensors and Actuators.* Y. Osada and D. E. Derossi, editors, Springer-Verlag, Lausanne, 1998.

[46] J. Madden, P. Madden, and I. W. Hunter. Conducting polymer actuators as engineering materials. In *Proceedings of SPIE Smart Structures and Materials 2002: Electroactive Polymer Actuators and Devices*, volume 4695, pages 424–434, San Diego, CA, 2002.

[47] T. A. Bowers. *Modeling, Simulation, and Control of a Polypyrrole-Based Conducting Polymer Actuator.* Masters Thesis, Massachusetts Institute of Technology, 2004.

[48] L. Bay, N. Mogensen, S. Skaarup, P. Sommer-Larsen, M. Jorgensen, and K. West. Polypyrrole doped with alkyl benzenesulfonates. *Macromolecules*, 35(25):9345–9351, 2002.

[49] G. Spinks, D. Zhou, L. Liu, and G. Wallace. The amounts per cycle of polypyrrole electromechancial actuators. *Smart Materials and Structures*, 12:468–472, 2003.

[50] S. Hara, T. Zama, A. Sewa, W. Takashima, and Kaneto. Polypyrrole-metal coil composites as fibrous artificial muscles. *Chemistry Letters*, 32(9):800–801, 2003.

[51] G. Spinks, G. Wallace, J. Ding, D. Zhou, B. Xi, and J. Gillespie. Ionic liquids and polypyrrole helix tubes: Bringing the electronic braille screen closer to reality. In *Proceedings of SPIE Smart Structures and Materials 2003: Electroactive Polymer Actuators and Devices*, volume 5051, pages 372–380, San Diego, CA, 2003.

[52] Y. Sonoda, W. Takashima, and K. Kaneto. Characteristics of soft actuators based on polypyrrole films. *Synthetic Metals*, 119(1-3):267–268, 2001.

[53] Eamex Corporation. http://www.eamex.co.jp.

[54] A. Chen. *Large Displacement Fast Conducting Polymer Actuators.* Masters thesis, Massachusetts Institute of Technology, 2006.

[55] Sigma-Aldrich Corp. http://www.sigmaaldrich.com.

[56] Princeton Applied Research. http://www.princetonappliedresearch.com. Oak Ridge, TN, USA.

[57] Cincinnati Sub-Zero Products Inc. http://www.cszinc.com. Cincinnati, OH, USA.

[58] HTW Hochtemperatur-Werkstoffe GmbH. http://htw-germany.com. Gemeindewald 41, 86672 Thierhaupten, Germany.

[59] FeatureCAM. http://www.featurecam.com. Salt Lake City, UT, USA.

[60] Technic Inc. http://www.technic.com.

[61] Loctite. http://www.loctite.com.

[62] P. Pillai. *Conducting Polymer Actuator Enhancement through Microstructuring.* Masters Thesis, Massachusetts Institute of Technology, 2007.

[63] MatWeb. http://www.matweb.com.

[64] Alfa Aesar. http://www.alfa.com. Ward Hill, MA, USA.

[65] J. Madden, P. Madden, and I. Hunter. Polypyrrole actuators: Modeling and performance. In *SPIE Smart Structures and Materials 2001: Electroactive Polymer Actuators and Devices*, volume 4329, pages 72–83, San Diego, CA, 2001.

[66] A. H. Slocum. *Precision Machine Design.* Society of Manufacturing Engineers, Dearborn, 1992.

[67] S. T. Smith. *Flexures: Elements of Elastic Mechanisms.* CRC, 2000.

[68] L. L. Howell. *Compliant Mechanisms.* Wiley-Interscience, 2001.

[69] N. Lobontiu. *Compliant Mechanisms: Design of Flexure Hinges.* CRC, 2002.

[70] N. Lobontiu and E. Garcia. Analytical model of displacement amplification and stiffness optimization for a class of flexure-based compliant mechanisms. *Computers & Structures*, 81:2797–2810, 2003.

[71] ANSYS Inc. http://www.ansys.com. Canonsburg, PA, USA.

[72] Trotec Laser Inc. http://www.trotec.net. Ypsilanti, MI, USA.

[73] J. D. W. Madden, B. Schmid, M. Hechinger, S. R. Lafontaine, P. G. A. Madden, F. S. Hover, R. Kimball, and I. W. Hunter. Application of polypyrrole actuators: Feasibility of variable camber foils. *IEEE Journal of Oceanic Engineering*, 29(3):738–749, 2004.

[74] G. V. Lauder, P. Madden, R. Mittal, H. Dong, M. Bozkurttas, N. Davidson, J. Tangorra, and I. Hunter. Pectoral fin function in sunfish: Experimental hydrodynamics, computational fluid dynamics, and construction of a robotic model. *Integrative and Comparative Biology*, 45(6):1030–1030, 2005.

[75] G. V. Lauder, P. G. A. Madden, R. Mittal, H. Dong, and M. Bozkurttas. Locomotion with flexible propulsors: I. Experimental analysis of pectoral fin swimming in sunfish. *Bioinspiration & Biomimetics*, 1(4):S25–S34, 2006.

[76] J. L. Tangorra, S. N. Davidson, I. W. Hunter, P. G. A. Madden, G. V. Lauder, H. Dong, M. Bozkurttas, and R. Mittal. The development of a biologically inspired propulsor for unmanned underwater vehicles. *IEEE Journal of Oceanic Engineering*, 32(3):533–550, 2007.

[77] J. L. Tangorra, S. N. Davidson, P. G. Madden, G. V. Lauder, and I. W. Hunter. The development of a biorobotic pectoral fin. In *Proceedings of the IEEE Engineering in Medicine and Biology Society*, New York, NY, 2006.